Synthesis and Evaluation of Fluoro and Thia Lipids as Bioanalytical Tools

Gaynor Manuel

University of Cape Town

August 2014

Synthesis and Evaluation of Fluoro and Thia Lipids as Bioanalytical Tools

A thesis submitted to the

University of Cape Town

In fulfilment of the requirements for the degree of

Master of Science

By

Gaynor Manuel

Supervisors: Dr Anwar Jardine and Prof Kelly Chibale

Department of Chemistry

University of Cape Town

August 2014

Declaration

I declare that “Synthesis and Evaluation of Fluoro and Thia Lipids as Bioanalytical Tools”, is my own work and to the best of my knowledge has never been submitted for any degree or examination at any university. All sources of information used are cited and completely referenced.

Signed by candidate

…… *18 August 2014*

Ms Gaynor Manuel …….. Date

To My Parents

Always giving thanks to God the Father for everything,
in the name of our Lord Jesus Christ

Ephesians 5:20

Acknowledgements

I would like to thank the following people for their contribution to this thesis:

- My parents for their unconditional love, support and encouragement. You've taught me the importance of family, faith and love. I give praise to God for the amazing parents he has given me.
- My spiritual parents, Bishop Raymond and Rosetta Olckers. Thank you for always keeping me in your prayers.
- My primary supervisor, Dr Anwar Jardine. Thank you for your guidance, encouragement and patience. Thank you for giving me the opportunity to work with you and learn from you. My growth as a chemist and a person, I owe to you.
- My co-supervisor, Prof Kelly Chibale for financial support, your guidance and all the interesting discussions.
- Shakeela Sayed for all the strategic planning, silly talks and laughs. Thanks for always being by my side.
- Thank you to Chitalu Musonda, for your intellectual support, the pep talks and keeping me motivated.
- My sisters, Lauren and Gaylin Manuel for making sure my cup were always filled with hot chocolate during the writing of this thesis.
- The employees from Permoseal, especially my manager, Paul Jacobs for allowing me to spend time on my thesis during working hours. The rest of the people in the lab, Anitha Sookdeo and Bruno Santos and Jason Daniels for all their support and interesting discussions.
- I would like to thank everyone from the Department of Chemistry, especially Pete Roberts (NMR), Gianpiero Benincasa (Elemental analysis) and Deirdre Brooks (For helping me stay on track).
- To Carine Sao Emani for providing me with the M.smeg culture and the endless advice on growing and handling cultures.
- Dr Suhail Rafudeen and Faezah Davids for allowing me to do all the biological studies in their labs and their students for being so accommodating.
- The group at the Institute of Infectious Disease and Molecular Medicine for doing all the work on M.tb, especially Digby Warner and Krishnamoorthy Gopinath.
- Thank you to all my friends, Shakeela Sayed, Gadija Akleker, Shankari Nair, Muneebah Adams, Tameryn Stringer, Preshendren Govender, Dorothy Semenya and Nicholas Njuguna for all their advice and support.

Table of Contents

Abstract

Lipid catabolism plays a significant role in the survival of M.tb inside the host. The development of analytical techniques such as gas chromatography mass spectroscopy (GC-MS) and liquid chromatography mass spectroscopy (LC-MS) has become popular as metabolomics tools in the study of such catabolic pathways. The development of biomarkers and internal standards to perform quantitative and qualitative analysis of metabolites in the catabolic pathway would be an attractive tool. Thus, cholesterol derivatives were synthesized as thia-, fluoro- and deuterium labeled analogs. Sulfur was incorporated into cholesterol at positions, C3 as well as C23. The 3β-mercaptocholest-5-ene was synthesized to block the initial stage of cholesterol catabolism and evaluate whether side chain degradation can still occur. Fluorine was integrated into the cholesterol backbone at C3 to evaluate the side-chain degradation in the absence of cholesterol oxidase activity. Steroids with fluorine at C6 are known to have good biological activity and were for this reason also synthesized. Deuterium labeled compounds were synthesized and used as internal standards for GC-MS analysis. As an alternative to cholesterol catabolism, fatty acids like stearic acid are important in producing building blocks for long chain mycolic acids which provides protection to the mycobacterium. For this reason thiastearic acid derivatives were synthesized and evaluated as biomarkers.

The compounds synthesized were characterized by ^{1}H NMR, ^{13}C NMR, FT-IR and elemental analysis. GC-MS was used to further support molecular identity. Growth curves of *Mycobacterium tuberculosis* (M.tb) and *Mycobacterium smegmatis* (M.smeg) were determined to establish whether the compounds can be utilized as carbon source by mycobacteria. Cholesterol displayed the highest growth in relation to its analogs in M.tb culture. Generally, better growth was observed with the compounds in an M.smeg culture. The stearic acid analysis displayed much better growth in both M.tb and M.smeg with only marginally lower growth observed as compared to the stearate standard.

Once it was established that the compounds synthesized in this study can be utilized as carbon sources by M.tb and M.smeg, the catabolic fate of the compounds were determined. Cholesterol oxidase experiments were performed to determine the enzyme activity in the presence of sulfur and fluorine.

Cholesterol oxidase or 3β-hydroxy-Δ(5)-steroid dehydrogenase (3β-HSD) is responsible for the conversion of cholesterol to cholestenone. The 3β-hydroxy steroids, cholesterol, 23-thiacholest-4-en-3β-ol and 6β-fluorocholestan-3β,5α-diol, were enzymatically oxidized via

cholesterol oxidase and the change in concentration monitored after 45 minutes. Oxidation products were detected and the concentrations determined.

In the absence of cholesterol oxidase activity, 3β-mercaptocholest-5-ene and 3α-fluorocholest-5-ene, side-chain degradation was evaluated.

The TIC of cholesterol incubation extracts displayed cholestenone as one of the catabolic products together with two other side-chain oxidations products. Standards and molecular mass data were used to identify these products. A decrease in degradation was observed when CYP450 inhibitor, econazole was added to the incubations. 23-Thiacholest-4-en-3β-ol was evaluated and the TICs of the incubation extract with showed oxidation forming 23-thiacholest-3-one as observed in cholesterol oxidase experiments.

The compounds were also evaluated as potential internal standards. Good extraction recovery percentages were obtained from culture which shows that the compounds can serve as internal standards. Thus, these lipids would be valuable for accurate quantification of cholesterol in analytical procedures.

The growth of M.tb and M.smeg was determined with thiastearic acids as the carbon sources. The concentration of the thiastearic acids were monitored after an incubation period of 24 hours. A decrease in concentration of thiastearic acids was noted for both 9- and 10-thiastearic acids while little change in concentration was observed with 11-thiastearic acid. This effect was also observed in the growth curves of M.smeg with the lowest growth observed with 11-thiastearic acid.

List of abbreviations

3-HSA	3-Hydroxy-9,10-seco-androst-1,3,5-triene-9,17-dione
3β-HSD	3β-Hydroxy-Δ(5)-steroid dehydrogenase
3,4-DHSA	3,4-Dihydroxy-9,10-seco-androst-1,3,5-triene-9,17-dione
4,9-DSHA	4,5-9,10-Diseco-3-hydroxy-5,9,17-trioxoandrosta-1,2-diene-4-oic acid
ACP	Acyl carrier protein
AD	4-Androstene-3,17-dione
ADD	1,4-Androstenediene-3,17-dione
AG	*D*-Arabino-*D*-galactan
$BF_3{\cdot}OEt_2$	Boron trifluoride etherate
BSA	Bovine serum albumin
EMB	Ethambutol
EtOH	Ethanol
$CaCl_2$	Calcium chloride
$CDCl_3$	Deuterated chloroform
$CeCl_3{\cdot}7H_2O$	Cerium (III) chloride heptahydrate
C. elegans	*Caenorhabditis elegans*
CrO_3	Chromium trioxide
CYP450	Cytochrome P450
DAST	Diethylaminosulfur trifluoride
DCM	Dichloromethane
DMAP	4-Dimethylaminopyridine
DOHNAA	9,17-Dioxo-1,2,3,4,10,19-hexanorandrostan-5-oic acid

DSA	*N*-decanesulfonylacetamide
EIC	Extracted ion chromatograph
FAD	Fatty acid desaturase
FAME	Fatty acid methyl ester
FAS	Fatty acid synthesis
FT-IR	Fourier transform-infrared
GC-MS	Gas chromatography mass spectroscopy
HCl	Hydrochloric acids
H_2O	Water
H_2SO_4	Sulfuric acid
HHD	2-Hydroxy-hexy-2,4-dienoic acid
HNO_3	Nitric acid
HPLC	High performance liquid chromatography
Hrs	Hours
INH	Isoniazid
ISO	Isoxyl
KatG	Catalase-peroxidase enzyme
KOH	Potassium hydroxide
LC-MS	Liquid chromatography-mass spectroscopy
LG	Lipoglycan
m-CPBA	meta-Chloroperoxybenzoic acid
MeOH	Methanol
$MgSO_4$	Magnesium sulfate
M.smeg	Mycobacterium smegmatis

M.tb	Mycobacterium tuberculosis
$NaBH_4$	Sodium borohydride
$NaBD_4$	Sodium borodeuteride
NaCl	Sodium chloride
$NaHCO_3$	Sodium bicarbonate
NaOH	Sodium hydroxide
NMR	Nuclear magnetic resonance
OD	Optical density
OSA	*N*-octanesulfonylacetamide
PG	Peptidoglycan
PI	Phosphatidyl inositols
Ppm	Parts per million
PZA	Pyrazinamide
RMP	Rifampicin
RT	Room temperature
S	Streptomycin
SLOS	Smith-Lemli-Opitz syndrome
TACO	Tryptophan-aspartate-containing coat protein
TIC	Total ion current
TLC	Thin-layer chromatography
TB	Tuberculosis
TMS	Tetramethylsilyl
TTA	Tetradecylthioacetic acid
$ZnSO_4$	Zinc sulfate

Chapter 1

Mycobacteria and the role of lipid metabolism in pathology and therapy

1.1. Background

Tuberculosis (TB) is an infectious airborne disease caused by various strains of Mycobacteria, primarily *Mycobacterium tuberculosis* (M.tb). Transmission of TB occurs *via* the spread of aerosol droplets carrying the bacteria from person to person during sneezing, coughing and talking.[1] Most TB infections remain asymptomatic and latent, but can become active and, if left untreated, could lead to death. TB can be diagnosed and detected by several techniques.[1] These techniques include chest X-rays, tuberculin skin tests and sputum analysis.

TB typically affects the lungs and is known as pulmonary TB. Symptoms of pulmonary TB include chest pains, fever and weight loss.[2] The central nervous system, lymphatic system, kidneys, bones and the joints can also be affected and this is known as extrapulmonary TB. A form of extrapulmonary TB, known as miliary TB, occurs when the bacterium move into the blood stream and infect various organs through the circulatory system. Atypical TB involves a group of Mycobacteria known as colonizers that do not cause disease.[1] These bacteria may, however, cause infection that is clinically similar to typical TB.

TB continues to be a major problem worldwide with more than 500 new cases per 100 000 population in South Africa (2012), while 1.8 million deaths occur globally per annum (Figure 1.1).[3] The current drug treatments against TB can have adverse side effects and due to the extensive treatment time, therapy often remains incomplete, leading to further problems such as drug resistance.

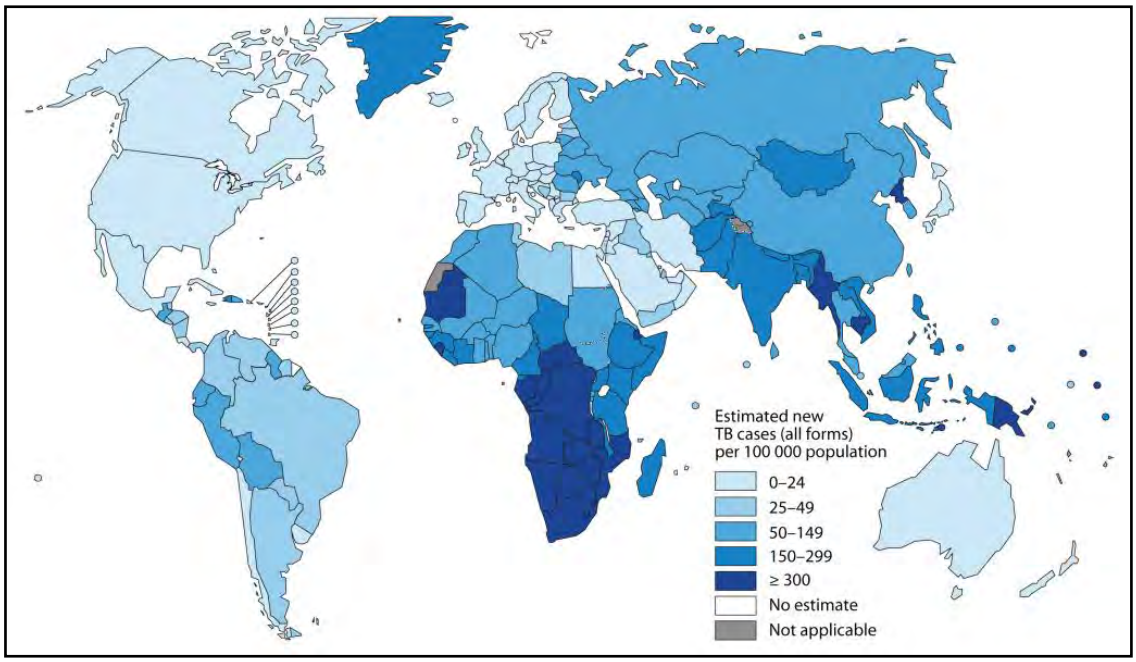

Figure 1.1: *Estimated tuberculosis incidence rate, 2012.*[3]

1.2. Mycobacterium tuberculosis: the pathogen

1.2.1. The cell wall envelope

One of the key factors that contribute to the success of M.tb infection is the unique composition of its thick lipid-rich cell wall (Figure 1.2). This unique design of the cell wall aids in the prevention of dehydration and affords protection against available drugs, which makes therapy so difficult. Since the cell wall is the outermost component of the bacterium, it interacts with host cells and plays a major role in bacterial virulence. The gram-positive cell wall is composed of two segments, an inner core and an outer core. The inner core is governed by covalently linked mycolic acids, *D*-arabino-*D*-galactan (AG) and peptidoglycan (PG). The constituents of the outer core include free lipids, lipoglycans (LG) and phosphatidyl inositols (PI) and are involved in the adaption of the bacterium during host immune evasion. These lipid molecules play an important role in the functioning of the pathogen and the manner in which the host responds during infection.[4]

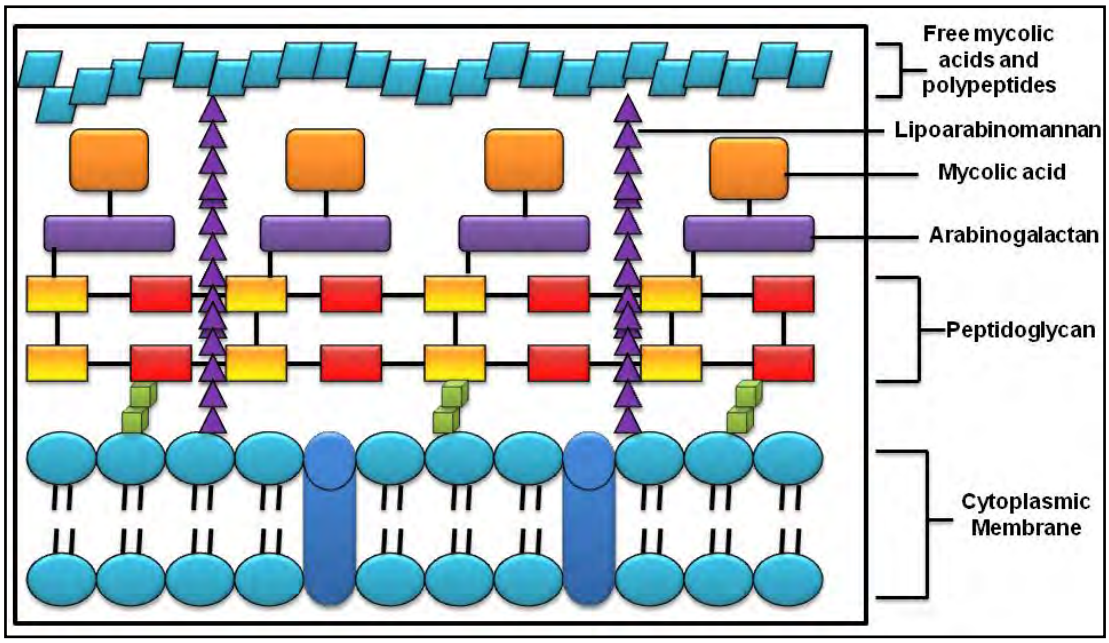

Figure 1.2: *Mycobacterial cell wall.*[5]

Mycolic acids

Mycolic acids are important mycobacterial cell wall components and are high molecular weight α-alkyl-β-hydroxy fatty acids with species-specific chain lengths of C_{60} – C_{90} atoms.[6,7] Mycolic acids are usually found as bound esters, albeit, extractable free mycolic acids are also present, usually as trehalose-6,6‟-dimycolate.[8] M.tb synthesizes three classes of mycolic acids; α-mycolic acids, methoxymycolic acids and ketomycolic acids (Figure 1.3).[8,7] These acids are modified with cyclopropane rings, methyl groups, ketones and methoxy-groups to form the different types of mycolic acids.

Mycolic acids are the outermost shield of the mycobacterial cell wall and most certainly involved in cellular recognition and immunity. Three dominant fibro-nectin binding proteins, Ag85A, Ag85B and Ag85C are important proteins that helps to assemble the mycobacterial cell wall and are collectively known as the antigen 85 complex.[9] These antigen proteins are secretory proteins of actively growing cells which efficiently generate immunity to M.tb.[10] Sensitization of these antigens occurs in the first phase of infection and can therefore be considered to be utilized as possible vaccine candidates against TB.[11]

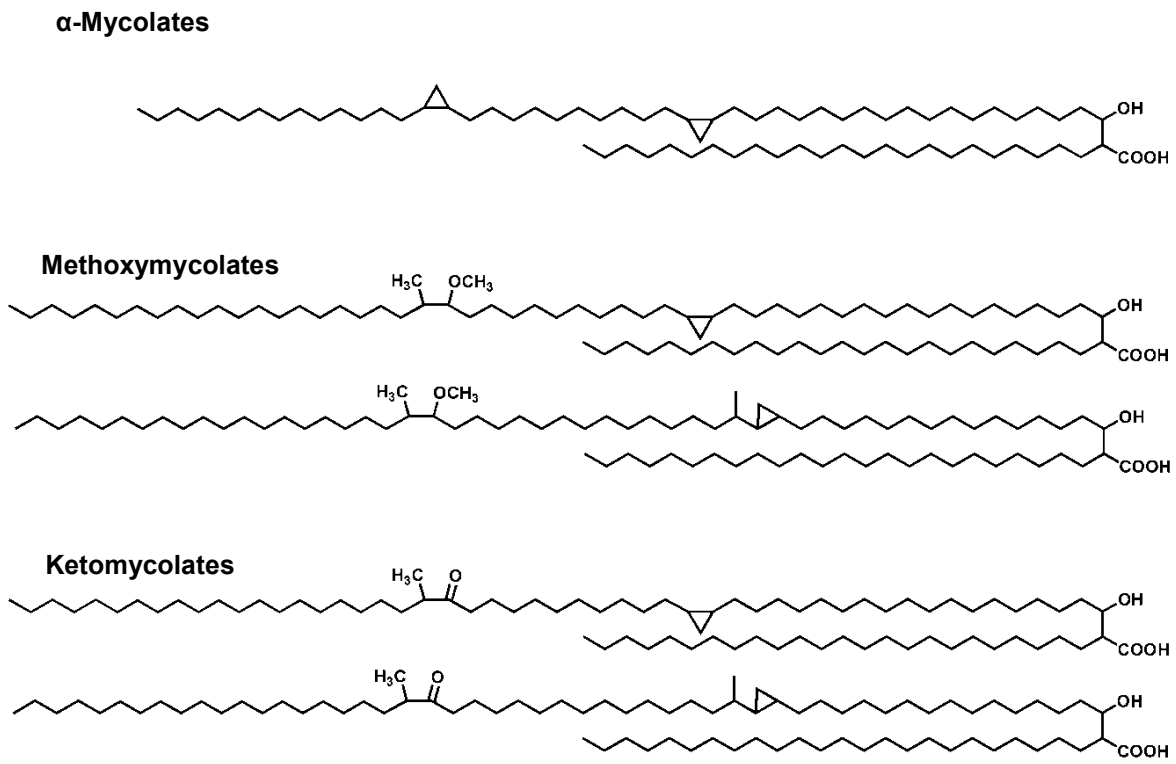

Figure 1.3: *Chemical structures of α-mycolic acid, methoxymycolic acid and ketomycolic acid.*[9]

1.3. Current tuberculosis chemotherapy

Clinical antituberculosis drugs include isoniazid (INH), rifampicin (RMP), pyrazinamide (PZA), ethambutol (EMB) and streptomycin (S) (Figure 1.4).[12] In order to rapidly treat the disease and minimize the chance of resistance developing, combination therapy is part of the public health policy. Streptomycin was the first drug to become available in 1946. It was the most successful antimycobacterial agent at the time.[12] By 1955, a treatment consisting of a combination of streptomycin, isoniazid and *p*-aminosalicylic acid was administered. Today, clinical TB treatment advocates the following two regimens:

- A two month long treatment which includes S, EMB, INH, RMP and PZA, followed by
- A four month treatment consisting of INH and RMP.

These first-line drugs are more efficient than both the second and third-line drugs and exhibit a lower level of toxicity.[1]

The mechanism of action of most M.tb drugs is well established. The focus in this review will be on drugs that affect mycolic acid synthesis.

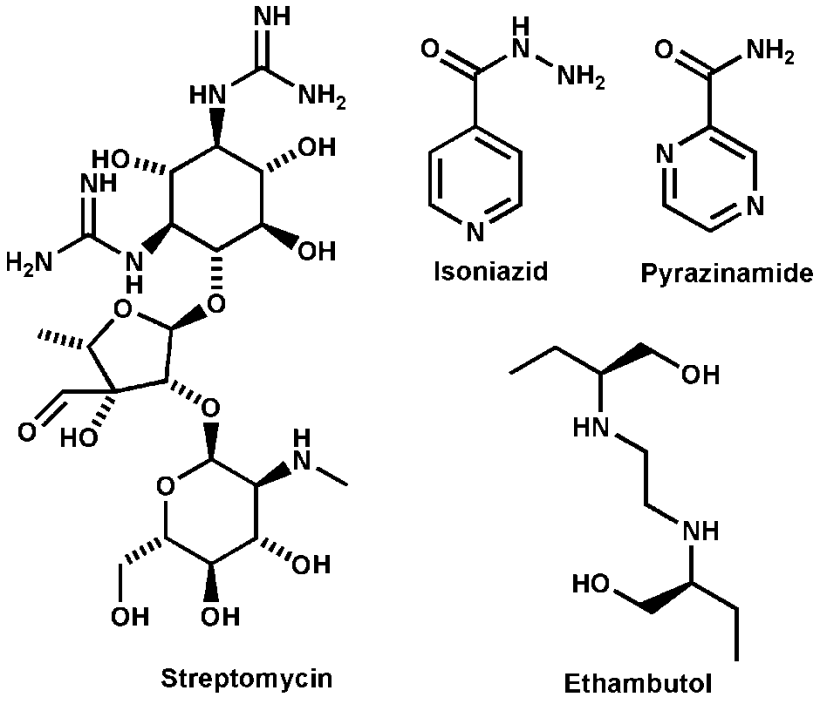

Figure 1.4: *Structures of available antituberculosis drugs, isoniazid, pyrazinamide, ethambutol and streptomycin.*[12]

1.3.1. Isoniazid (INH)

The most common antituberculosis drug used is isoniazid which has been in clinical use since the 1950's. INH was first discovered by Domagk in 1952 and still today remains one of the most effective antimycobacterial agents.[1] The existence of INH as an antituberculosis treatment came about through random screens.[13–15] Even though INH is one of the oldest synthetic antituberculosis drugs, its mode of action only became known in the late 1990's.[15]

Mechanism of action of Isoniazid (INH)

INH is a prodrug, which requires activation by a multifunctional mycobacterial catalase-peroxidase enzyme (KatG) *via* peroxidation.[16] As a result, a range of reactive carbon, oxygen or nitrogen intermediates are derived, which can cause detrimental modification to intracellular lipids, proteins and amino acids of M.tb cells.[17] INH inhibits TB by inhibiting mycolic acid synthesis which is a major element of the mycobacterium cell wall.[17] FabI (InhA) is a NADH-dependent enoyl acyl carrier protein reductase responsible for bacterial mycolic acid synthesis. When INH is activated in the presence of NAD and FabI, a covalent INH-NAD adduct is formed. The INH-NAD adduct can then bind to the NADH recognition site of FabI, which prevents further synthesis of mycolic acids.[13] This increases the permeability of the mycobacterial cell wall, thus allowing entry of other antimycobacterial drugs which aids in further inhibition of bacterial cell growth. The mode of action of INH is shown in Figure 1.5.

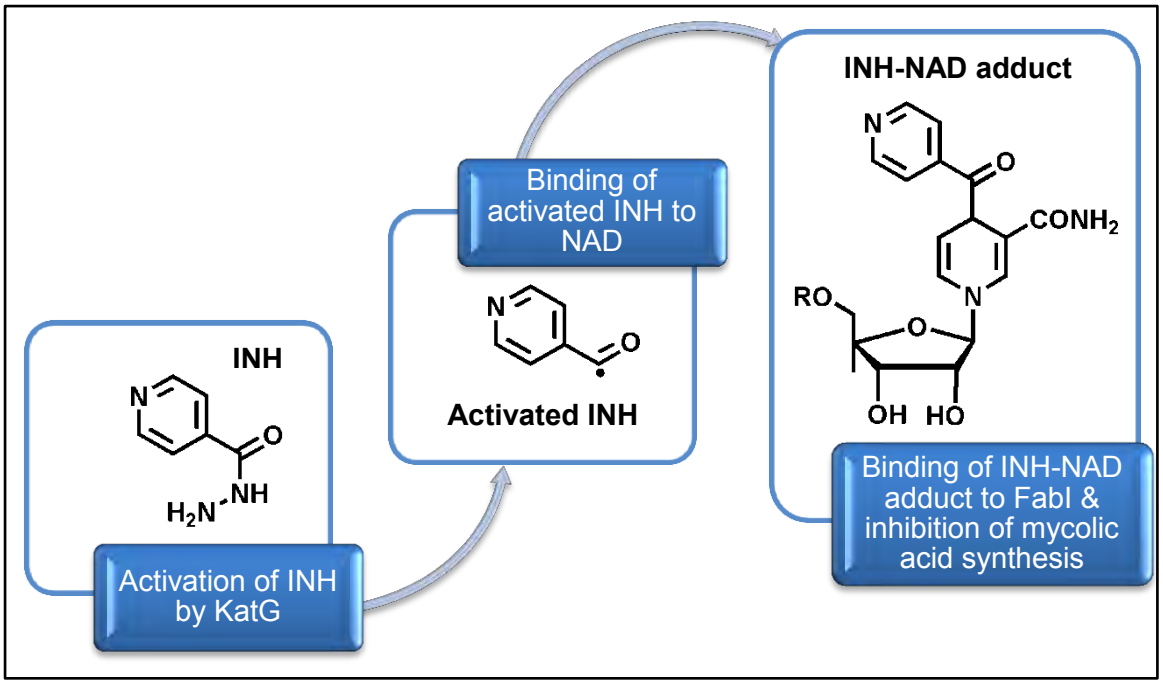

Figure 1.5: *Mode of action of INH.*[16]

Due to the evolving nature of the mycobacterium pathogen, various strains have become resistant to the action of INH. One such resistant mechanism is due to a mutation in the KatG gene. The KatG gene is responsible for encoding the catalase-peroxidase enzyme. Due to the occurrence of mutations such as deletions and missense in the KatG gene, one third of M.tb strains are unable to activate INH and hence are resistant to INH.[15]

Early antituberculosis drugs such as isoxyl are also known to inhibit mycolic acid synthesis.

1.3.2. Isoxyl (ISO)

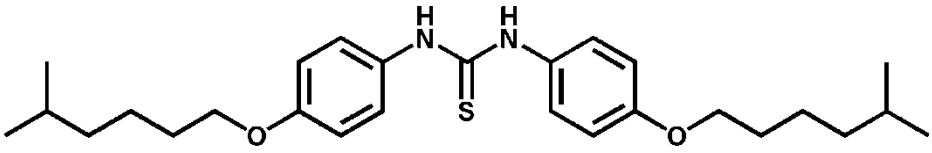

Figure 1.6: *Chemical structure of isoxyl.*[15]

Isoxyl (ISO) was effectively used as an antituberculosis drug in the 1960's.[18] It is a diaryl thiourea derivative and is believed to have antimycobacterial properties by inhibiting both mycolic acid and short chain fatty acid synthesis.[8] ISO is thought to inhibit a Δ^9-desaturase, DesA3, together with a Δ^9-stearoyl desaturase.[8] Desaturases play an important role in the biosynthesis of unsaturated fatty acids that serves as building blocks for mycolic acid synthesis.

Urbancik *et al.* demonstrated that with monotherapy of ISO, moderate activity was observed against TB and that 25 % of chronically positive patients were cured within 6 to 8 weeks.[19] With combination therapy of INH and ISO, improved mycobacterial activity compared to monotherapy was observed.

The danger of TB due to the resistance against available drugs has extended from single drug resistance to multidrug resistance to extremely drug resistant strains. With more than 10 000 confirmed multidrug resistant cases in South Africa in 2011 and with only half of those patients treated at the end of that year, development of improved drug treatments has become sought-after.[3] The success in developing new drugs is dependent on targeting essential processes that play important roles in the survival of the pathogen. *In vivo*, mycobacteria can switch from carbohydrates to fatty acids as a carbon and energy source.[20] Thus, processes such as fatty acid biosynthesis and catabolism and desaturation of fatty acids can be investigated as possible drug targets.

1.4. Biosynthesis and transport of fatty acids

Bacterial fatty acid synthesis (FAS) follows a biochemical pathway nearly identical to that found in humans.[21] Due to differences in protein amino sequences, the enzyme active sites are entirely different and this allows for distinct bacterial fatty acid inhibitors to be generated.[22] Additionally, in humans, a single polypeptide is the key contributor to the biosynthesis of fatty acids, whereas in bacteria each step in the synthetic process is carried out by individual proteins.[23] The fatty acid biosynthesis pathway found in humans is known as FAS I and the process in bacteria, plants and protozoa is known as FAS II. Mycobacteria are known to have both FAS I and FAS II pathways.[24] FAS II was adapted from an *E.coli* model as shown in Figure 1.7. Fatty acid biosynthesis (Fab) genes are responsible for the synthesis of long chain fatty acids from acetyl-CoA and malonyl-CoA.[21] Malonyl-CoA is conjugated to an acyl carrier protein (ACP), malonyl-ACP. Subsequent catalysis through processes such as condensation, reduction and dehydration using various Fab genes produce phospholipids. Ultimately phospholipids serve as the basis for the synthesis of other lipids such as mycolic acids. Enzymes responsible for mycolic acid synthesis are essential for the survival of mycobacteria and therefore are excellent drug targets.[25] Interference with acylation of ACP thus constitutes a key drug target. Modified FAs that resist chemical transformation have also proved to be good inhibitors. Parrish *et al.* evaluated a β-sulfonyl carboxamide, namely *N*-octanesulfonylacetamide (OSA), as an inhibitor of mycolic acid synthesis.[24] OSA (Figure 1.8) derivatives are known to function as transition state compounds involving processes of fatty acid elongation. The mode of inhibition is yet to be

established and other derivatives such as *N*-decanesulfonylacetamide (DSA) have also been found to have inhibitory effects.[26]

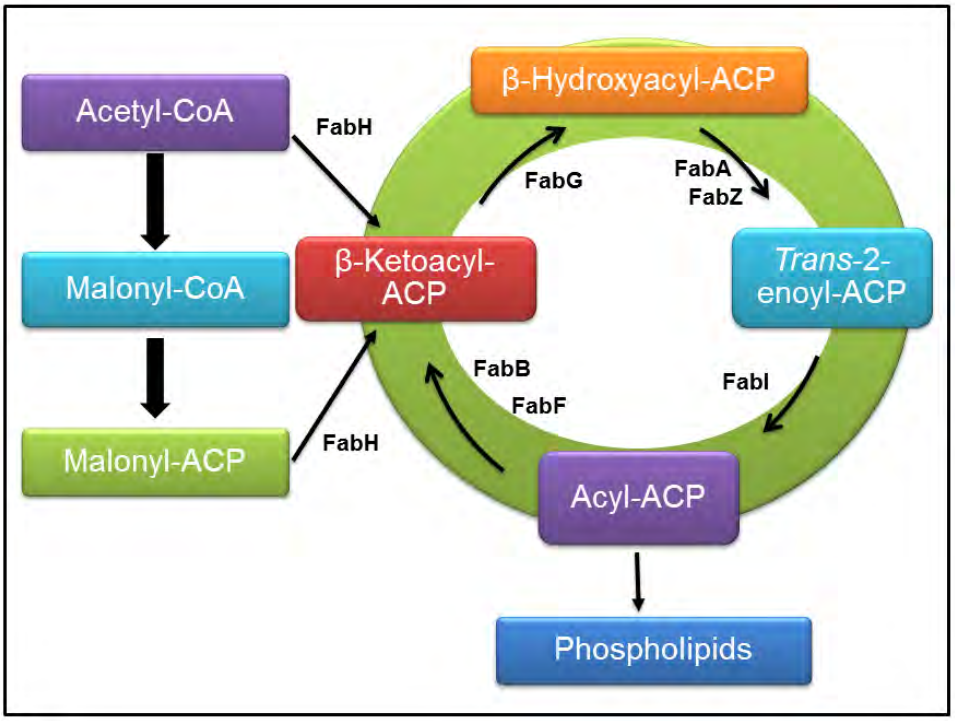

Figure 1.7: *Bacterial fatty acid biosynthesis pathway.*[25]

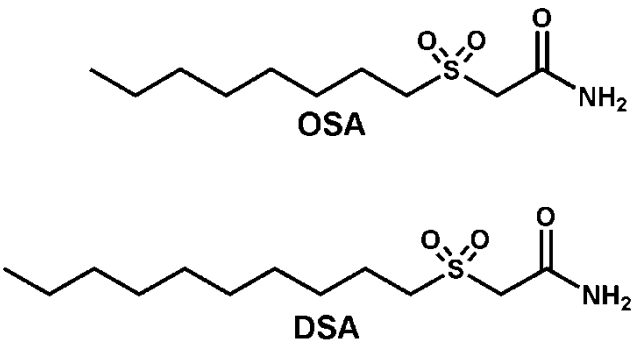

Figure 1.8: *Structures of OSA and DSA.*[24,26]

1.5. Catabolism of fatty acids

Titgemeyer *et al*. studied the carbohydrate uptake in *Mycobacterium smegmatis* (M.smeg) and M.tb where it was established that M.tb only has 5 sugar permeases compared to the 28 found in M.smeg.[27] This, together with the absence of genes encoding for sugar metabolism, led researchers to believe that M.tb relies on an alternative carbon source in host cells, i.e. fatty acids. Fatty acid catabolism follows two pathways: a β-oxidation pathway and an anaplerotic glyoxylate shunt pathway.[28] The β-oxidation pathway is used for the degradation

of fatty acids to acetyl-CoA while the glyoxylate shunt pathway uses the acetyl-CoA units to produce biosynthetic C-4 precursors essential for mycobacterial cells.[20]

1.6. Desaturation and alkylation of fatty acid chains

The ability of M.tb to modify its cell wall properties according to the cell cycle stage or environmental conditions is partly the reason for its robustness. Fatty acid desaturation involves the introduction of a *cis* double bond into an acyl fatty acid chain using enzymes called fatty acid desaturases (Fad).[29] The result of this unsaturation of membrane fatty acids is an increase in fluidity.[30] The introduction of methyl side chains as well as the characteristic cyclopropyl groups along the mycolic acid chain also requires unsaturated precursors. Desaturation occurs in numerous fatty acids, but the favoured substrates in M.tb are palmitoyl-and stearoyl-CoA (due to its higher content) which is converted to palmitoleoyl- and oleoyl-CoA, respectively.[31]

A significant step in the synthesis of monounsaturated fatty acids is the desaturation at the C9 position. The iron-containing stearoyl CoA Δ^9-desaturase is responsible for the catalysis and regulation of this desaturation.[32] The first step is slow and includes a C-H (9^{th} position) activation which produces a carbon-centred radical.[33] A second hydrogen atom (10^{th} position) is rapidly lost in a *syn* fashion in a subsequent step to produce a *cis*-olefin as shown in Figure 1.9. This is supported by mechanistic probes previously synthesized that showed efficient oxidation when the methylene group at the 9^{th} position was substituted with a sulfur atom (Figure 1.9).[34]

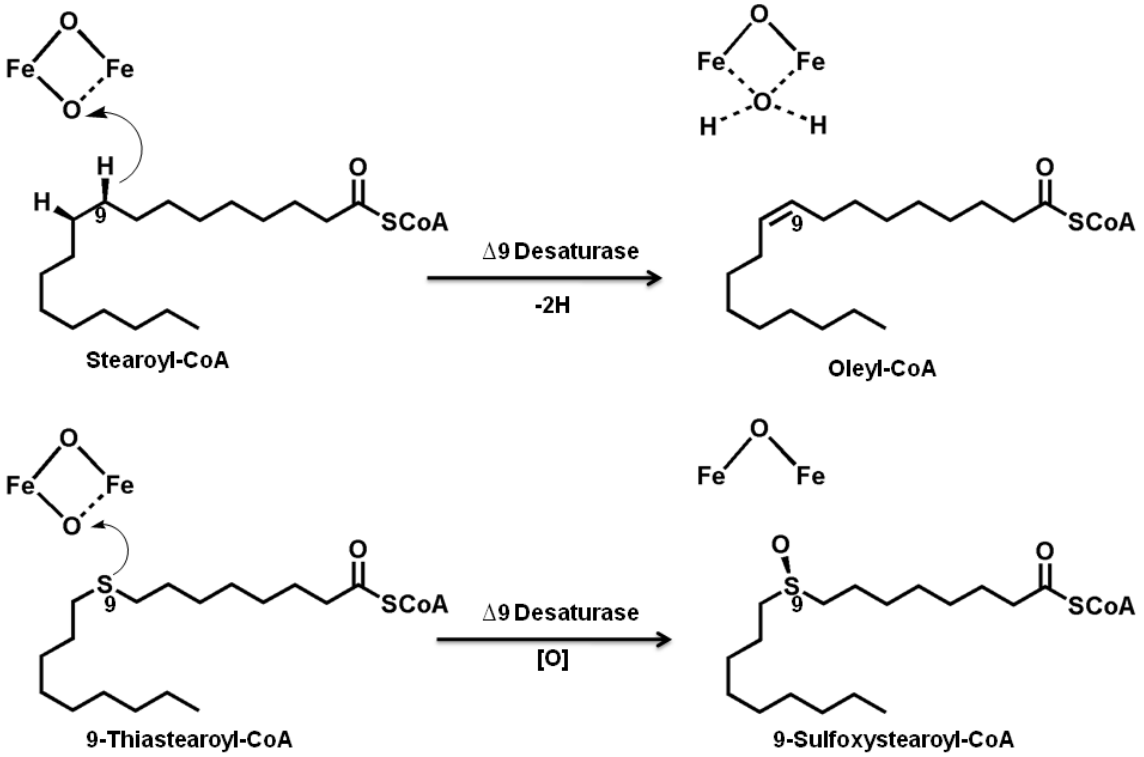

Figure 1.9: *Δ^9-Desaturase of stearoyl CoA and 9-thiastearoyl CoA.*[35]

The biosynthesis of unsaturated fatty acids is important since these acids serve as substrates for cyclopropanation to produce long chain fatty acids that are eventually converted into mycolic acids. Dihydrosterculic acid (Figure 1.10) is a cyclopropanated fatty acid that play a key role in the growth of various bacteria and plants, including pathogenic species such as *Leishmania*.[36] The biosynthesis of this fatty acid would be an effective drug target since cyclopropane fatty acids are absent in mammals.[36] Pascal *et al.* evaluated 10-thiastearic acid as an inhibitor of dihydrosterculic acid synthesis in *Crithidia fasciculate*.[36] It is believed that during the cyclopropanation of 10-thiastearic acid, the sulfonium ion is formed due to the methyl transfer from S-adenosylmethionine. This ion then acts as an inhibitor and prevents the synthesis of dihydrosterculic acid, and hence the growth of the protozoan (Figure 1.10).

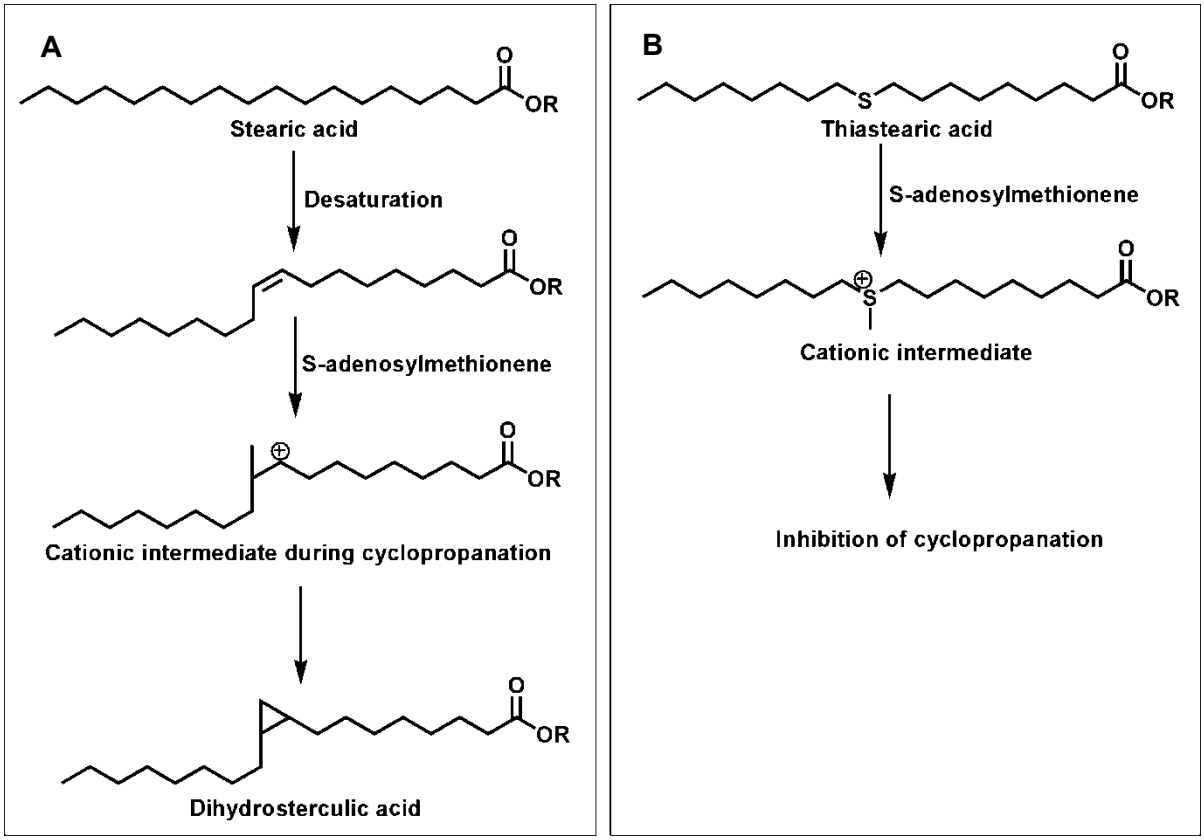

Figure 1.10: *Cyclopropanation of* ***A:*** *stearic acid and* ***B:*** *10-thiastearic acid.*[36]

Other thia-fatty acids analyzed include 3-thia- and 4-thia-fatty acids.[37,38] Hvattum *et al.* synthesized 4-thiastearic acid and its sulfoxide derivative and evaluated its metabolism in whole rats, rat hepatocytes and rat liver mitochondria.[37] The study concluded that 4-thiastearic acid and its sulfoxide derivative are utilized as a carbon source by rats and that 4-thiastearic acid is integrated into phospholipids and triacylglycerol faster than the natural stearic acid. The incorporation of 3-thiafatty acids has been shown to increase the presence of oleic acid in the liver of rats due to an increased gene expression of Δ^9-desaturase.[38]

1.7. Synthesis, properties and applications of thia-fatty acids

Thia-fatty acids are fatty acid derivatives with the sulfur atom substituting a methylene group within the fatty acid chain. Due to the more polar nature of the thia-fatty acid, they are more water soluble than the typical fatty acid.[39] High performance liquid chromatography (HPLC) revealed that thia-fatty acids have a reduced elution volume compared to the original fatty acid and gas chromatography mass spectroscopy (GC-MS) analysis showed an increase in retention time on both polar and non-polar columns.[39]

1.7.1. Natural thia-fatty acids

Naturally occurring thia-fatty acids have been isolated from onions, a wide range of garlic species as well as various microorganisms. Reseman *et al.* evaluated the oil content in onions as potential flavour carriers.[40] The lipid extract from onions was analyzed using GC-MS and 3-(methylsulfinyl)alanine was identified as a constituent. The fatty acid composition of a garlic species, *Allium sativum,* was determined using GC-MS and is shown in Figure 1.11.[41] These thia-fatty acids include fatty acids with sulfur present in position C10 and isolation of such fatty acids could lead to further investigation as possible inhibitors of dihydrosterculic acid synthesis in *Crithidia fasciculate* (Section 1.5). Dembitsky *et al.* identified various saturated and unsaturated fatty acids as well as a cyclic thia-fatty acid.[41] Other thia-fatty acids were also isolated from garlic which including 3-(methylsulfinyl)alanine and 3-allylthiopropionic acid.

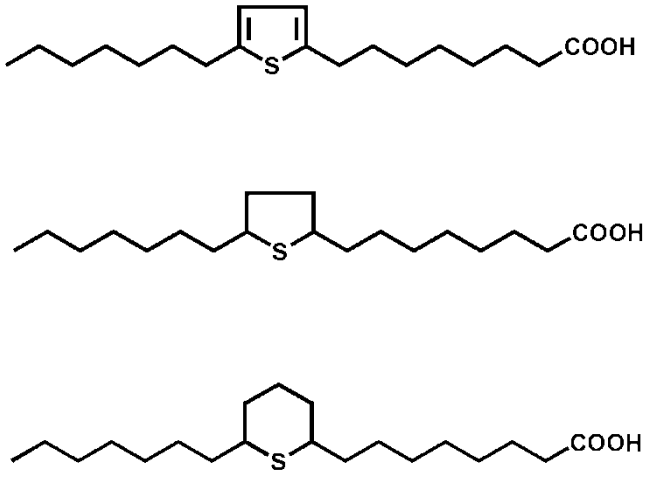

Figure 1.11: *Isolated thia-fatty acids from Allium sativum.*[41]

Various epithio stearic acids have been isolated from canola oil by Wijesundera *et al*.[42] Gas chromatography and mass spectroscopy was used to analyze these fatty acids. It was found that sulfur was included as part of a 5-membered ring. *Streptomyces* species also synthesize thia-fatty acids when grown in the presence of methionine, 3-methylpropionic acid and *trans*-3-methylthioacrylic acid are synthesized.

1.7.2. Synthetic thia-fatty acids

Saturated thia-fatty acids can be prepared from alkylbromides and ω-mercaptocarboxylic acids as well as from alkylmercaptanes and ω-bromocarboxylic acids.[43,44] Thia-fatty acids can also be prepared from alkylthiols and ethylacrylate and by reacting alkylthiols with propiolic acid.[45,46]

Dyroy *et al.* evaluated the anti-inflammatory effects of tetradecylthioacetic acid (TTA), a 3-thia-fatty acid.[47] β-oxidation of TTA does not occur but rather ω-oxidation and sulfur oxidation as well as desaturation. Although there is no clear mode of action of TTA, it was established that TTA inhibits tumour necrosis endothelial cell activation.

Mechanistic thia-fatty acid probes previously synthesized provided significant information about the active site of desaturases.[35] The insertion of a sulfur atom in a fatty acid chain produces very little distortion and the chemical properties of thia-fatty acids are similar to those of the usual fatty acids.[39] However, thia-fatty acids may produce different metabolic effects, depending on the position of the sulfur atom within the fatty acid chain.[39]

In *Saccharomyces cerevisiae*, it was found that desaturation still occurs when thiastearic acids contained sulfur in the 5^{th}, 6^{th}, 7^{th}, 12^{th} and 13^{th} positions. However, when sulfur was substituted in the 8^{th}, 9^{th} , 10^{th} and 11^{th} positions, desaturation was inhibited.[39] Similarly, Hovik *et al.* demonstrated that 9- and 10-thia-fatty acids are strong inhibitors of Δ^9-desaturase in rats whereas desaturation in the presence of 3-thia fatty acids could still occur.[48]

Thia-fatty acids are useful as probes for the study of biochemical systems due to the bioisosteric nature of the sulfur atom with a methylene group.[49] It was shown by Funk *et al.* and Corey *et al.* that thia-fatty acids can act as enzyme inhibitors.[50,51] Funk *et al.* synthesized a range of sulfur-containing octadecanoic acid derivatives and concluded that these fatty acids inhibit oxygenation of linoleic acid. The thia-fatty acids synthesized by Corey *et al.* were evaluated as possible inhibitors of leukotriene synthesis to help control inflammation as well as allergic responses.

Pinilla *et al.* examined thia-fatty acids as tracers for the biosynthesis of moth sex pheromones.[49] A series of thiatetradecanoic acid derivatives were prepared and the metabolism of these derivatives evaluated in *Spodoptera littoralis*. The study determined that 8-thiatetradecanoic acid and 13-thiatetradecanoic acid were incorporated into the biosynthetic pathway and metabolized by desaturation. The 9, 10, 11 and 12-thiatetradecanoic acid was not metabolized and no S-oxidation products were observed from the GC-MS results obtained.

In addition to thia-fatty acids, fluoro and fluorothia-fatty acids were synthesized and used as mechanistic probes in *Saccharomyces cerevisiae* for the study of Δ^9-desaturase mediated oxidation.[35,52] ^{19}F NMR was successfully used as an analytical tool to monitor the unique chemical shifts of ω-fluorothia-fatty acids induced by the vicinal sulfur oxidation.

Labeled ^{18}F-4-thia-oleate and ^{18}F-6-thia-heptadecanoate were used as probes for positron emission topography of myocardial fatty acid oxidation imaging.[53] In this manner, these probes can play a major role in the fatty acid oxidation imaging in cardiovascular disorders, cancer and possibly neurology.

1.7.3. Analysis of fatty acids

The analysis of fatty acids often includes a derivatization step to a more stable fatty acid methyl ester (FAME) form. FAMEs are usually quantified using (GC) coupled to a mass spectrometer which allows for good fractionation.[54] The technique is sensitive and allows for detection at exceptionally low FAME quantities. The utilization of GC-MS allows not only for the separation of FAME but also allows one access to structural information and molecular mass data of individual FAMEs.[55]

Mayakova *et al*. successfully took advantage of GC-MS coupled with selective ion monitoring to study M.tb lipid extracts.[56] The results consisted of 13 fatty acids, including stearic acid. In addition to GC-MS, ^{1}H-decoupled and ^{19}F NMR can be used to study fluoro tagged thia-fatty acids.[57]

The exploitation of HPLC for the fractionation of fatty acids has increased due to the availability of Hilic columns as well as the lower temperatures required unlike GC. When using HPLC, the mobile phase can be modified to vary the potential retention times of fatty acids.[56]

In this review, thia-fatty acid derivatives have been reported as mechanistic probes as well as inhibitors to assess fatty acid metabolism in various organisms. As with fatty acids, cholesterol can also be utilized as a carbon and energy source by M.tb. The complete mode of action of the catabolism of cholesterol in M.tb has only recently come to light and the pathway has received a lot of attention as it lends itself to exploitation for possible new drug targets.

1.8. Cholesterol metabolism

1.8.1. Metabolism of cholesterol in humans

Cholesterol is a significant component in cellular membranes and plays an important role in mammals as it is a precursor for various steroid hormones such as androgens and progesterone that are crucial to the reproductive systems of males and females, respectively.[58] Essential substances like vitamin D_3 are also synthesized from cholesterol in

the presence of ultraviolet light.[58] The brain is the organ with the highest concentration of cholesterol and therefore regulation of cholesterol is critical for the functioning of the brain and the central nervous system.[59] Thus, cholesterol has been implicated in diseases such as Alzheimer"s, Huntington"s and Parkinson"s disease. Regulation of cholesterol is carried out through excretion *via* bile acids or conversion to oxysterols which increases the polarity and helps with transport to the plasma.[59] Cholesterol plays a vital role in gene transcription and the functioning of both the immune system and number of enzymes.[59] Cholesterol is obtained either through the diet or *de novo* synthesis *via* 21 steps which is initiated by acetate where the liver is believed to be the major source of newly synthesized cholesterol.[60] Disruption of cholesterol biosynthesis during pregnancy can cause Smith-Lemli-Opitz syndrome (SLOS) due to the lack of cholesterol availability to the fetus which causes abnormal development.[61] SLOS is an autosomal recessive disorder characterized by severe mental retardation and behavioural problems.[62] Cytochrome P450s (CYP450s) are enzymes that are responsible for the degradation of cholesterol into various biologically significant steroids. CYP450s are haem-containing monooxygenases and have various roles in different metabolic pathways with many implicated in the catabolism of steroids, fatty acids and other lipophilic compounds.[63,64] The name is derived from the unusual spectral properties of CYP450s which typically exhibit absorption at 450 nm due to the cysteine thiolate group present.[65] CYP450 was first discovered in mammalian liver but is also present in plants, fungi and bacteria.[61] CYP450s are divided into four classes based on the mode of electron transport from the NAD(P)H.[66] In humans, over 50 CYP450s have been identified and are key players in metabolism and detoxification of substances in the liver.[67] The metabolic fate of cholesterol in humans is outlined in Figure 1.12 and includes hormone precursors such as pregnenolone which is converted to progesterone and androgens as well as bile acids such as cholic acid and lithocholic acid. Cholesterol esters are stored in cells and are present in plasma where they get incorporated into lipoproteins.[68] The rest of the cholesterol gets excreted through bile either as bile acids or as cholesterol itself.

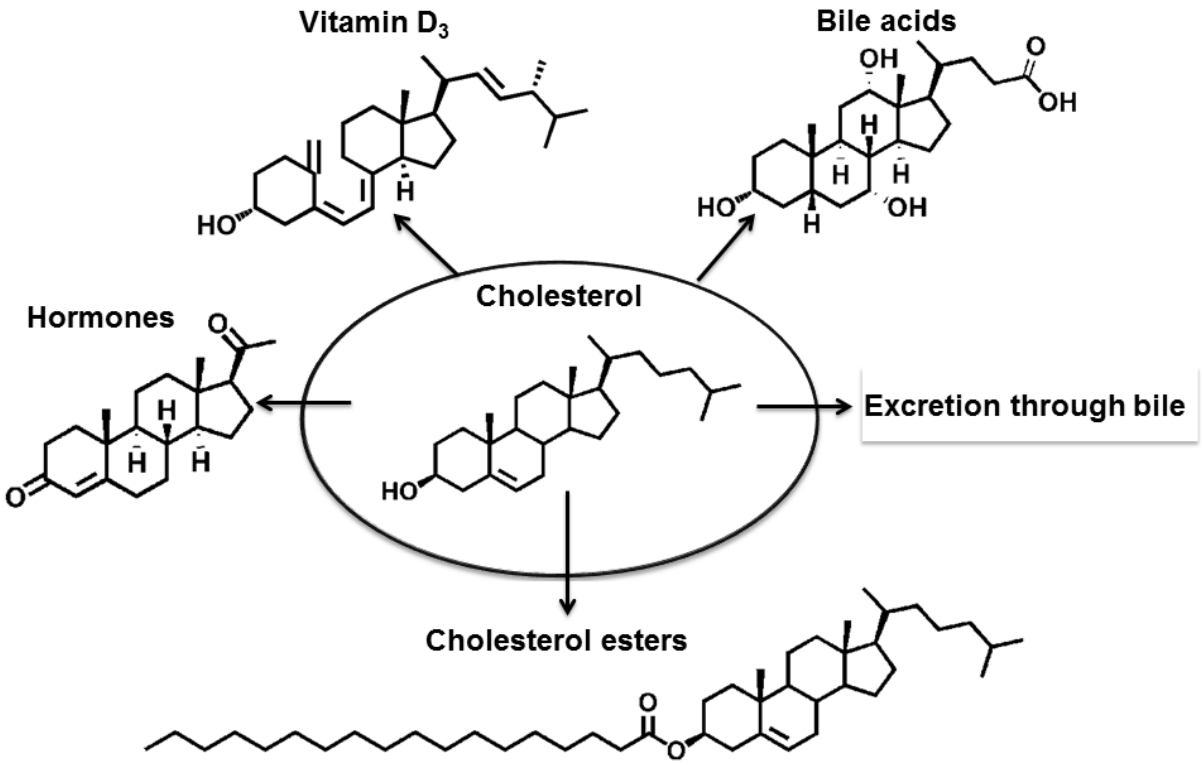

Figure 1.12: Cholesterol metabolism in humans.[60]

1.8.2. Mycobacterium tuberculosis and cholesterol

Cholesterol as a carbon source

Cholesterol and other naturally occurring sterols are abundant molecules in the environment and are therefore common carbon sources for a diverse range of microorganisms.[69] M.tb is one such organism that possesses the ability to use cholesterol as a carbon and energy source through catabolism.[70] The bacterium itself, however, does not synthesize its own cholesterol. M.tb adapts to the host environment by switching its metabolic pathways from carbohydrates to lipids during infection.[71] The ability of the organism to use nutrients from the host is but one mechanism that assists in the success of the pathogen.[72]

1.8.3. The role of cholesterol during host cell entry

M.tb has developed several techniques to gain entry into the host macrophage and *in vitro*, phagocytosis can occur through binding to multiple receptors.[73] In addition to binding to these receptors, M.tb can interact with cholesterol present in the plasma membrane of host cells.[74] Cholesterol plays a crucial role not only in the entry into macrophages, but also in the mediation of the phagosomal association of tryptophan-aspartate-containing coat protein (TACO) that prevents mycobacterial degradation in lysosomes.[75] Thus, M.tb entering macrophages at high cholesterol areas and delivery to lysosomes which in turn assist in the

survival of M.tb.[75] A human receptor, Ck, is responsible for regulating the transcriptional expression of a gene that codes for TACO.[75] Kaul *et al.* evaluated the presence of surface receptors in M.tb and found that the organism possesses a cholesterol-specific „Ck-like" receptor.[75] The study concluded that the interaction of the „Ck-like" receptor with the cholesterol-rich membrane helps to form a „synaptic-junction" between M.tb and the macrophage, resulting in signalling events that are responsible for entry into and survival within macrophages.

1.8.4. Cholesterol catabolism by M.tb

A catabolic pathway for cholesterol degradation was published by Ouellet *et al*.[76] The catabolism of cholesterol is carried out by CYP450 enzymes and consists of two steps:

- the degradation of the aliphatic side-chain and
- the degradation of the sterol rings.

The aliphatic chain is degraded by either CYP125 or CYP142 enzymes through a series of hydroxylation processes (Scheme 1.1). Sterol rings are degraded by enzymes such as KshA, KshB, HsaA, HsaB HsaC and HsaD (Scheme 1.3).

Side-chain degradation of cholesterol

Cholesterol catabolism is initiated by the conversion of cholesterol to cholest-4-en-3-one. This step is catalyzed by 3β-hydroxy-Δ(5)-steroid dehydrogenase (3β-HSD) or cholesterol oxidase.[63] Hydroxylation at C26 is required for side-chain degradation to occur which is followed by further oxidation to form the C26-oic acid. Degradation of the resulting acid occurs until C22-oic acid is formed. Propionyl-CoA and acetyl-CoA is released in the process. Propionyl-CoA serves as an important precursor for other biosynthetic pathways. However, the accumulation of propionyl-CoA is toxic to the bacterium.[77] Propionyl-CoA is therefore further metabolized *via* the methylmalonyl pathway and the methylcitrate cycle to form essential metabolic precursors. Once side-chain degradation is completed, 4-androstene-3,17-dione (AD) is formed and further ring degradation can occur. The side-chain degradation pathway is shown in Scheme 1.1.

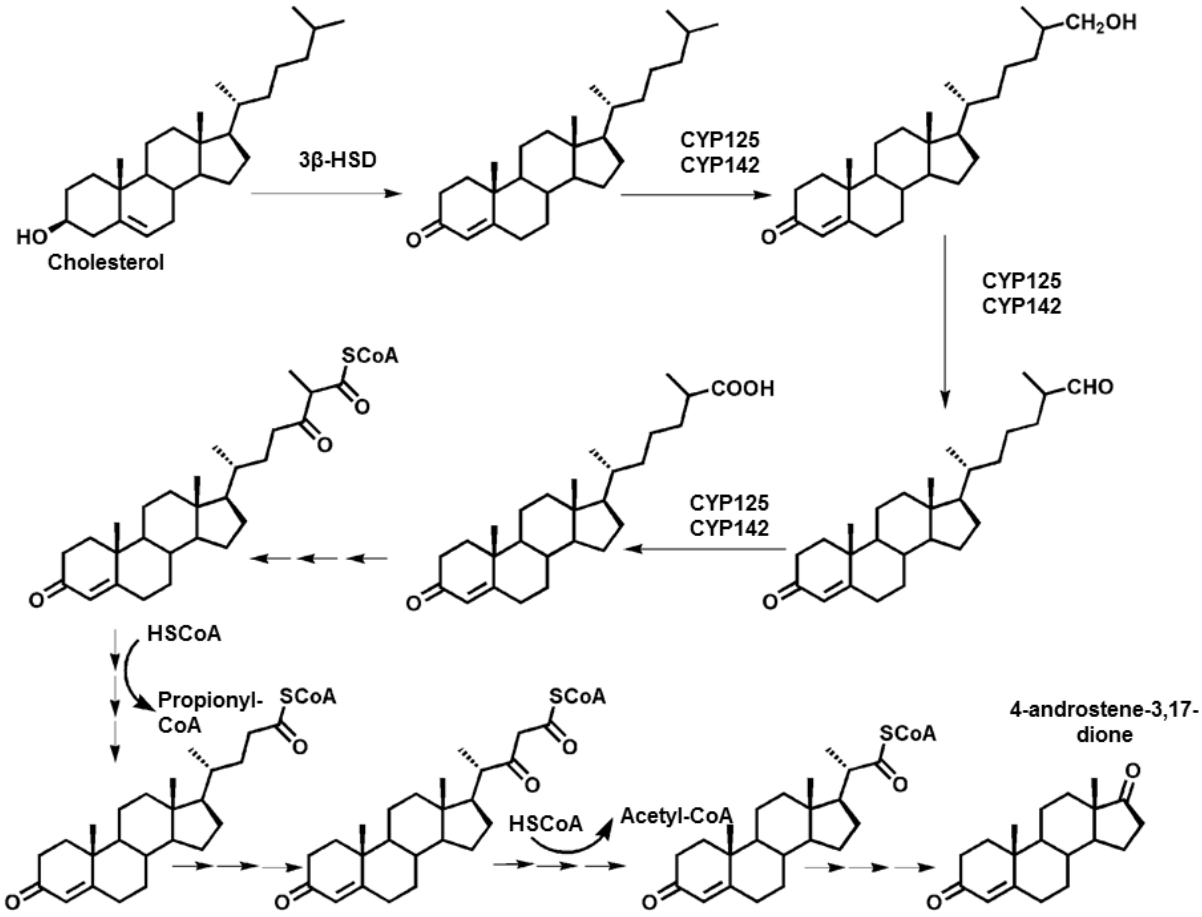

Scheme 1.1: Side-chain degradation of cholesterol.[76]

Cholesterol is a precursor for the synthesis of various signalling molecules that play a vital role in biological functions, such as metabolism and reproduction.[78] Dafachronic acid is a steroid hormone found in a nematode worm, *Caenorhabditis elegans* (C. elegans) and its presence is critical to ensuring that the worm develops into a reproductive adult.[78–81] Due to the short life span of *C. elegans*, geneticists have exploited it as a system of biological discovery for many years and thus holds scientific significance.[80,82] Cytochrome P450 proteins, DAF-9 and DAF-36 assist in the biosynthesis of dafachronic acids of both Δ^4 and Δ^7 (Scheme 1.2). Giroux and Corey reported the stereo-controlled synthesis of Δ^7-dafachronic acid which they called dafachronic acid A.[80] The synthesis was started with β-stigmasterol and was obtained through a 10-step synthesis. Due to the similarity in the chemical nature of dafachronic acids and the side-chain oxidation products of cholesterol catabolism, the cholesterol catabolism pathway is an alternative tool for the synthesis of such molecules for further biological evaluation.

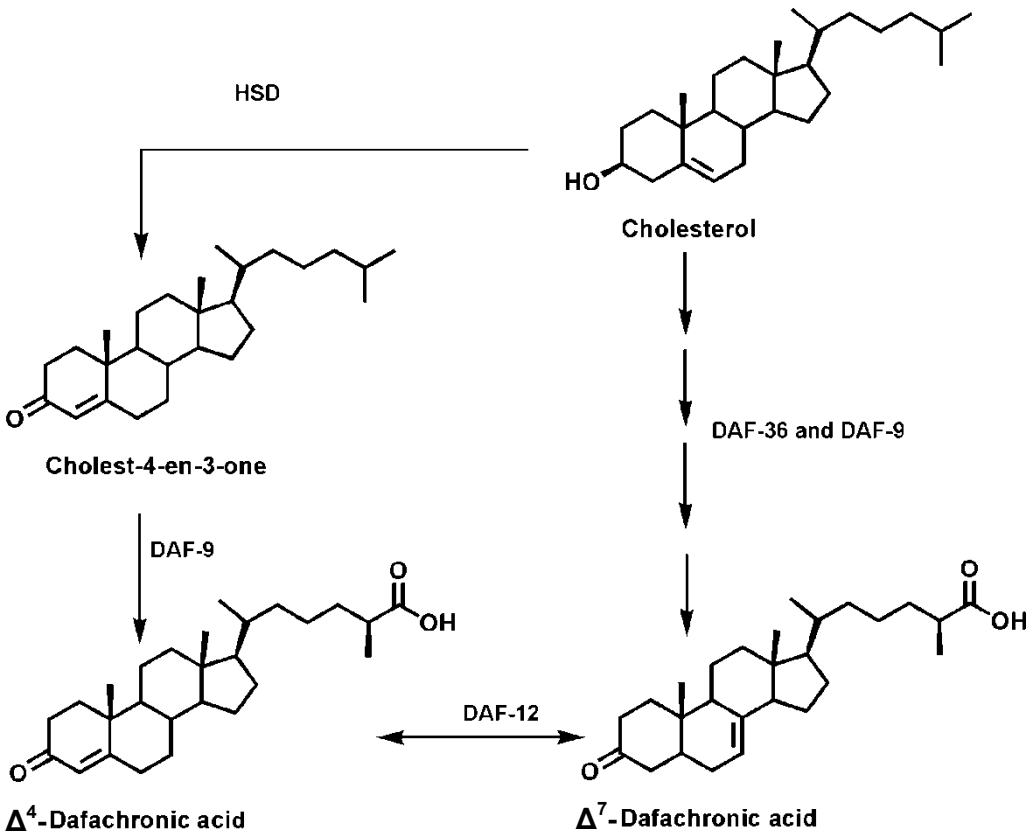

Scheme 1.2: Biosynthesis of dafachronic acids.[82]

Ring degradation of cholesterol

KstD is a protein that catalyzes the trans-axial elimination of hydrogen at C1 and C2 in the A-ring of 3-ketosteroids.[76] The product of side-chain degradation, 4-androstene-3,17-dione (AD) is derivatized to 1,4-androstenediene-3,17-dione (ADD) from the action of KstD. The activity of KstD can also act on derivatives with partially degraded side-chains. The oxygenases, KshA and KshB, uses oxygen and NADH to open up ring B and aromatize ring A to form 3-hydroxy-9,10-seco-androst-1,3,5-triene-9,17-dione (3-HSA). HsaA and HsaB proteins are responsible for hydroxylating 3-HSA to form 3,4-dihydroxy-9,10-seco-androst-1,3,5-triene-9,17-dione (3,4-DHSA). The next step involves HsaC and is dependent on iron and oxygenates and cleaves 3,4-DHSA to 4,5-9,10-diseco-3-hydroxy-5,9,17-trioxoandrosta-1,2-diene-4-oic acid (4,9-DSHA). HsaD cleaves carbon-carbon bonds of 4,9-DSHA to form 9,17-dioxo-1,2,3,4,10,19-hexanorandrostan-5-oic acid (DOHNAA) and 2-hydroxy-hexy-2,4-dienoic acid (HHD). HHD is eventually converted to propionyl-CoA and pyruvate.[76] Until recently, it was unknown whether DOHNAA is further catabolized. According to Casabon *et al*. DOHNAA is further catabolized by FadD3 to the CoA-derivative

and unlike KstD, FadD3 does not transform metabolites with incomplete side-chain degradation.[83] The ring degradation pathway of ADD is shown in Scheme 1.3.

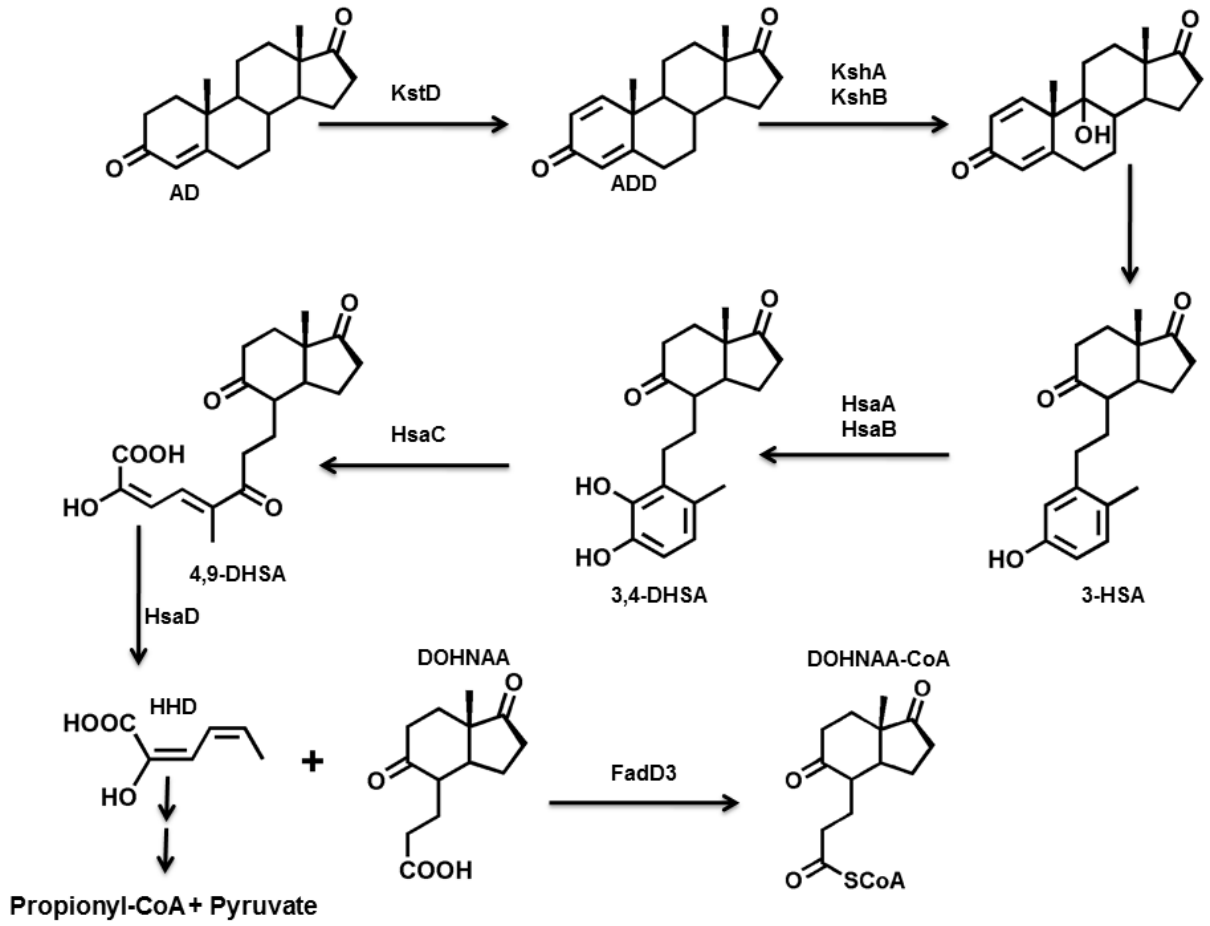

Scheme 1.3: Ring degradation of cholesterol.[76]

The CYP450s involved in the catabolism of cholesterol in M.tb have different amino acid sequences as compared to those found in humans, and therefore make excellent drug targets.[84] Compared to the 57 CYP450s found in humans, 20 have been identified in M.tb which is a significant number as it is relatively rare in other bacteria.[84,85] McLean *et al.* isolated the CYP125 cytochrome and demonstrated the role of CYP125 in the hydroxylation of cholesterol at C26 and hence degradation of the cholesterol side-chain.[86]

Binding of cholesterol to CYP125

The haem co-factor of CYP125 is present between helical sheets and the active site cavity approaching the haem. A CYP125-cholesterol complex was modeled and the structure is shown in Figure 1.13.[86] The most favourable conformation was where the alkyl chain of cholesterol appears towards the haem, with C26 positioned towards the haem iron. Residues within the active site pocket of CYP125 include Ile 97, Leu 117, Val 267, Phe 316

and Trp 414. The hydrophobic nature of these amino acids allows for interaction with the hydrophobic cholesterol, which aids in the stabilization of the CYP125-cholesterol complex.

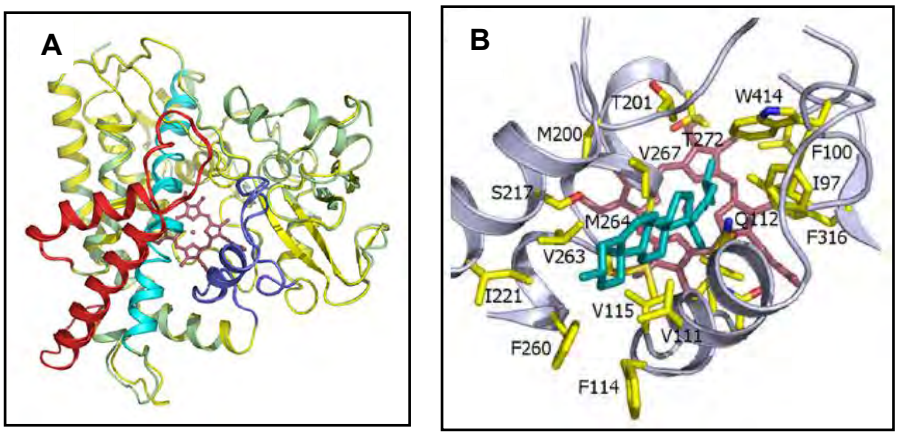

Figure 1.13: Crystal structures of A: CYP125 and B: CYP125-cholesterol complex.[86]

The importance of the 3β-OH of cholesterol to the binding with CYP125

The binding of 3β-cholesterol derivatives to CYP450 was investigated by Heyl *et al.*[87] They demonstrated that the group at the C3 is required to have an appropriate stereochemistry. Cholesterol contains a 3β-hydroxyl and binds to the CYP125 enzyme, whereas epi-cholesterol contains a 3α-hydroxyl and does not bind to the enzyme. Binding of cholesterol is limited to the size of the substituent at the 3β-position. Hydrogen bonding at this position was found not to be a necessity, although bonding of the β-oxygen is a requirement. The 3β-position was modified and the binding of these derivatives analyzed as a function of the 3β-substituent. These 3β-cholesterol derivatives include 3β-thiocholesterol and 3β-chlorocholesterol and no binding was observed with CYP125.

1.8.5. Cholesterol catabolism inhibitors

The cholesterol catabolism pathway has great potential as a drug target as inhibition of the pathway can lead to deprivation of carbon and eventually cell death.[76]

Antifungal azole drugs

Antifungal azole drugs have been shown to have antimycobacterial activity.[76] Ahmad *et al.* illustrated that clotrimazole and econazole (Figure 1.14) have effective antimycobacterial activity.[88] It has been proposed that the azole drugs inhibit cholesterol metabolism by targeting the P450 enzymes (CYP125, CYP142 and CYP124). These enzymes are responsible for catalyzing the side chain degradation of cholesterol. The azole drugs showed a synergistic effect when used in conjunction with RMP and INH. Azole drugs, especially

econazole, demonstrated antimycobacterial activity against both dormant and multidrug resistant strains.[76]

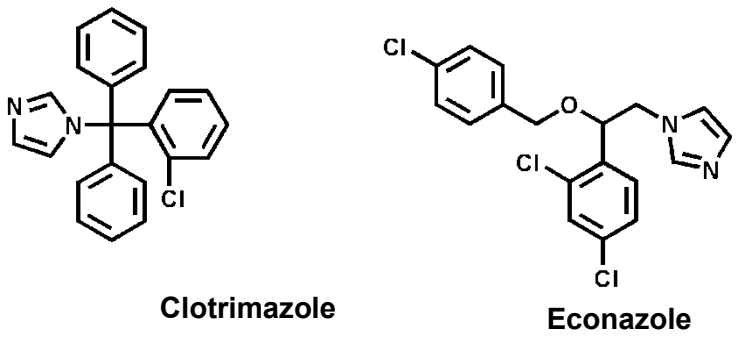

Clotrimazole **Econazole**

Figure 1.14: *Chemical structures of clotrimazole and econazole.*[76]

Azasteroids

Thomas *et al.* synthesized a range of 6-azasteroids and 4-azasteroids with various side chain modifications.[89] The study concluded that the 6-azasteroids (Figure 1.15) were the best inhibitors with an indication of strong competitive binding to 3β-HSD which is responsible for initiating cholesterol catabolism.

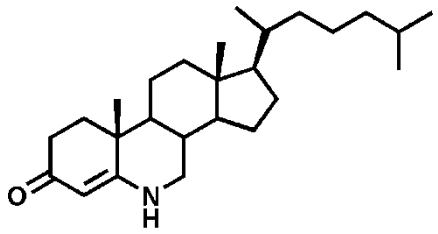

Figure 1.15: *Chemical structure of a 6-azasteroid.*[89]

Thiacholesterol derivatives

Previous utilization of (*20S, 22R*)-22-thiacholesterol (Figure 1.16) as a mechanistic probe revealed the diastereoselective conversion to (*20S,22R*)-22-thiacholesterol S-oxide.[90] The oxygen of the oxide then binds to the active site of the P450 haem, thus blocking further interaction with competitive substrates and inhibiting cholesterol catabolism.

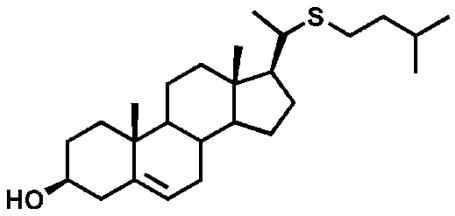

Figure 1.16: *Chemical structure of a* (*20S, 22R*)-22-thiacholesterol.[90]

Other steroid derivatives

Antinarelli *et al.* synthesized a range of conjugated aminoquinoline steroid derivatives and tested the activity of these compounds against both Leishmaniasis disease and TB.[91] Quinolines are extensively used as antimalarial agents and have shown activity against both HIV and TB. Due to the favourable properties of steroids as drug carriers, aminoquinoline steroid conjugates have been synthesized. These conjugates have improved antimycobacterial activity as compared to the native quinoline with MIC values comparable to current antituberculosis drugs.

Although the cholesterol catabolic pathway holds promise as a good drug target, much can be gained by exploiting the pathway for commercial purposes.

1.8.6. Commercial exploitation of bacterial cholesterol catabolism

As already mentioned, cholesterol is one of the most common steroids in nature and is therefore a common carbon source for many microorganisms, including M.tb.[92] As a result, much attention has been drawn to utilizing cholesterol degradation by bacteria as an economical route for the synthesis of bioactive molecules.[92] Possible biotechnological applications include biosensors for cholesterol analysis, bioconversions of regio- and stereoselective steroids and diagnosis of lipid disorders by cholesterol oxidases.[92–94]

1.8.6.1. Biotechnological applications of bacterial enzymatic processes

Steroids play a significant role in the pharmaceutical industry and are used as various drugs and hormones.[95] The synthesis of such steroids requires regio- and stereoselective production with selective side-chain cleavage.[96] The result of chemical reactions often leads to a low conversion rate with little economical turnover and the production of various unwanted by-products. Microbial biotransformation holds a cost-effective alternative with greater conversion rates, is non-toxic and less time consuming.[96]

Applications of Cholesterol Oxidase

Cholesterol oxidase is an enzyme that catalyzes the initial step in cholesterol catabolism, converting cholesterol to cholestenone.[97] This enzyme catalyzes the conversion of 3β-OH steroids to the keto-derivative and subsequent isomerization of $\Delta^5 \rightarrow \Delta^4$ steroids. Cholesterol oxidase is produced by both pathogenic- and non-pathogenic bacteria. Pathogenic bacteria utilize cholesterol oxidase for host cell infection and cholesterol catabolism, while non-pathogenic bacteria require cholesterol oxidase for cholesterol catabolism. Cholesterol oxidase is found only in microorganisms and holds applications both clinically and industrially. Clinically, cholesterol oxidase is used to determine total cholesterol in biological samples and is used as a tool for diagnosis of lipid disorders such as atherosclerosis and hypercholesterimia.[93] The activity of cholesterol oxidase as a biosensor was evaluated and an analytical method established with the assistance of HPLC for the quantitation of cholesterol in cultured cells.[98] Cholesterol oxidase is often used as a biocatalyst to catalyze conversion of cholesterol along with other steroids that, for example, can be utilized as standards for structure determination of steroids synthesized by patients suffering from SLOS.[99] Due to the conversion properties of cholesterol oxidase, it has the ability to alter cell membranes and can therefore be used in the treatment of bacterial infections.[93] Industrially, cholesterol oxidase is used as an insecticidal. Cotton boll weevil (*Anthonum grandis*) is a beetle that is difficult to control on account of the lack of direct contact with chemical sprays. Cholesterol oxidase has potent activity by causing developmental arrest and death as well as fecundity of female boll weevil larvae.[100]

1.8.7. Analysis of steroids

Steroids are traditionally extracted from solid material by organic solvents followed by grinding, freeze-drying or homogenization.[101] Subsequent purification using liquid-liquid extraction or solid-phase extraction provide extracts for analysis using GC-MS, LC-MS, HPLC and/or NMR.[102]

NMR is widely used for the analysis of steroids. High field resolution (>400 MHz) is required for proper analysis as CH_2 and CH groups appear as a cluster in the range of 0.5 – 2.5 ppm in the ^{1}H NMR. However, the use of 2-D NMR can help with the complete analysis of novel steroid compounds.

GC-MS and LC-MS analyses remain as the preferred tools for the characterization of steroids. These techniques allow for detection and identification of both known and unknown steroids.

A GC-MS program was developed by Amaral *et al.* to quantify steroids present in amniotic fluids.[102] These steroids include cholesterol, 7-dehydroxycholesterol, desmosterol, lathosterol and sitosterol.[103] Lamb *et al.* studied the sterol biosynthetic pathway in M.smeg by analyzing the lipid extract by GC-MS.[104] LC-MS analysis allowed for analysis of cholesterol and cholesteryl esters at 1ng/mL quantities.[105] Fluorescent probes synthesized and analyzed by LC-MS allowed for detection of conversion products for cholesterol-converting oxidoreductases.[106]

The use of HPLC for the analysis of steroids remains favourable due to the lower temperatures required. Mast *et al.* studied the binding of cholesterol and a triol-cholestane derivative to CYP450 and used HPLC to identify the conversion products present as a result of binding.[106]

Biosynthesis of cholesterol in humans is vital as it plays a major role in maintaining the fluidity of cell membranes. Cholesterol is also important in the homeostasis of the central nervous system as poor regulation of cholesterol can lead to various diseases. On the contrary, catabolism of cholesterol occurs in M.tb exploiting the presence of host lipids such as cholesterol and fatty acids as a sole carbon and energy source. Due to the importance of the various lipid metabolic pathways for the existence and success of M.tb growth and virulence, molecular biomarkers or internal standards can be synthesized as bioanalytical tools to assess specific activity of molecular targets within these pathways.

1.9. Aims and Objectives

1.9.1. General Aims

The utilization of biomarkers and internal standards is valuable in the field of lipidomics for efficient, qualitative bioanalysis of key metabolic processes in mammals and pathogenic organisms such as M.tb. Therefore, the aim is to synthesize thia-, fluoro- and deuterium labeled cholesterol derivatives as well as thiastearic acid derivatives and establish a protocol to evaluate these derivatives as mechanistic probes for lipid metabolism in M.tb and M.smeg. Establishing such tools would allow for identification of metabolically processed metabolites within a specific pathway. Previously, thiastearic acid derivatives were synthesized and evaluated as both probes and inhibitors in protozoan species, rats and hepatoma cells.[37,107–109] However, the utilization of such molecules has not been exploited in M.tb. Thus, another aim is to evaluate the catabolism of thiastearic acid in M.tb and M.smeg, respectively. Similarly, thia-steroid derivatives have been used to probe the CYP450 enzymes in *Rhodococcus jostii RHA1* and bovine adrenal as well as evaluated as inhibitors of growth of *Candida albicans* but have not been assessed for steroid metabolism in M.tb.[63,110,111]

1.9.2. Specific Objectives

The specific objectives of this study are outlined as follows;

- Synthesize and characterize a range of fluoro, thia- and deuterium labeled cholesterol and stearic acid derivatives.
- Evaluate synthesized molecules as internal standards for GCMS, whereby natural molecule modification entails a substitution of a methylene group ($-CH_2-$) for a sulfur atom (-S-). Thus providing a mass increase of 18amu for the thia-derivative amenable to S-oxidation to further help establish identity after extraction from a complex matrix.
- Establish whether the compounds synthesized can be utilized as carbon sources by M.tb and M.smeg, respectively, and hence, serve as potential biomarkers.
- Establish a tool to evaluate whether cholesterol side-chain degradation can occur while blocking 3β-HSD activity.
- Evaluate synthesized compounds as potential downstream catabolic pathway inhibitors (prodrugs).
- Deliberately inhibit enzyme activity using azole drugs in the presence of steroids in a cell-free system.

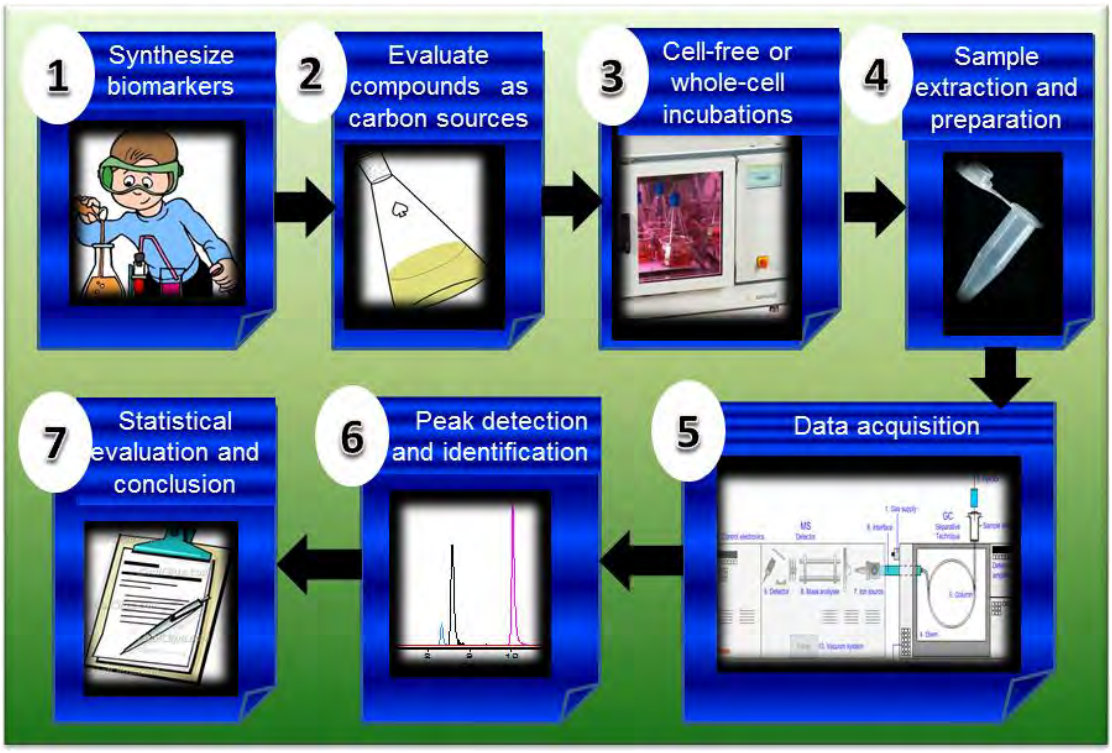

Scheme 1.4: *Objectives of the current study.*[112–114]

1.9.3. Cholesterol derivatives

Based on the proposed catabolic pathway of cholesterol (Scheme 1.1 and Scheme 1.3), the possible degradation of the synthesized compounds and the proposed metabolically produced products are shown in the figures (Figure 1.17 – Figure 1.20) to follow.

The action of 3β-HSD was prevented by blocking the 3β-position of cholesterol. The compound 3β-mercaptocholest-5-ene was synthesized to evaluate whether side-chain degradation can still occur. If side-chain degradation does occur in the absence of 3β-HSD activity, the side-chain of 3β-mercaptocholest-5-ene is expected to become oxidized to form products such as C26-OH and C26-COOH as shown in Figure 1.17. Further degradation can also occur with products consisting of the C22-oic acid.

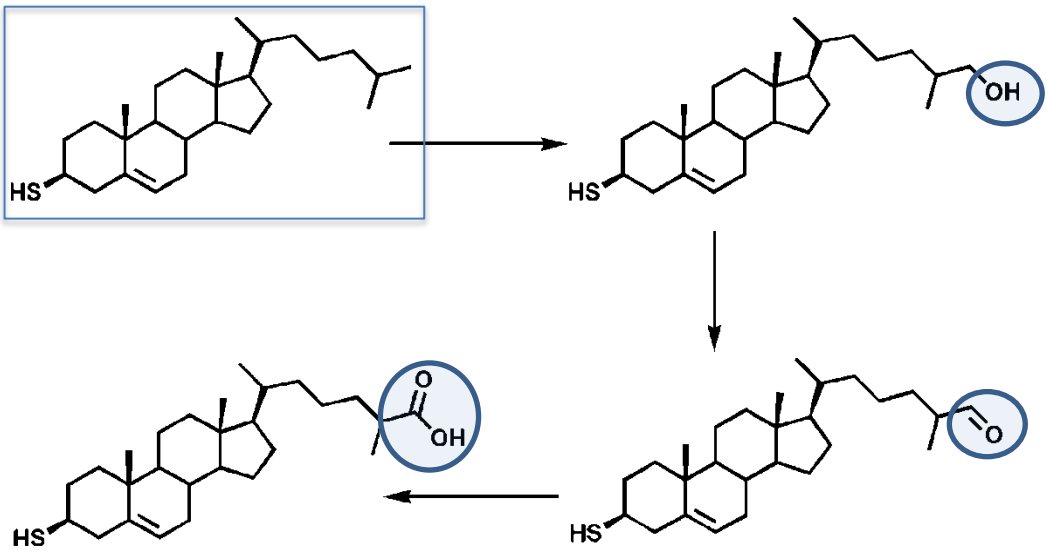

Figure 1.17: *Expected oxidation products of 3β-mercaptocholest-5-ene.*

From the cholesterol catabolic pathway (Scheme 1.1 and Scheme 1.3) side-chain oxidation occurs at even numbered positions (C22 and C24). Substitution of sulfur in position C22 was shown to inhibit the P450 enzymes, possibly due to the oxidation product itself; i.e. the sulfoxide.[110] To prevent possible inhibition, a sulfur atom was substituted in an odd position (C23) which will potentially allow the catabolic pathway to be followed further downstream. The 23-thiacholesterol derivatives (Figure 1.18) synthesized was expected to enzymatically form the keto-derivative as well as similar hydroxylation products at C26 as shown above.

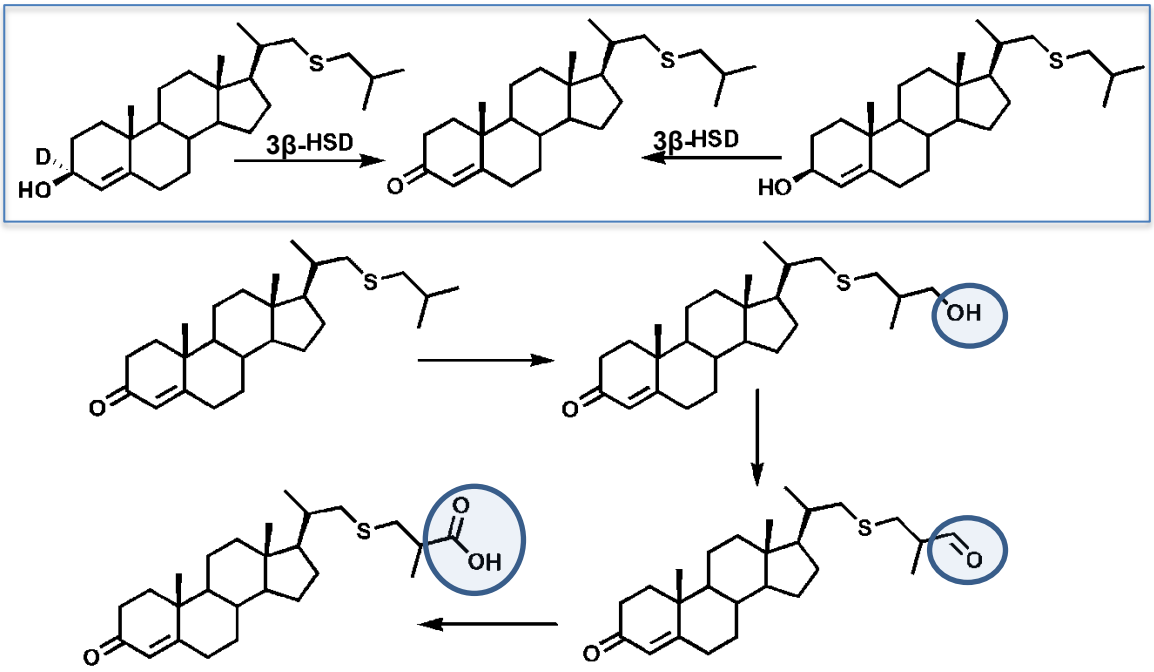

Figure 1.18: *Expected oxidation of 23-thiacholesterol derivatives.*

The fluoro-derivatives synthesized are shown in Figure 1.19 and Figure 1.20. The presence of a fluorine atom allows for ^{19}F NMR analysis of the cell-free extracts by monitoring the possible chemical shifts as a consequence of the formation of oxidation products. Due to the presence of a 3α-group of 3α-fluorocholest-5-ene, the activity of 3β-HSD is expected to be inhibited. However, side-chain degradation can still be evaluated and C26-OH, C26-CO and C26-COOH products are expected to form.

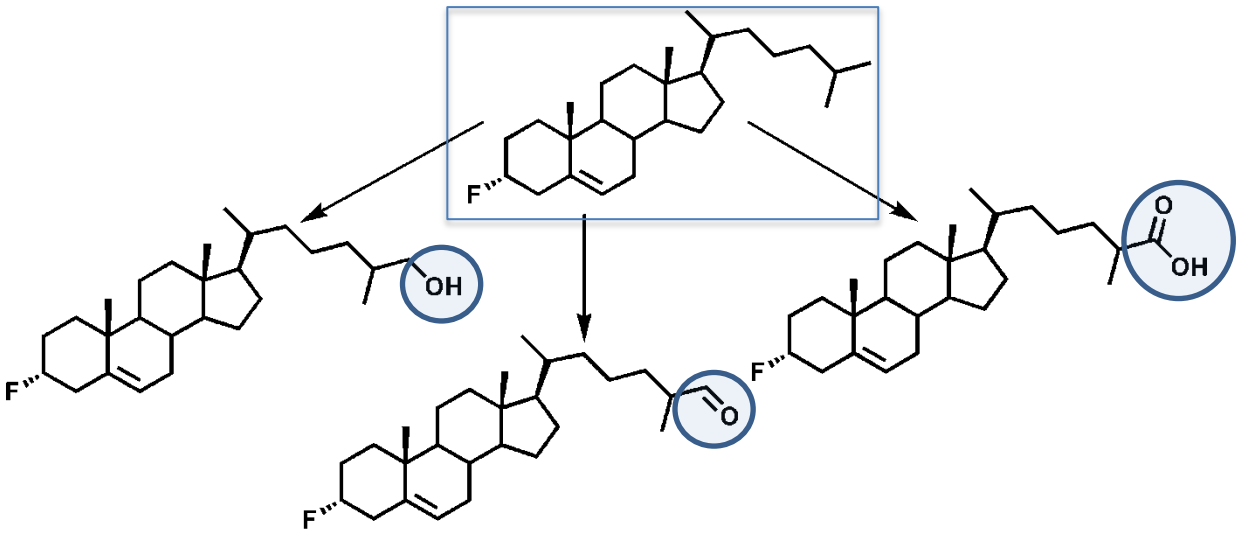

Figure 1.19: *Expected oxidation products of 3α-fluorocholest-5-ene.*

6β-Fluorocholestan-3β,5α-diol holds the advantage of the presence of a fluorine atom in position C6. Previous evaluation of 6-fluoro-steroids indicated highly biologically activated compounds of corticoids with activity exceptionally higher than the native cortisone.[115] Other 6-fluoro steroids include a series of 6-fluoroprogesterone derivatives synthesized by Bowers *et al*.[116] The study evaluated these compounds as alternative contraceptive agents as well as hormones for use in reproductive and obstetric dysfunctions. Biological activity revealed that together with the presence of the fluorine atom at C6 and the introduction of double bonds, enhanced activity was observed. In the current study, 6β-fluorocholestan-3β,5α-diol is evaluated as an alternative carbon source for M.tb and M.smeg in an attempt to pin point the fate of this compound as a result of catabolism. Due to the activity of 3β-HSD, 6β-fluorocholestan-3β,5α-diol is expected to be oxidized to 6β-fluorocholest-4-en-3-one (Figure 1.20). Bowers *et al.* synthesized the progesterone derivatives of both the hydroxyl and the ketone compounds, which were evaluated as oral progestational agents.[116] The hydroxyl compound was oxidized *via* two steps using CrO_3 and HCl/HOAc. The advantage of enzymatic oxidation is that only one step is required and is environmentally benign. The cholesterol catabolic pathway of *Mycobacteria* therefore holds for the possibility for the "green" synthesis of 6β-fluoro keto-steroids.

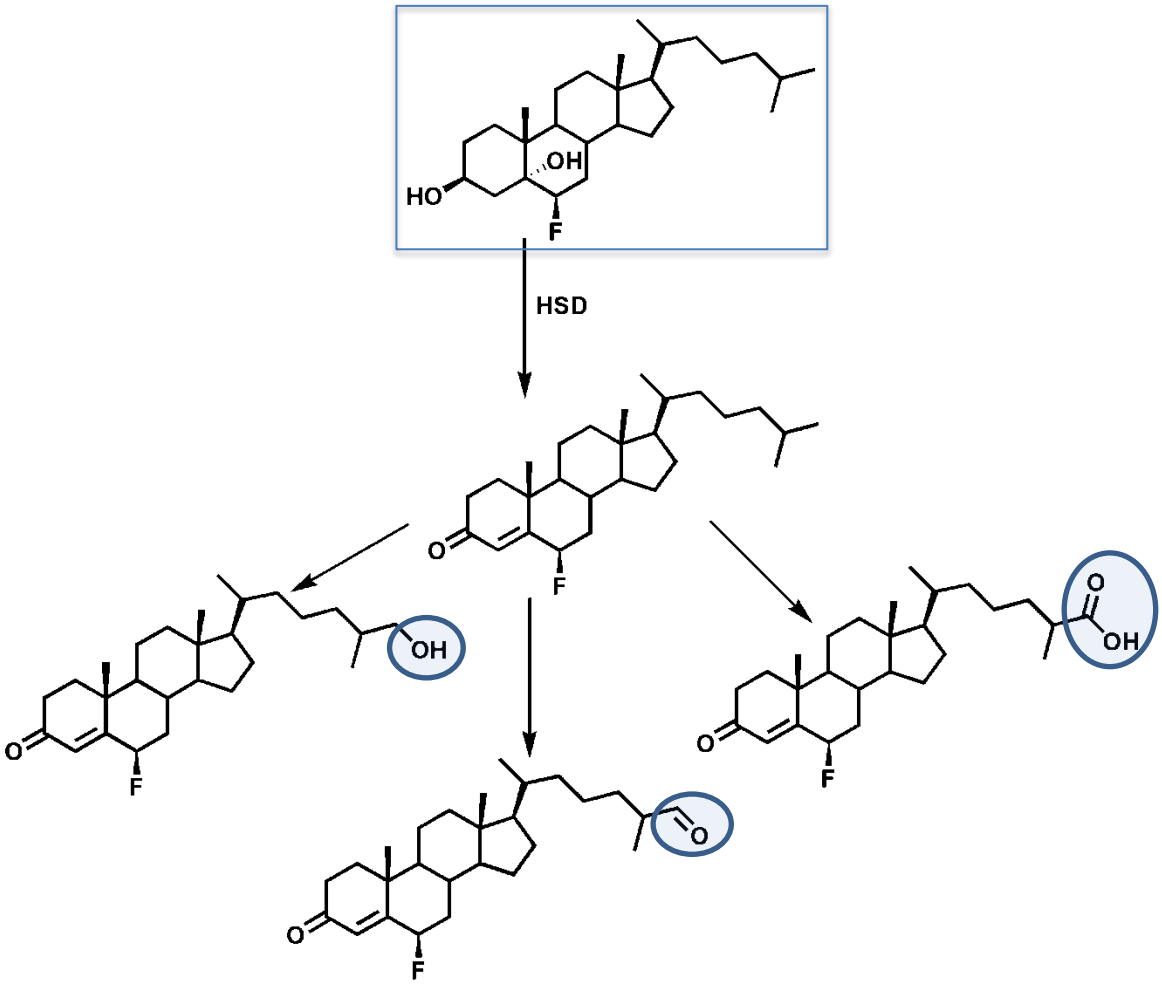

Figure 1.20: *Possible catabolic products of fluoro-cholesterol derivatives.*[117,118]

1.9.4. Stearic acid derivatives

Due to the higher content of stearic acid in M.tb, stearic acid is a favourite substrate for desaturation and was therefore chosen to be derivatized to various thiastearic acid derivatives (Figure 1.21) to be evaluated as potential molecular probes. Fatty acids play a vital role in the synthesis of mycolic acids, thus utilization of probes to establish a method of detection and analysis would aid in establishing more specific drug targets. Previous evaluation of various thiastearic acids revealed that 9-thiastearic acid was a poor inhibitor of *Trypanosoma cruzi* growth while 10-thiastearic acid displayed good inhibition. The poor inhibition activity of 9-thiastearic acid suggests that it can possibly be employed to probe fatty acid desaturases and establish the fate of stearic acid.[119] In Morris hepatoma cells, however, both 9-thiastearic acid and 10-thiastearic acid allowed binding to the desaturase to produce the thia-fatty acid sulfoxide (Figure 1.21), which prevented desaturation from taking place and therefore resulted in good inhibition.[48] Rahman *et al.* studied 9-, 10- and 11-thiastearic acid as inhibitors of *Crithidia fasciculate* growth and found that 10- and

11-thiastearic acid inhibited the growth of the protozoan.[108] The synthesis of thia-fatty acids is well established and its utilization has been exploited in various microorganisms. However, the evaluation of such markers in M.tb has yet to be exploited. In this study, the aim is to synthesize thiastearic acids and their sulfoxide derivatives and evaluate the potential of these compounds as mechanistic probes in M.tb and M.smeg.

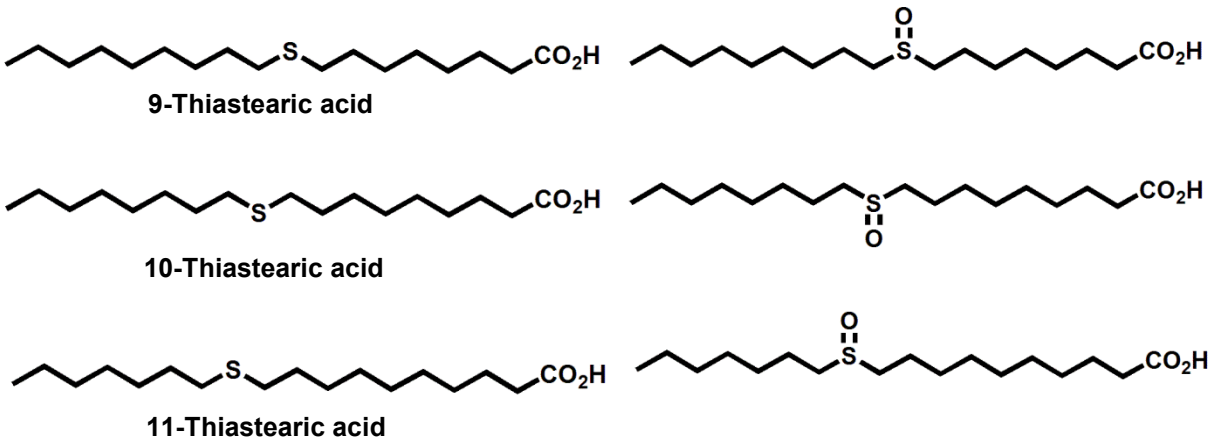

Figure 1.21: *Thiastearic acids and .sulfoxide derivatives.*[57,108]

1.10. References

1. L. Kumar and V. Sharma, *Asian J. Pharm. Res*, 2012, **2**, 59–62.

2. A. Brzostek, B. Dziadek, A. Rumijowska-Galewicz, J. Pawelczyk and J. Dziadek, *FEMS Microbiol. lett.*, 2007, **275**, 106–112.

3. World Health Organisation, *Global Tuberculosis Control*, World Health Organisation, Geneva, 2012.

4. V. Briken, S. A. Porcelli, G. S. Besra and L. Kremer, *Mol. Microbiol.*, 2004, **53**, 391–403.

5. G. Kaiser, *Doc Kaiser's Microbiol.*, http://faculty.ccbcmd.edu/courses/bio141/labmanua/lab16/diseases/mtuberculosis/u1fig11.html, 2005, (Accessed February 2012).

6. L. A. Davidson and K. Takayama, *Notes*, 1979, **16**, 104–105.

7. E. Dubnau, J. Chan, C. Raynaud, V. P. Mohan and M. Lane, *Mol. Microbiol.*, 2000, **36**, 630–637.

8. E. K. Schroeder, O. N. de Souza, D. S. Santos, J. S. Blanchard and L. A. Basso, *Curr. Pharm. Biotechnol.*, 2010, **3**, 197–225.

9. L. Kremer, W. N. Maughan, R. A. Wilson, L. G. Dover and G. S. Besra, *Lett. Appl. Microbiol.*, 2002, **34**, 233–237.

10. S. I. Bentley-Hibbert, X. Quan, T. Newman, H. P. Godfrey, X. I. N. Quan and K. Huygen, *Infect. Immun.*, 1999, **67**, 581–588.

11. H. Huygen, J. Conten, O. Denis, D. L. Montgomery, A. M. Yawman, R. R. Deck, C. M. DeWitt, I. M. Orme, S. Baldwin, C. D'Souza, A. Drowart, E. Lozes, P. Vandenbussche, J. Van Vooren, M. A. Liu and J. B. Ulmer, *Nat. Med.*, 1996, **2**, 893–898.

12. Y. L. Janin, *Bioorg. Med. Chem.*, 2007, **15**, 2479–2513.

13. F. Bardou, C. Raynaud, C. Ramos, M. A. Laneelle and G. Laneelle, *Microbiology*, 1998, **144**, 2539–2544.

14. C. Vilcheze, H. R. Morbidoni, T. R. Weisbrod, H. Iwamoto, M. Kuo, J. C. Sacchettini and W. R. Jacobs, *J. Bacteriol.*, 2000, **182**, 4059–4067.

15. I. Chopra and P. Brennan, *Tuber. Lung Dis.*, 1998, **78**, 89–98.

16. K. Mdluli, R. A. Slayden, Y. Zhu, S. Ramaswamy, X. Pan, D. Mead, D. D. Crane, J. M. Musser and C. E. Barry, *Science*, 1998, **280**, 1607–1610.

17. A. Somoskovi, L. M. Parsons and M. Salfinger, *Respir. Res.*, 2001, **2**, 164–168.

18. B. Phetsuksiri, M. Jackson, H. Scherman, M. McNeil, G. S. Besra, A. R. Baulard, R. A. Slayden, A. E. DeBarber, C. E. Barry, M. S. Baird, D. C. Crick and P. J. Brennan, *J. Biol. Chem.*, 2003, **278**, 53123–53130.

19. B. Urbancik, *Tubercle*, 1966, **47**, 283–288.

20. E. J. Muñoz-Elías and J. D. McKinney, *Nat. Med.*, 2005, **11**, 638–644.

21. J. W. Campbell and J. E. Cronan, *Annu. Rev. Microbiol.*, 2001, **55**, 305–332.

22. Y. M. Zhang, S. W. White and C. O. Rock, *J. Biol. Chem.*, 2006, **281**, 17541–17544.

23. D. J. Payne, P. V Warren, D. J. Holmes, Y. Ji and J. T. Lonsdale, *Drug Discov. Today*, 2001, **6**, 537–544.

24. N. M. Parrish, T. Houston, P. B. Jones, J. D. Dick and C. Townsend, *Antimicrob. Agents Chemother.*, 2001, **45**, 1143–1150.

25. A. Bhatt, V. Molle, G. S. Besra, W. R. Jacobs and L. Kremer, *Mol. Microbiol.*, 2007, **64**, 1442–1454.

26. N. M. Parrish, C. G. Ko and J. D. Dick, *Tuberculosis*, 2009, **89**, 325–327.

27. F. Titgemeyer, J. Amon, S. Parche, M. Mahfoud, J. Bail, M. Schlicht, N. Rehm, D. Hillmann, J. Stephan, B. Walter, A. Burkovski and M. Niederweis, *J. Bacteriol.*, 2007, **189**, 5903–5915.

28. A. Miczak, B. Chen, E. J. Mun, W. Chan, D. Swenson, J. C. Sacchettinik, W. R. Jacobs and D. G. Russell, *Nature*, 2000, **261**, 735–738.

29. J. Shanklin and E. B. Cahoon, *Annu. Rev. Plant Physiol. Plant Mol. Biol.*, 1998, **49**, 611–641.

30. K. Hashimoto, *Synthesis*, 2006, **17**, 173–183.

31. J. M. Ntambi, *J. Lipid Res.*, 1999, **40**, 1549–1558.

32. J. M. Ntambi and M. Miyazaki, *Curr. Opin. Lipidol.*, 2003, **14**, 255–261.

33. B. Behrouzian and P. H. Buist, *Prostag. Leukotr. Ess.*, 2003, **68**, 107–112.

34. A. E. Tremblay, N. Tan, E. Whittle, D. J. Hodgson, B. Dawson, P. H. Buist and J. Shanklin, *Society*, 2010, **3**, 1322–1328.

35. J. Hodgson, K. Y. Y. Lao, B. Dawson and P. H. Buist, *Helv. Chim. Acta*, 2003, **86**, 3688–3697.

36. R. A. Pascal, S. J. Mannarelli and D. L. Ziering, *J. Biol. Chem.*, 1986, **261**, 12441–12443.

37. E. Hvattum, S. Skrede, J. Bremer and M. Solbakken, *Biochem. J.*, 1992, **286**, 879–887.

38. L. Froyland, L. Madsen, W. Sjursen, A. Garras, O. Lie, J. Songstad, A. C. Rustan and R. K. Berge, *J. Lipid Res.*, 1997, **38**, 1522–1534.

39. S. Skrede, H. N. Sorensen, L. N. Larsen, H. H. Steineger, K. Hovik, O. S. Spydevold, R. Horn and J. Bremer, *Biochim. Biophys. Acta*, 1997, **1344**, 115–131.

40. J. Resemann and R. Carle, *J. Food. Agric. Environ.*, 2003, **1**, 104–111.

41. V. M. Dembitsky, S. Abu-Lafi and L. O. Hanuš, *Acta Chromatograhica*, 2007, 206–216.

42. R. C. Wijesundera and A. G, *J. Am. Oil Chem. Soc.*, 1988, **65**, 959–963.

43. M. J. Pitt, C. J. Easton, A. Ferrante, A. Poulos and D. A. Rathjen, *Chem. Phys. Lipids*, 1998, **92**, 63–69.

44. V. M. Dembitsky and M. Srebnik, *Prog. Lipid Res.*, 2002, **41**, 315–367.

45. P. Wu and J. Bremer, *Biochim Biophys Acta.*, 1994, **1215**, 87–92.

46. S. Lau, R. K. Brantley and C. Thorpe, *Biochemistry*, 1988, **27**, 5089–5095.

47. E. Dyroy, A. Yndestad, T. Ueland, B. Halvorsen, J. K. Damås, P. Aukrust and R. K. Berge, *J. Am. Hear. Assoc.*, 2005, **25**, 1364–1369.

48. K. E. Hovik, O. S. Spydevold and J. Bremer, *Biochim Biophys Acta.*, 1997, **1348**, 251–256.

49. A. Pinilla, E. Mas, F. Camps and G. Fabria, *Insect Biochem. Mol. Biol.*, 2001, **31**, 401–405.

50. M. O. Funk and A. W. Alteneder, *Biochem Biophys Res Commun.*, 1983, **114**, 937–943.

51. E. J. Corey, J. R. Cashman, T. M. Eckrich and D. R. Corey, *J. Am. Chem. Soc.*, 1985, **107**, 713–715.

52. P. H. Buist, K. A. Alexopoulos, B. Behrouzian and B. Black, *J. Chem. Soc. Perkin Trans.*, 1997, **1**, 2617–2624.

53. M. K. Pandey, A. Bansal and T. R. Degrado, *Heart Metab.*, 2011, **51**, 15–19.

54. G. C. Burdge, P. Wright, A. E. Jones and S. A. Wootton, *Br. J. Nutr.*, 2000, **84**, 781–787.

55. A. Cert, W. Moreda and M. C. Perez-Camino, *J. Chromatogr. A*, 2000, **881**, 131–148.

56. T. I. Mayakova, E. E. Kuznetsova, M. G. Kovaleva and S. A. Plyusnin, *J. Chromatogr. B. Biomed. Appl.*, 1995, **672**, 133–137.

57. D. J. Hodgson, K. Y. Y. Lao, B. Dawson and P. H. Buist, *Helv. Chim. Acta*, 2003, **86**, 3688–3697.

58. B. Lewis, *Postgrad. Med. J.*, 1959, **35**, 208–215.

59. K. J. McLean, M. Hans and A. W. Munro, *Biochem. Soc. Trans.*, 2012, **40**, 587–593.

60. S. M. Grundy, *West. J. Med.*, 1978, **128**, 13–25.

61. D. F. Lewis, *Cytochromes P450*, Taylor & Francis, London, 1996.

62. G. S. Tint, M. Irons, E. R. Elias, A. K. Batta, R. Frieden, T. S. Chen and G. Salen, *N. Engl. J. Med.*, 1994, **330**, 107–113.

63. K. Z. Rosłoniec, M. H. Wilbrink, J. K. Capyk, W. W. Mohn, M. Ostendorf, R. van der Geize, L. Dijkhuizen and L. D. Eltis, 2009, **74**, 1031–1043.

64. K. J. McLean, P. Lafite, C. Levy, M. R. Cheesman, N. Mast, I. A Pikuleva, D. Leys and A. W. Munro, *J. Biol. Chem.*, 2009, **284**, 35524–35533.

65. F. Hannemann, A. Bichet, K. M. Ewen and R. Bernhardt, *Biochim. Biophys. Acta*, 2007, **1770**, 330–344.

66. F. P. Guengerich, *Chem. Res. Toxicol.*, 2001, **14**, 611–650.

67. K. Schmidt, C. Hughes, J. A. Chudek, S. R. Goodyear, R. M. Aspden, R. Talbot, T. E. Gundersen, R. Blomhoff, C. Henderson, C. R. Wolf and C. Tickle, *Mol. Cell. Biol.*, 2009, **29**, 2716–2729.

68. M. Norlin, PhD Thesis, Uppsala University, 2000.

69. I. Uhía, B. Galán, S. L. Kendall, N. G. Stoker and J. L. García, *Environ. Microbiol. Rep.*, 2012, **4**, 168–182.

70. A. Brzostek, J. Pawelczyk, A. Rumijowska-Galewicz, B. Dziadek and J. Dziadek, *J. Bacteriol.*, 2009, **191**, 6584–6591.

71. H. Ouellet, S. Guan, J. B. Johnston, E. D. Chow, P. M. Kells, A. L. Burlingame, J. S. Cox, L. M. Podust and P. R. O. de Montellano, *Mol. Microbiol.*, 2010, **77**, 730–742.

72. D. Schnappinger, S. Ehrt, M. I. Voskuil, Y. Liu, J. A. Mangan, I. M. Monahan, G. Dolganov, B. Efron, P. D. Butcher, C. Nathan and G. K. Schoolnik, *J. Exp. Med*. 2003, **198**, 693–704.

73. E. N. G. Houben, L. Nguyen and J. Pieters, *Curr. Opin. Microbiol.*, 2006, **9**, 76–85.

74. S. Munoz, B. Rivas-Santiago and J. A. Enciso, *Culture*, 2009, **70**, 256–263.

75. D. Kaul, P. K. Anand and I. Verma, *Mol. Cell. Biochem.*, 2004, **258**, 219–222.

76. H. Ouellet, J. B. Johnston and P. R. O. de Montellano, *Trends Microbiol.*, 2011, **19**, 530–539.

77. S. Savvi, D. F. Warner, B. D. Kana, J. D. McKinney, V. Mizrahi and S. S. Dawes, *J. Bacteriol.*, 2008, **190**, 3886–3895.

78. T. Li, J. Chen, X. Li, X. Ding, Y. Wu, L. Zhao, S. Chen, X. Lei and M. Dong, *Am. Chem. Soc.*, 2013, **85**, 9281–9287.

79. R. Martin, F. Däbritz, E. V Entchev, T. V Kurzchalia and H.-J. Knölker, *Org. Biomol. Chem.*, 2008, **6**, 4293–4295.

80. S. Giroux and E. J. Corey, *J. Am. Chem. Soc.*, 2007, **129**, 9866–9867.

81. R. B. Beckstead and C. S. Thummel, *Cell*, 2006, **124**, 1137–1140.

82. F. C. Schroeder, *ACS Chem. Biol.*, 2006, **1**, 198–200.

83. I. Casabon, A. M. Crowe, J. Liu and L. D. Eltis, *Mol. Microbiol.*, 2013, **87**, 269–283.

84. D. R. Nelson, *Arch. Biochem. Biophys.*, 1999, **369**, 1–10.

85. K. J. McLean, K. R. Marshall, A. Richmond, I. S. Hunter, K. Fowler, T. Kieser, S. S. Gurcha, G. S. Besra and A. W. Munro, *Microbiology*, 2002, **148**, 2937–2949.

86. K. J. McLean, P. Lafite, C. Levy, M. R. Cheesman, N. Mast, I. A. Pikuleva, D. Leys and A. W. Munro, *J. Biol. Chem.*, 2009, **284**, 35524–35533.

87. B. L. Heyl, D. J. Tyrrell and J. D. Lambeth, *J. Biol. Chem.*, 1986, **261**, 2743–2749.

88. Z. Ahmad, S. Sharma and G. K. Khuller, *Microbiol. Lett.*, 2005, **251**, 19–22.

89. S. T. Thomas, X. Yang and N. S. Sampson, *Bioorg. Med. Chem. Lett.*, 2011, **21**, 2216–2219.

90. J. Cloutier, A. Nagahisa and C. Byon, *Biochemistry*, 1995, 8415–8421.

91. L. M. Antinarelli, A. M. Carmo, F. R. Pavan, C. Q. F. Leite, A. D. Da Silva, E. S. Coimbra and D. B. Salunke, *Bioorg. Med. Chem. Lett.*, 2012, **2**, 16–23.

92. J. L. García, I. Uhía and B. Galán, *Microb. Biotechnol.*, 2012, **5**, 679–699.

93. L. Kumari and S. S. Kanwar, *Adv. Appl. Microbiol.*, 2012, **2**, 49–65.

94. M. S. Andhale and S. A. Sambrani, *Indian J. Biotechnol.*, 2006, **5**, 389–393.

95. S. M. Rao, K. Thakkar and K. Pawar, *Quest*, 2013, **1**, 16–20.

96. F. Naghibi, M. T. Yazdi, M. Sahebgharani and M. R. N. Daloii, *J. Sci. Islam. Repub. Iran.*, 2002, **13**, 103–106.

97. L. Pollegioni, L. Piubelli and G. Molla, *FEBS J.*, 2009, **276**, 6857–6870.

98. J. A. Contreras, M. Castro, C. Bocos, E. Herrera and M. A. Lasunción, *J. Lipid Res.*, 1992, **33**, 931–936.

99. L. Guo, W. K. Wilson, J. Pang and C. H. L. Shackleton, *Steroids*, 2003, **68**, 31–42.

100. D. R. Corbin, R. J. Grebenok, T. E. Ohnmeiss, J. T. Greenplate and J. P. Purcell, *Plant Physiol.*, 2001, **126**, 1116–1128.

101. H. Noppe, B. Le Bizec, K. Verheyden and H. F. de Brabander, *Anal. Chim. Acta*, 2008, **611**, 1–16.

102. C. Amaral, E. Gallardo, R. Rodrigues, R. Pinto Leite, D. Quelhas, C. Tomaz and M. L. Cardoso, *J. Chromatogr. B.*, 2010, **878**, 2130–2136.

103. D. C. Lamb, D. E. Kelly, N. J. Manning and S. L. K. Y, *FEBS Lett.*, 1998, **437**, 142–144.

104. Y. Wang, L. Li, A. Leger, A. Altobelli, A. Cohen and B. Wang, *Poster Present.*, 2007.

105. Y. V Faletrov, K. I. Bialevich, I. P. Edimecheva, D. G. Kostsin, E. V Rudaya, E. I. Slobozhanina and V. M. Shkumatov, *J. Steroid Biochem. Mol. Biol.*, 2013, **134**, 59–66.

106. N. Mast, D. Murtazina, H. Liu, S. E. Graham, I. Bjorkhem, J. R. Halpert, J. Peterson and I. A. Pikuleva, *Biochemistry*, 2006, **45**, 4396–404.

107. R. A. Pascal and D. L. Ziering, *J. Lipid Res.*, 1986, **27**, 221–224.

108. M. D. Rahman, D. L. Ziering, S. J. Mannarelli, K. L. Swartz, D. S. Huang and R. A. Pascal, *J. Med. Chem.*, 1988, **31**, 1656–1659.

109. K. E. Hovik, O. S. Spydevold and J. Bremer, *Biochim. Biophys. Acta*, 1997, **1349**, 251–256.

110. E. Miao, S. Joardar, C. Zuo, N. J. Cloutier, A. Nagahisa, C. Byon, S. R. Wilson and W. H. Orme-Johnson, *Biochemistry*, 1995, **34**, 8415–8421.

111. M. A. Ator, S. J. Schmidt, J. L. Adams, R. E. Dolle, L. I. Kruse, C. L. Frey and J. M. Barones, *J. Med. Chem.*, 1992, **35**, 100–106.

112. *http://triadmomsonmain.com/my-blog/rainy-day-activities-for-kids-of-all-ages*, 2012, (Accessed January 2014).

113. *Crawford Scientific, http://www.chromacademy.com/resolver-november2010_understanding_gcms_part_1.html, (Accessed January 2014).*

114. *Acclaim Imagery, http://www.clipartguide.com/_pages/0511-1001-2709-2952.html, (Accessed January 214).*

115. A. Bowers and H. J. Ringold, *J. Am. Chem. Soc.*, 1958, **80**, 4423–4424.

116. A. Bowers, L. C. Ibanez and H. J. Ringold, *J. Am. Chem. Soc.*, 1959, **81**, 5991–5993.

117. J. Liu, PhD Thesis, Texas Tech University, 2008.

118. A. Bowers and H. J. Ringold, *Tetrahedron*, 1958, **3**, 14–27.

119. E. Dyroy, H. Wergedahl, J. Skorve, O. A. Gudbrandsen, J. Songstad and R. K. Berge, *Lipids*, 2006, **41**, 169–177.

Chapter 2

Synthesis and characterization of thia-, fluoro- and deuterium labeled cholesterol derivatives

2.1. Thia-cholesterol derivatives

The synthesis and characterization of sulfur containing cholesterol and other steroid analogues is well established in the literature.[1–4] These compounds have found applications as growth inhibitors of various organisms as well as probes for the study of metabolic processes in several species except M.tb. In the current study, the aim was to synthesize and characterize a range of thia-cholesterol derivatives that could be used to probe the activity of CYP450 enzymes of M.tb. These compounds include 3β-mercaptocholest-5-ene and 23-thiacholestene derivatives. The compounds synthesized were chosen based on the strategic placement of a sulfur atom as determined by the cholesterol catabolic pathway published by Quellet *et al*.[5] In this study the synthesized compounds were evaluated as alternative substrates for M.tb and hence evaluated as mechanistic probes for lipid catabolism. Derivatives that do not degrade within at least 1 hour in a cell-free matrix will be considered as potential internal standards for steroid analysis.

2.1.1. Synthesis of 3β-mercaptocholest-5-ene

Cholesterol catabolism in M.tb is initiated by the conversion of cholesterol to cholest-4-en-3-one as shown in Figure 2.1. This step is catalyzed by 3β-hydroxy-Δ(5)-steroid dehydrogenase (3β-HSD) or cholesterol oxidase (Section 1.5.3). 3β-HSD is responsible for both oxidizing cholesterol to cholest-5-ene-3-one and the subsequent isomerization to cholest-4-ene-3-one.[6] Armstrong and co-workers performed a cholesterol oxidase assay of steroids by substituting the 3β-OH of cholesterol with 3α-OH (epi-cholesterol) and 3β-SH (3β-mercaptocholest-5-ene) (Figure 2.1).[7] The study demonstrated that the sulfur atom in 3β-mercaptocholest-5-ene was not oxidized due to the action of 3β-HSD.[7] Therefore, in the current study, 3β-mercaptocholest-5-ene was synthesized to determine whether side-chain degradation can occur irrespective of the absence of 3β-HSD activity at the 3β-position.

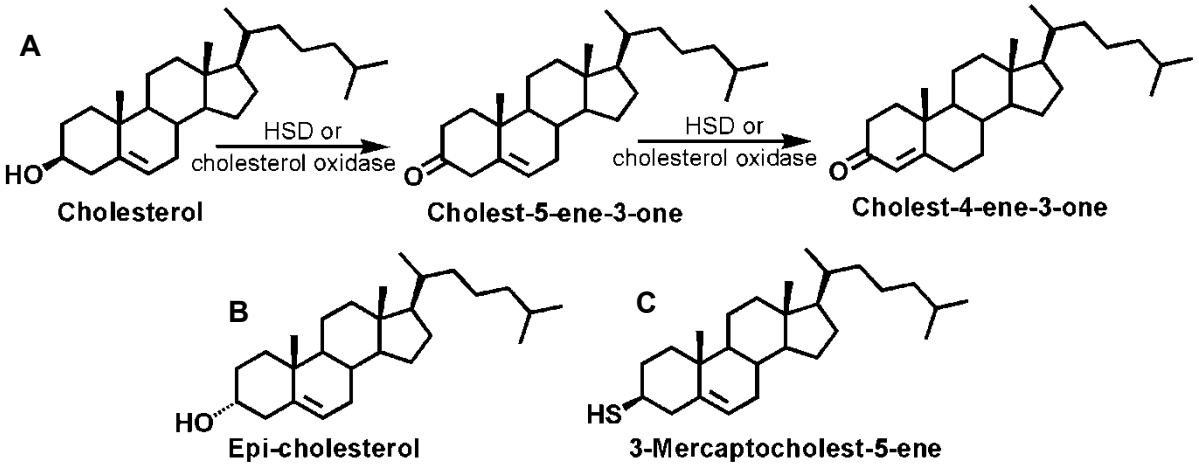

Figure 2.1: A: *Enzymatic synthesis of cholest-4-ene-3-one from cholesterol.* ***B:*** *epi-cholesterol and* ***C:*** *3β-mercaptocholest-5-ene.*[7]

3β-Mercaptocholest-5-ene (**3**) was synthesized from cholesteryl tosylate (**1**) *via* cholesterylisothiouronium tosylate (**2**) as shown in Scheme 2.1.

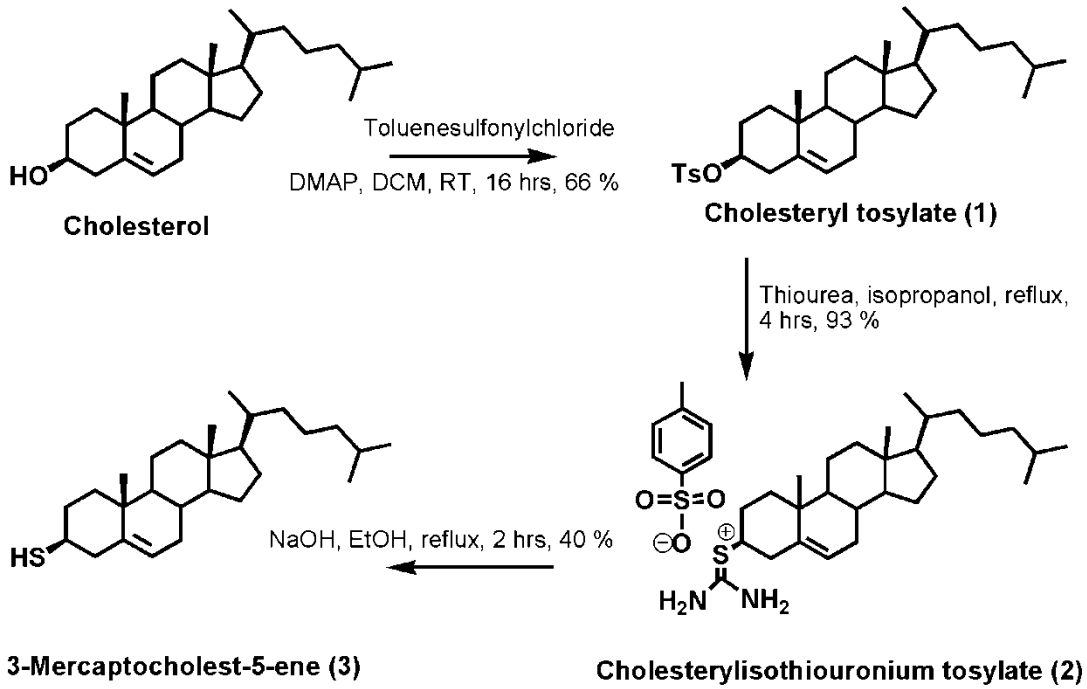

Scheme 2.1: *Synthesis of 3β-mercaptocholest-5-ene (**3**).*[8]

Cholesteryl tosylate (**1**) was synthesized *via* a substitution reaction by reacting toluenesulfonylchloride with commercially available cholesterol following the method of Bajaj *et al*.[9] Isolation of the product by filtration produced a white crystalline solid in a yield of 66 %. Since the oxygen at C3 of (**1**) has a better configuration, the stereochemistry was retained and a 3β-tosylate derivative formed.

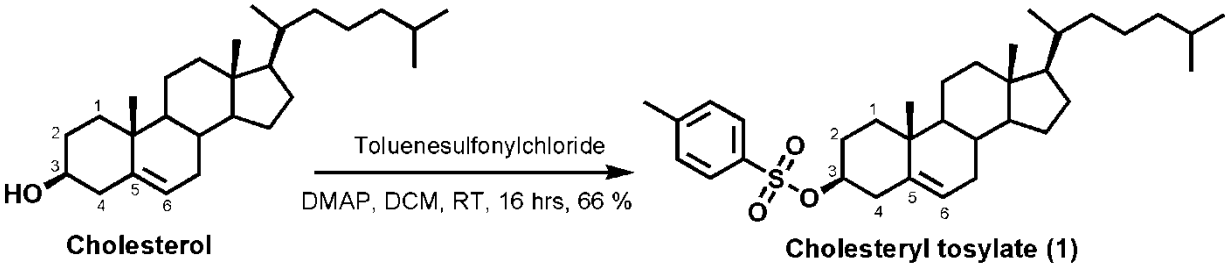

Scheme 2.2: *Synthetic route to cholesteryl tosylate (**1**).*[9]

*^{1}H NMR and ^{13}C NMR analysis of cholesteryl tosylate (**1**)*

The formation of (**1**) was confirmed by ^{1}H NMR and ^{13}C NMR analysis. The presence of the *para*-disubstituted phenyl protons were confirmed by a distorted doublet of doublets at 7.32 ppm (H3‟, H5‟) and 7.79 ppm (H2‟, H6‟) which integrated for two protons each. The methyl protons of the tosylate group (H7‟) were confirmed by a singlet at 2.44 ppm. Distinct methyl groups of the cholesterol backbone appeared in the region of 0.66 – 0.97 ppm as shown in Figure 2.2, with H18 appearing as the most upfield signal at 0.66 ppm which was confirmed by means of a COSY NMR spectrum. A doublet of doublets was observed at 2.27 ppm and was assigned to $H4_B$. The two *J* values associated with this peak is due to the axial/equatorial coupling with H3 (4.9 Hz) and the geminal coupling with $H4_A$ (13.1 Hz), respectively. The most deshielded proton, H6, appeared as a doublet at 5.31 ppm. The ^{1}H NMR of (**1**) agrees with that presented by Bajaj *et al*.[9] The ^{13}C NMR analysis further confirmed the formation of (**1**) with the presence of 34 carbon signals as expected with resonances in the region of 127.6 ppm – 138.9 ppm confirming the presence of the aromatic group.

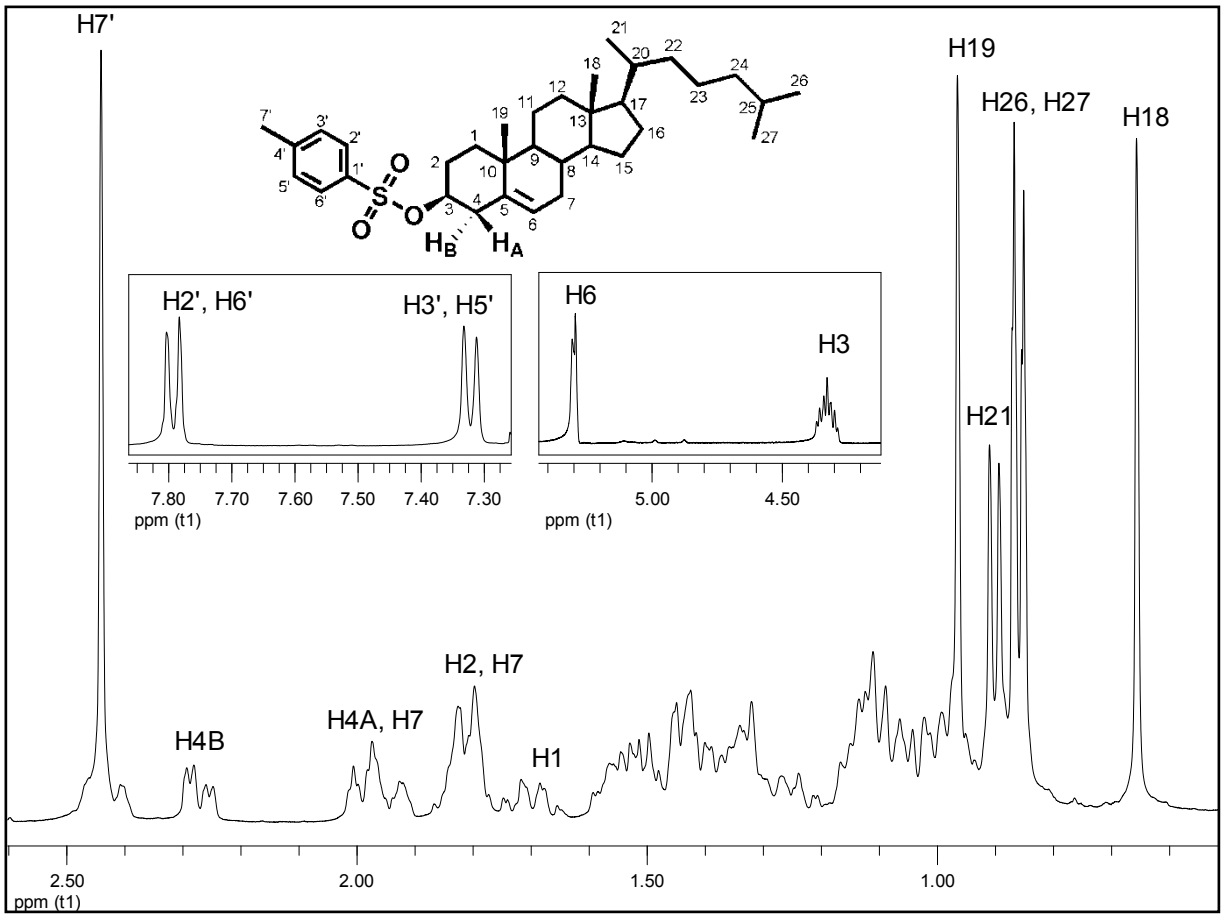

Figure 2.2: *^{1}H NMR cholesteryl tosylate (**1**) in $CDCl_3$.*

*FT-IR, elemental analysis and melting point analysis of cholesteryl tosylate (**1**)*

The presence of the aromatic tosylate moiety of (**1**) was confirmed by *FT-IR*. The C=C symmetric and asymmetric stretching vibrations of the aromatic group appeared as strong, sharp bands at 1599 cm^{-1} and 1470 cm^{-1}, respectively. The asymmetric stretching vibration of C-H (aromatic) gave rise to a strong broad band in the region of 2943 cm^{-1}, confirming the successful tosylation of cholesterol. Elemental analysis determined for (**1**) showed good correlation with the calculated values agreeing within a range of 0.0 – 1.1 %. The melting point range of (**1**) was determined to be 132 – 133 °C which agreed with the literature value of 132 – 133 °C.[9]

The synthesis of cholesterylisothiouronium tosylate (**2**) was carried out according to the procedure described by Ralls *et al*.[10] A suspension of cholesteryl tosylate (**1**), thiourea and dry isopropanol was refluxed under anhydrous conditions and a white solid was obtained as the product in a yield of 93 % as shown in Scheme 2.3.

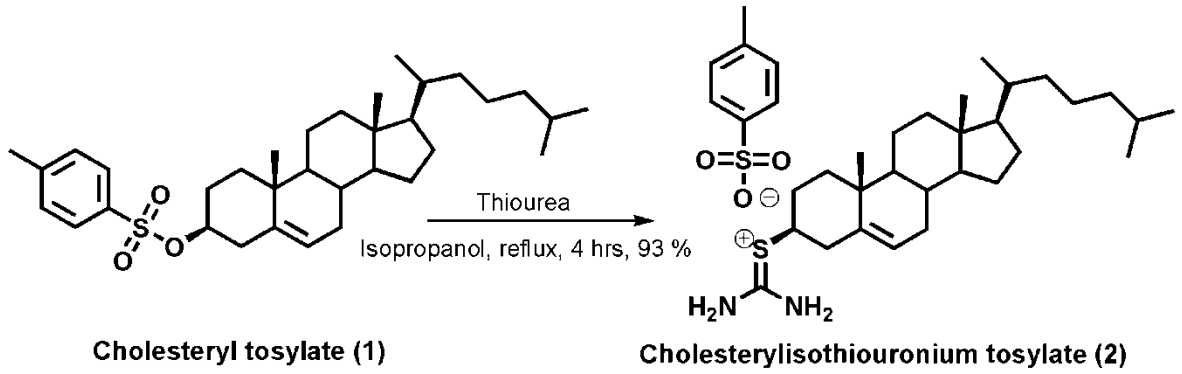

Scheme 2.3: *Synthesis of cholesterylisothiouronium tosylate (**2**).*

*Mechanism of formation of cholesterylisothiouronium tosylate (**2**)*

Riegel *et al.* described a mechanism for the synthesis of (**2**).[11] This mechanism occurs *via* a nucleophilic substitution of (**1**) at C3 by which an *i*-cholesteryl derivative is initially formed as shown in Scheme 2.4, pathway (ii).[11] A kinetic study completed by Pearson *et al*. concluded that 67 % of the reaction follows pathway (ii), whereby *i*-cholesteryl is formed first, followed by a nucleophilic attack from thiourea to form (**2**).[12] A direct reaction without the formation of *i*-cholesteryl accounts for 33 % of the reaction as shown in pathway (i).

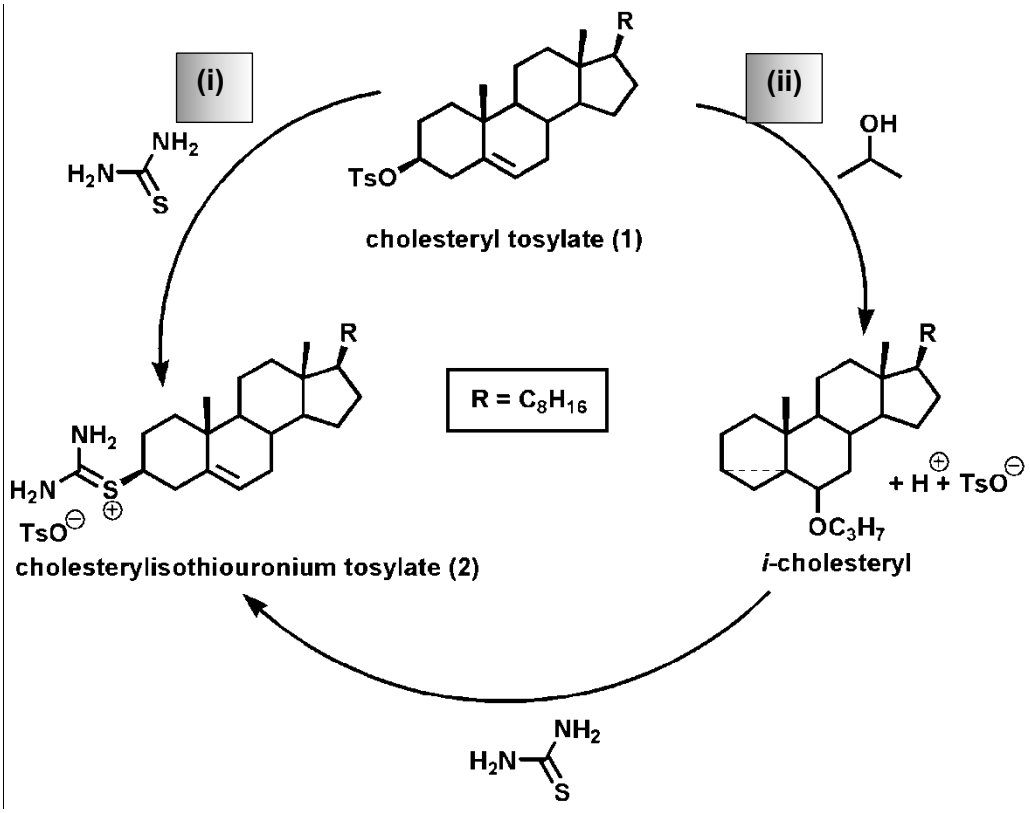

Scheme 2.4: *Mechanism of formation of cholesterylisothiouronium tosylate (**2**).*[12]

Due to solubility constraints, (**2**) could not be characterized using liquid state NMR spectroscopy. Elemental analysis, melting point and *FT-IR* was used to characterize (**2**).

FT-IR, elemental analysis and melting point analysis of cholesterylisothiouronium tosylate (2)

The IR spectrum of (**2**) revealed bands at 3492 cm^{-1} and 3430 cm^{-1} due to the N-H stretch of the primary amines while the N-H bending vibration was confirmed by a band at 1655 cm^{-1}. A sharp, strong band was observed at 1208 cm^{-1} which corresponded to the C-N stretch. A decrease in bands associated with the bound tosylate group in (**1**) as compared to cholesteryl tosylate further confirmed the successful synthesis of (**2**). Elemental analysis results were in close agreement with calculated values and agreed within a range of 0.0 – 0.6 %, excluding sulfur. The melting point range of 237 – 239 °C agreed with the literature melting point range presented by Ternay *et al*.[8]

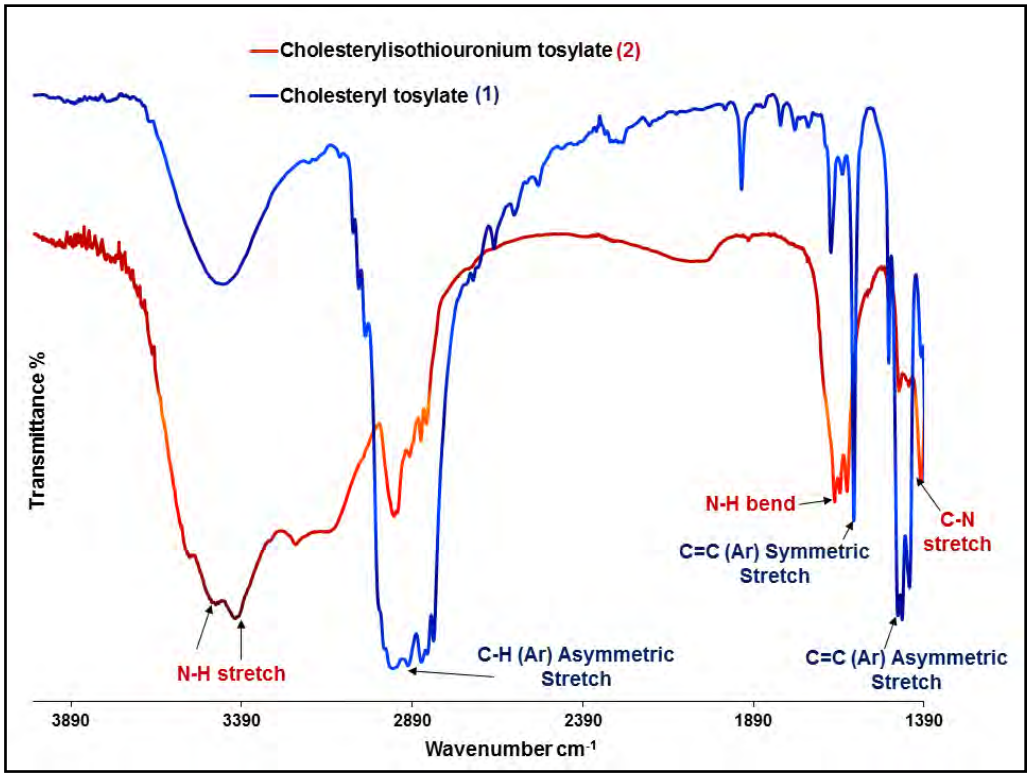

Figure 2.3: *IR spectrum of cholesteryl tosylate (**1**) and cholesterylisothiouronium tosylate (**2**).*

3β-Mercaptocholest-5-ene (**3**) was prepared according to the procedure reported by Ternay *et al*.[8] The product was synthesized by refluxing cholesterylisothiouronium tosylate (**2**) with ethanolic NaOH to yield a yellow solid (40 %) with concomitant loss of *p*-toluene sulfonate and ammonium carbonate. The base mediated elimination of urea from the thiouronium tosylate gave the thiocholesterol derivative (**3**)

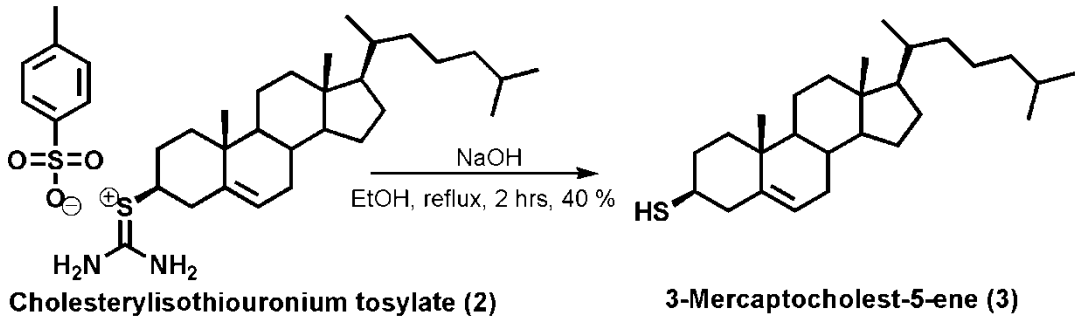

Scheme 2.5: *Synthesis of 3β-mercaptocholest-5-ene (**3**).*

*^{1}H NMR and ^{13}C NMR analysis of 3β-mercaptocholest-5-ene (**3**)*

The formation of (**3**) was confirmed by the upfield shift of H3 from 4.33 ppm in cholesteryl tosylate (**1**) to 2.67 ppm in (**3**) (Figure 2.4). This is due to the presence of the less electronegative sulfur at C3 as compared to the oxygen present in (**1**). In addition, the presence of the SH functional group was confirmed by the multiplet at 1.83 ppm which integrated for 1 proton.

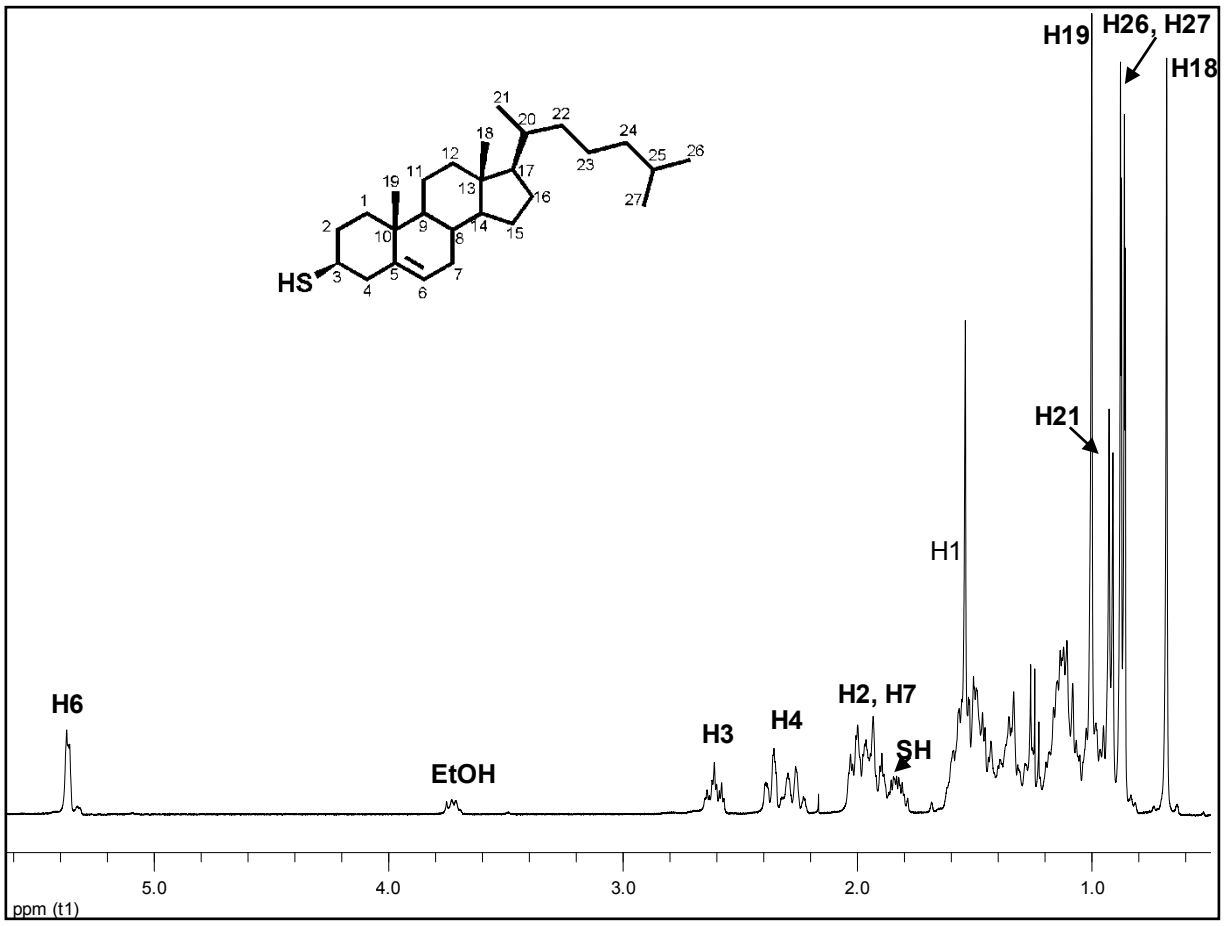

Figure 2.4: *^{1}H NMR spectrum of 3β-mercaptocholest-5-ene (**3**) in $CDCl_3$.*

*FT-IR and elemental analysis of 3β-mercaptocholest-5-ene (**3**)*

The microanalysis of (**3**) agreed within 0.1 % (except for sulfur) of the calculated values. In the IR spectrum of (**3**) (Figure 2.5), the N-H stretch of the thiourea present in (**2**) was observed at 3492 cm^{-1} and 3430 cm^{-1} and the absence of these bands in the IR spectrum of (**3**) combined with the appearance of a new broad band at 2897 cm^{-1} representing the S-H stretch, further confirmed the successful synthesis of (**3**).

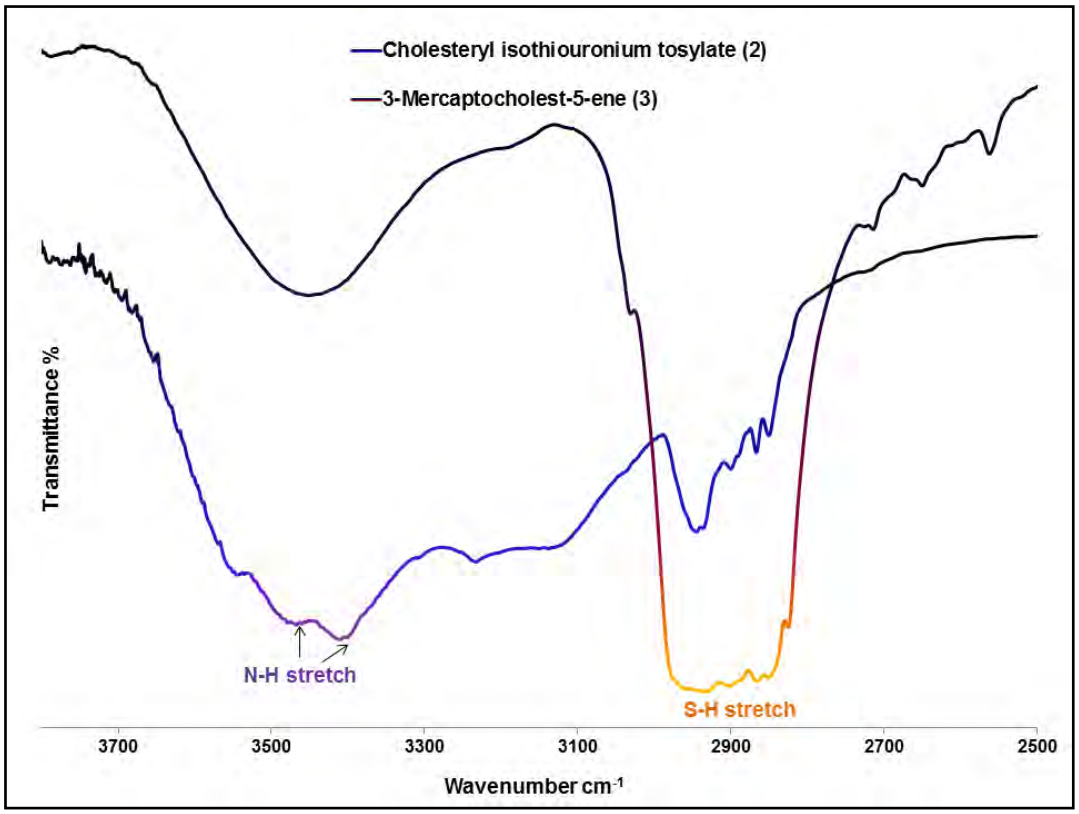

Figure 2.5: *IR spectrum of 3β-mercaptocholest-5-ene (**3**).*

Other thiacholesterol derivatives were synthesized where the side-chain of cholesterol was modified to include sulfur in position C23.

2.1.2. Synthesis of 23-thiacholest-4-en-3-one (4) and 23-thiacholest-4-en-3β-ol (5)

Thia-cholesterol derivatives were synthesized to probe the side-chain degradation of cholesterol by M.tb. Sulfur was substituted in position C23 to produce 23-thiacholest-4-en-3-one (**4**) and 23-thiacholest-4-en-3β-ol (**5**), respectively. Previously, the cholestane derivative, 23-thia-5α-cholestan-3β-ol, was synthesized and studied as an inhibitor of ergosterol biosynthesis and growth in *Crithidia fasciculate,* a parasitic protozoan utilizing various mosquito species as vectors.[13] However, it was found that this compound

was a poor inhibitor and had no adverse effect on the growth of the parasite. In the current study, 23-thiacholest-4-en-3β-ol (**5**) was synthesized to evaluate whether it"s potential as a carbon source for M.tb, and hence, as a mechanistic probe. Other ergosterol biosynthesis inhibitors include 25-thialanosterol where a sulfur atom was substituted in position C25.[14] The good inhibitory effect may indicate biological significance at this position which prevents further degradation from taking place.[14]

According to the cholesterol catabolic pathway, successive oxidation occurs for even numbered carbons (C22 and C24) during side chain degradation.[5] In the event of the oxidation product itself acting as an inhibitor, sulfur was placed in an odd numbered position (C23) instead. Compound (**5**) was obtained by a two-step synthesis as shown in Scheme 2.6. First, 23-thiacholest-4-en-3-one (**4**) was synthesized from hydroxymethylprogesterone tosylate (delta-4-HMP-tosylate) *via* a substitution reaction with 2-methyl-1-propanethiol followed by a reduction with $NaBH_4$ and $CeCl_3{\cdot}7H_2O$ to give 23-thiacholest-4-en-3β-ol (**5**). Delta-4-HMP-tosylate can be prepared from stigmasterol as previously discussed by Jungyeob *et al*.[15]

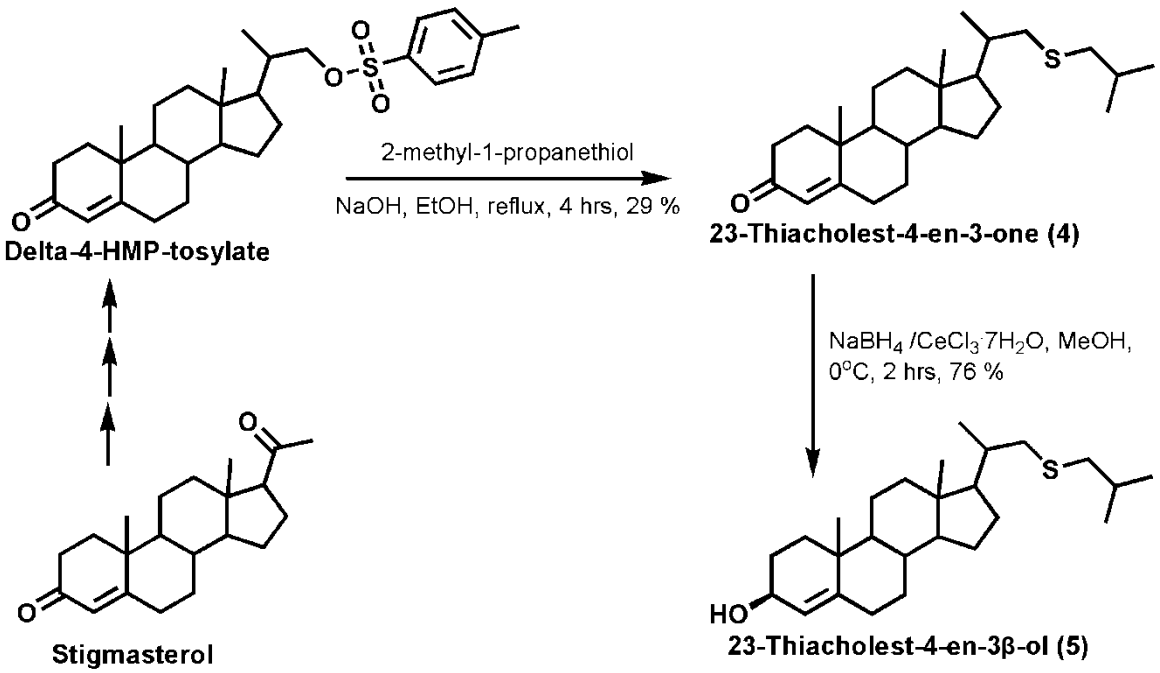

Scheme 2.6: *Synthesis of 23-thiacholest-4-en-3β-ol (**5**).*

*^{1}H NMR and ^{13}C NMR spectroscopy analysis of 23-thiacholest-4-en-3-one (**4**)*

The ^{1}H NMR spectrum of delta-4-HMP-tosylate revealed a doublet of doublets at 7.78 ppm and 7.35 ppm due to the aromatic protons of the tosylate group while the aromatic methyl group was observed as a singlet at 2.45 ppm. The alkene proton, H4, appeared as a singlet at 5.72 ppm while H22 appeared as a doublet at 3.80 ppm. The methyl protons of the steroid

moiety, H21, H19 and H18 were observed between 0.68 ppm and 1.17 ppm as three distinct singlets. The ^{1}H NMR spectrum of (**4**) confirmed the formation of the anticipated product, which could be seen by the disappearance of the aromatic proton signals. New methyl proton signals were observed due to C26 and C27, which appeared as a doublet at 0.98 ppm. H22 shifted further upfield due to the absence of the electron withdrawing tosylate group which is now substituted by a sulfur atom. The synthesis of (**4**) was also confirmed using ^{13}C NMR spectroscopy which showed 26 carbon signals as expected with no resonances in the aromatic region. The melting point range of compound (**4**), a novel compound, was recorded as 101 – 103 °C.

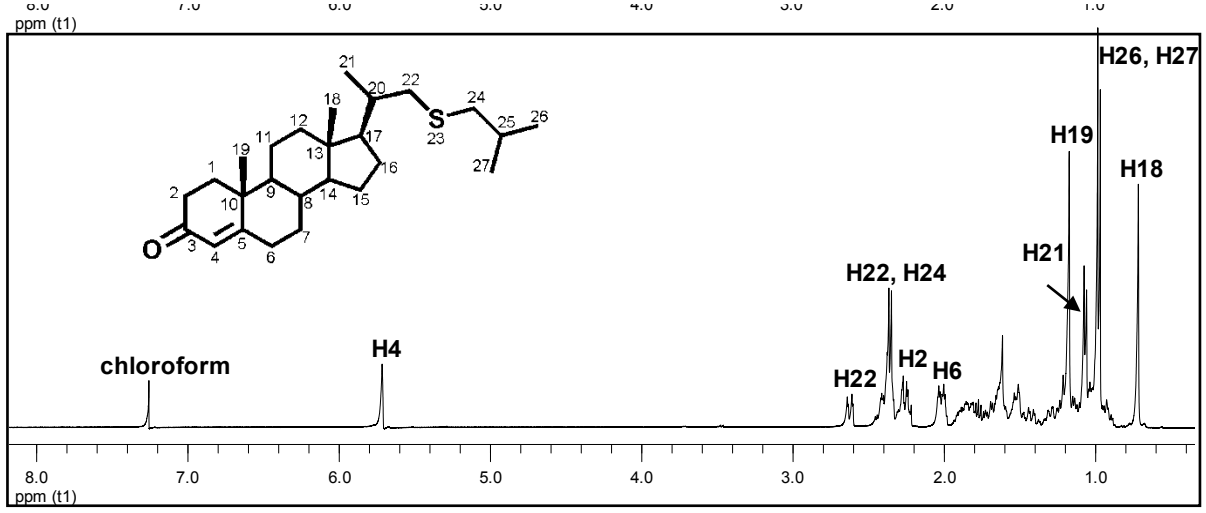

Figure 2.6: *^{1}H NMR of 23-thiacholest-4-en-3-one (**4**) in $CDCl_3$.*

*FT-IR and elemental analysis of 23-thiacholest-4-en-3-one (**4**)*

The synthesis of 23-thiacholest-4-en-3-one (**4**) was further confirmed by *FT-IR*. The IR spectrum of (**4**) revealed a sharp band at 1669 cm^{-1}, which corresponds to the ketone moiety while no bands corresponding to a phenyl group could be observed. This confirms that the substitution reaction was successful. Elemental analysis agreed within a range of 0 – 0.9 % with the calculated values.

23-Thiacholest-4-en-3β-ol (**5**) was synthesized by the addition of $NaBH_4$ and $CeCl_3{\cdot}7H_2O$ to 23-thiacholest-4-en-3-one (**4**) in methanol. Recrystallization from diethyl ether afforded (**5**) as a white crystalline solid in good yield (76 %). $CeCl_3{\cdot}7H_2O$ was added to ensure that the formation of the alkene derivative becomes favoured. The double bond at C4 is produced as a result of the first step in the degradation of cholesterol which is later further catabolized in the pathway resulting in ring degradation of 4-androstene-3,17-dione (Section 1.7.4). It is also of interest to evaluate 23-thiacholest-4-en-3β-ol (**5**) as substrate for 3β-HSD and cholesterol oxidase. The synthesis of 23-thiacholest-5-en-3β-ol was attempted via the

reduction of cholestenone to the corresponding enol acetate. The isolation of pure products proved to be challenging and was therefore not included into the study.

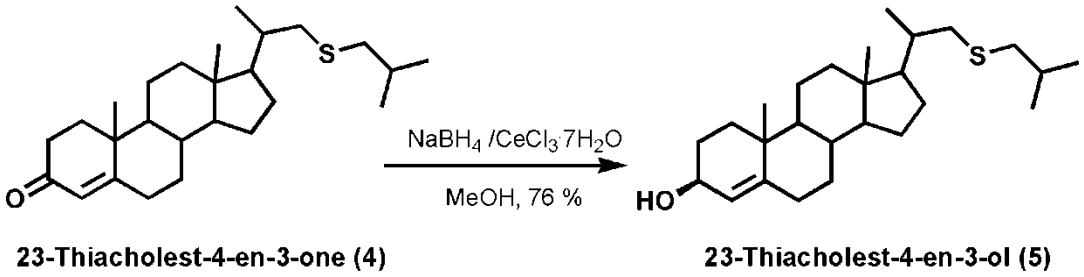

23-Thiacholest-4-en-3-one (4) **23-Thiacholest-4-en-3-ol (5)**

Scheme 2.7: *Synthesis of 23-thiacholest-4-en-3β-ol (**5**).*

*Proposed mechanism of the formation of 23-thiacholest-4-en-3β-ol (**5**)*

The synthesis of (**5**) was carried out *via* a Luche reduction which is generally used for the reduction of α,β-unsaturated ketones. $NaBH_4$ is a soft nucleophile and therefore favours a 1,4-addition while exclusive 1,2-attack can be achieved by the addition of $CeCl_3$ as shown in Scheme 2.8. This lanthanide acts as a Lewis acid and aids in the degradation of BH_4^- in the presence of methanol. The Ce^{3+} cation coordinates with the methanol and this makes the methanolic proton more acidic. The result is that the reaction rate between BH_4^- and methanol is increased to produce the alkoxyborohydride derivative that can act as a harder reagent to favour 1,2-attack. The carbonyl is activated through hydrogen bonding *via* the methanol-Ce^{3+} complex. The hard alkoxyborohydride attacks the hard carbonyl carbon to afford the desired product (**5**).[16] The mechanism of formation of (**5**) is shown in Scheme 2.9.

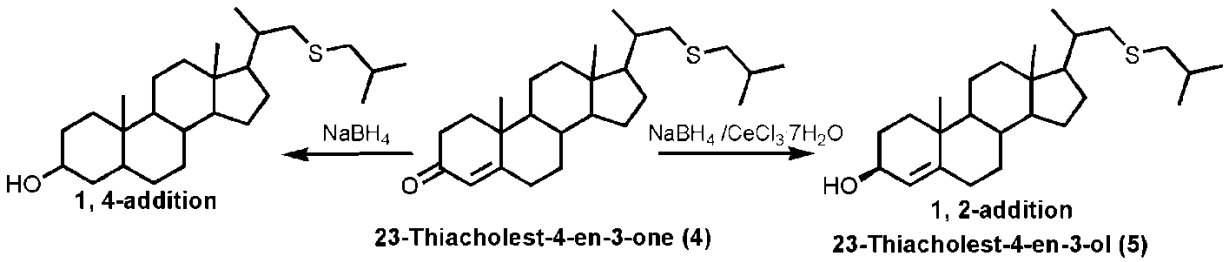

23-Thiacholest-4-en-3-one (4) **23-Thiacholest-4-en-3-ol (5)**

Scheme 2.8: *Possible reduction outcomes of 23-thiacholest-4-en-3-one (**4**) using $NaBH_4$.*

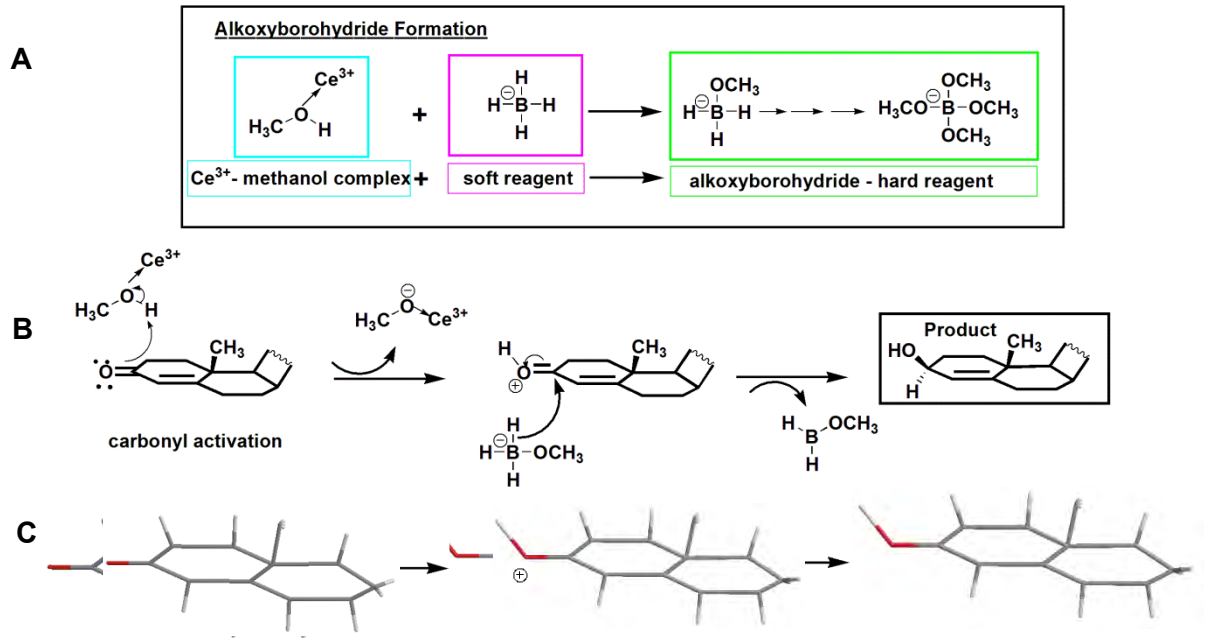

Scheme 2.9: *Proposed mechanism of formation of 23-thiacholest-4-en-3β-ol (**5**). **A:** Formation of alkoxyborohydride, **B:** Formation of 3β-sterol and **C:** 3D representation of of the formation of the 3β-sterol.*

*^{1}H NMR and ^{13}C NMR spectroscopy analysis of 23-thiacholest-4-en-3β-ol (**5**)*

The ^{1}H NMR spectrum of 23-thiacholest-4-en-3β-ol (**5**) is shown in Figure 2.7. A similar pattern was observed as in the ^{1}H NMR spectrum of (**4**) with the exception of a downfield shift of H4 due to the presence of the hydroxyl group in (**5**). In addition, the reduction of (**4**) was confirmed by the appearance of two signals at 4.15 ppm and 3.48 ppm, which was assigned to the hydroxyl proton (OH) and H3, respectively.

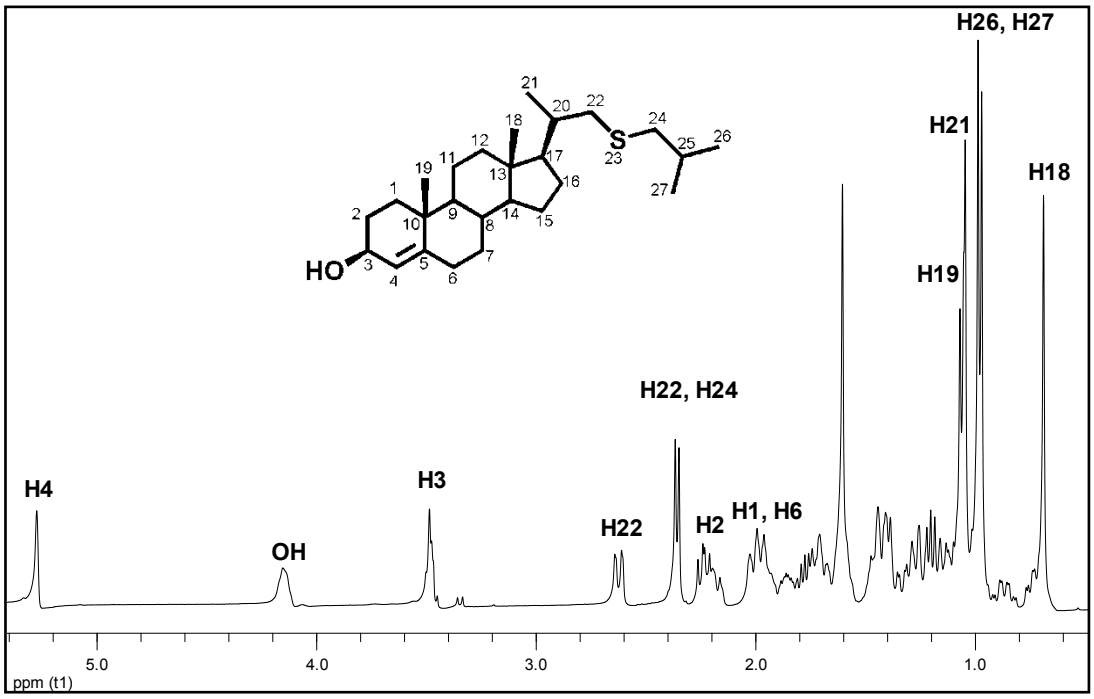

Figure 2.7: *^{1}H NMR 23-thiacholest-4-en-3β-ol (**5**) in $CDCl_3$.*

*FT-IR and elemental analysis of 23-thiacholest-4-en-3β-ol (**5**)*

FT-IR analysis confirmed the successful synthesis of (**5**) (Figure 2.8). The appearance of a new broad band at 3486 cm^{-1} confirms the presence of the hydroxyl group in (**5**). In addition, the band at 1673 cm^{-1} associated with a C=O stretching vibration in (**4**) was no longer present in (**5**). The melting point range of (**5**) was 76 – 78 °C and elemental analysis agreed well with the calculated values. Over reduction of (**4**) can result in the production of the cholestane derivative. Elemental analysis and mass spectroscopy, however, account for the successful formation of (**5**).

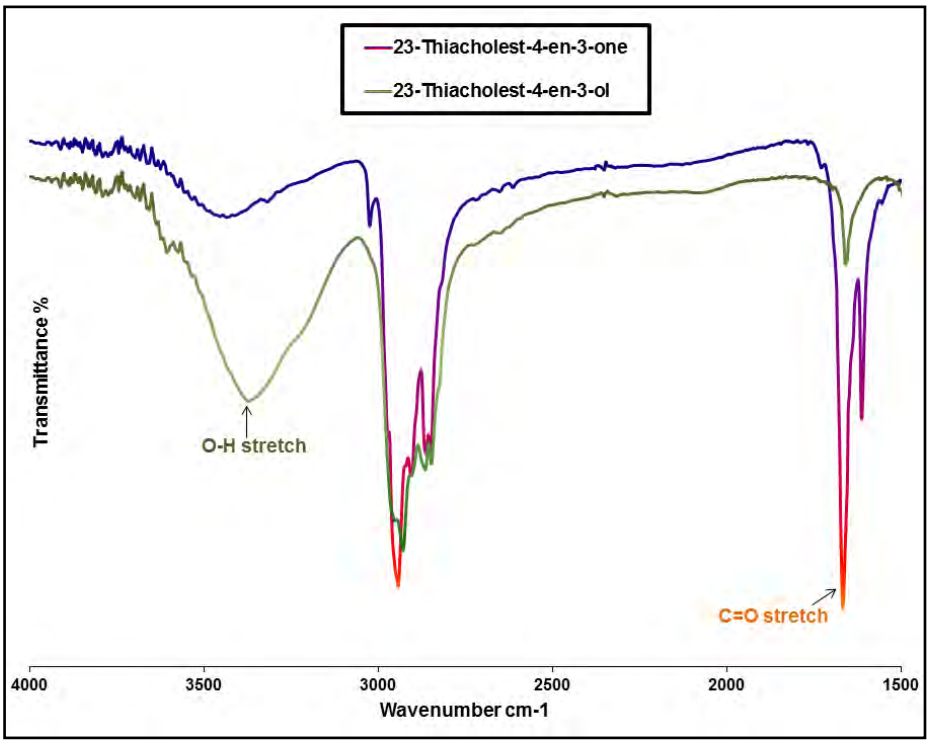

Figure 2.8: *IR spectra of 23-thiacholest-4-en-3-one (**4**) and 23-thiacholest-4-en-3β-ol (**5**).*

2.1.3. Synthesis of 22-mercapto-20-methylpregna-4-en-3-one (7)

As already stated, one of the aims of this project was to evaluate whether or not the compounds synthesized can be utilized as alternative carbon sources for M.tb. Due to the expected degradation of 23-thiacholest-4-en-3β-ol (**5**), 22-mercapto-20-methylpregna-4-en-3-one (**7**) was synthesized to be utilized as a possible reference compound for GC-MS analysis. The synthesis was carried out from delta-4-HMP-tosylate using the same procedure as described for the synthesis of 3β-mercaptocholest-5-ene (**3**) as shown in Scheme 2.10. Delta-4-HMP-tosylate was prepared by a member of the group as described by Jungyeob *et al*.[15]

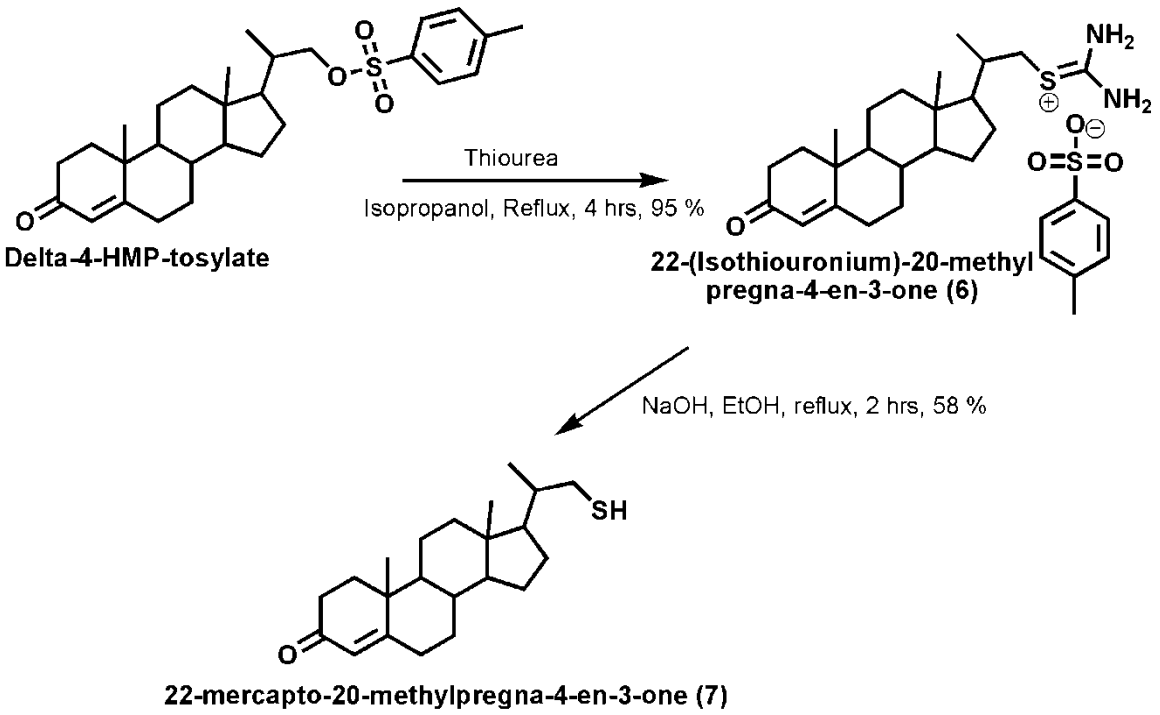

Scheme 2.10: *Synthesis of 22-mercapto-20-methylpregna-4-en-3-one (**7**).*

22-(Isothiouronium)-20-methylpregna-4-en-3-one (**6**) was obtained by refluxing of delta-4-HMP-tosylate in the presence of thiourea. A white solid in a yield of 95 % was obtained. Due to poor solubility in deuterated solvents, NMR analysis was not possible. However, elemental analysis, melting point range and *FT-IR* were carried out instead.

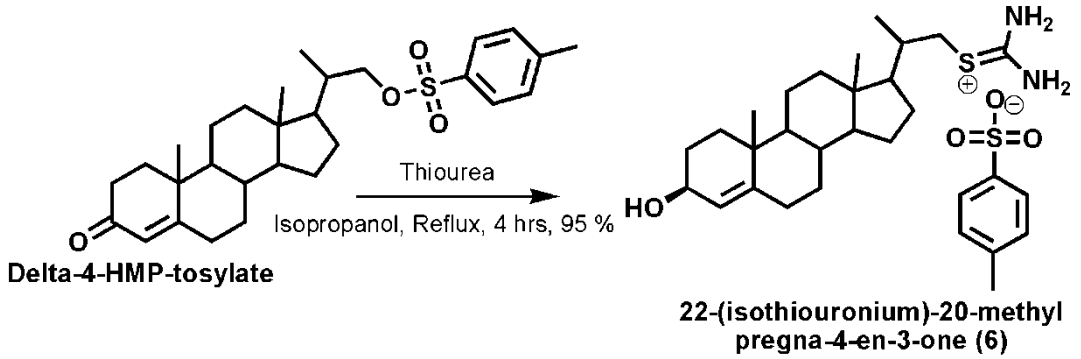

Scheme 2.11: *Synthesis of 22-(isothiouronium)-20-methyl pregna-4-en-3-one (**6**).*

*FT-IR and elemental analysis of 22-(isothiouronium)-20-methylpregna-4-en-3-one (**6**)*

IR spectroscopy was used to confirm the presence of the newly formed amine groups in (**6**). Two strong absorption bands appeared at 1673 cm^{-1} and 1212 cm^{-1} and were assigned to the N-H bending and C-N stretching vibrations, respectively, while the N-H stretch could be seen at 3376 cm^{-1}. The calculated elemental analysis agreed within a range of 0.0 – 1.0 % with the experimental values.

The synthesis of (**7**) was carried out by the addition of solid NaOH to a solution of 22-(isothiouronium)-20-methylpregna-4-en-3-one (**6**) in ethanol and allowing the mixture to reflux under anhydrous conditions for 2 hours. An orange solid was isolated and recrystallized from ethanol with a yield of 58 %. Ferraboschi *et al*. first synthesized (**7**) indirectly from the corresponding thioacetate anion, which was synthesized from (**6**) using potassium thioacetate in polyethylene glycol 400.[17] The subsequent reaction of the acetate with aqueous NaOH generated the thiol derivative (**7**).

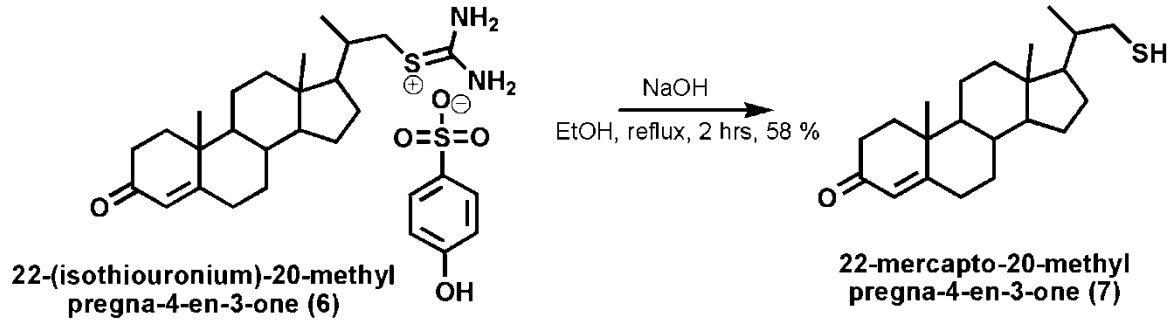

Scheme 2.12: *Synthesis 22-mercapto-20-methylpregna-4-en-3-one (**7**).*

*^{1}H NMR and ^{13}C NMR spectroscopy analysis of 22-mercapto-20-methylpregna-4-en-3-one (**7**)*

The ^{1}H NMR spectrum of (**7**) is shown in Figure 2.9. The alkene proton, H4, appeared as a multiplet at 5.64 ppm while H2 resonated at 3.65 ppm. H22 appeared as a doublet at 2.85 ppm while the methyl protons H18, H19 and H21 occurred between 0.68 – 1.12 ppm. The successful synthesis of (**7**) was further confirmed by the ^{13}C NMR spectrum which displayed 22 signals as expected.

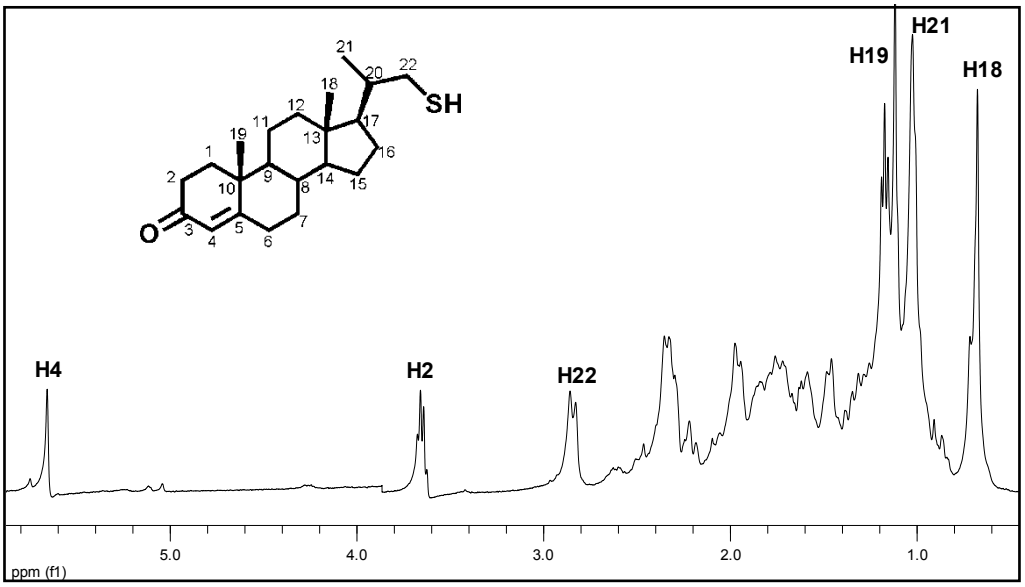

Figure 2.9: *^{1}H NMR22-mercapto-20-methylpregna-4-en-3-one (**7**) in $CDCl_3$.*

2.2. Deuterium labeled cholesterol derivatives

Deuterium labeled compounds is conventionally used as molecular biomarkers to evaluate metabolic pathways in various microorganisms. In this study, two deuterated cholesterol derivatives [3α-^{2}H]23-thiacholest-4-en-3β-ol (**8**) and [3α-^{2}H]cholest-4-en-3β-ol (**9**) were synthesized. Synthesizing the deuterium labeled derivative with sulfur substituted in position C23 allows for this compound to be utilized as an internal standard for cell-free assays of 23-thiacholest-4-en-3β-ol (**5**).

2.2.1. Synthesis of [3α-^{2}H]23-thiacholest-4-en-3β-ol (8) and [3α-^{2}H]cholest-4-en-3β-ol (9)

The following deuterium labeled derivatives were synthesized *via* a Luche reduction of the appropriate α,β-unsaturated ketone using $NaBD_4$ and $CeCl_3{\cdot}7H_2O$ following the procedure discussed for the synthesis of (**5**) (Scheme 2.13).

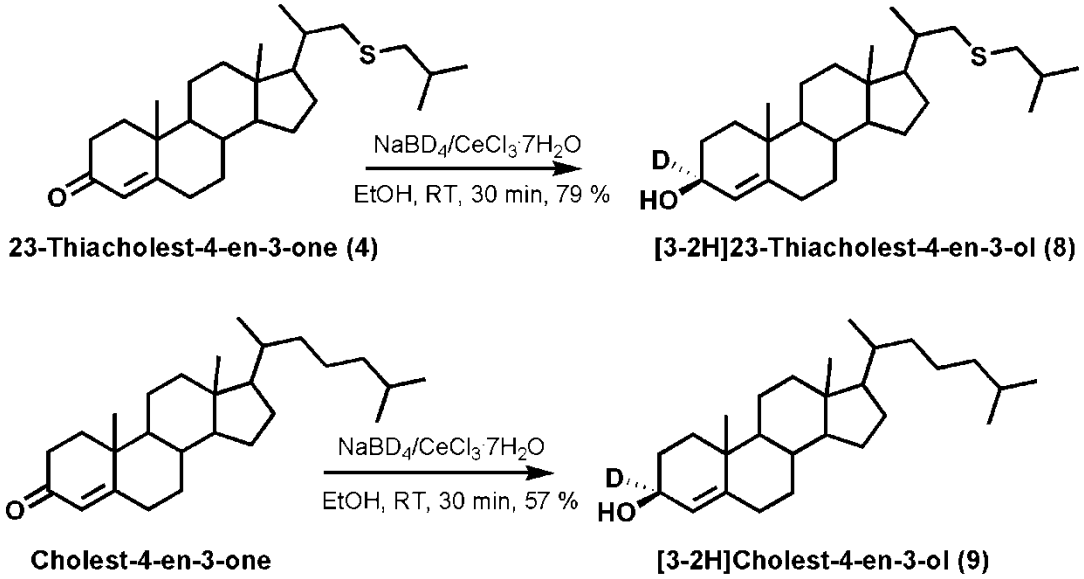

Scheme 2.13: *Synthesis of [3α-^{2}H]23-thiacholest-4-en-3β-ol (**8**) and [3α-^{2}H]cholest-4-en-3β-ol, (**9**).*

*^{1}H NMR and ^{13}C NMR analysis of [3α-^{2}H]23-thiacholest-4-en-3β-ol (**8**) and [3α-^{2}H]cholest-4-en-3β-ol (**9**)*

The ^{1}H NMR spectra of (**8**) and (**9**) are shown in Figure 2.10. Due to the presence of a deuterium atom, (**8**) and (**9**) could not be confirmed by a resonance due to H3 at 3.48 ppm as with the synthesis of 23-thiacholest-4-en-3β-ol (**5**). The successful synthesis of (**8**) was confirmed by the upfield shift from 5.72 ppm to 5.27 ppm of H4, which was also observed for (**5**). Similarly, an upfield shift from 5.72 ppm to 5.22 ppm for H4 was observed in the ^{1}H NMR spectrum of (**9**) compared to that of cholest-4-en-3-one. Furthermore, the formation of these compounds was confirmed by ^{13}C NMR spectroscopy. Due to the presence of sulfur in

position 23 of (**8**), 26 carbon signals were detected while 27 carbon signals were observed for (**9**).

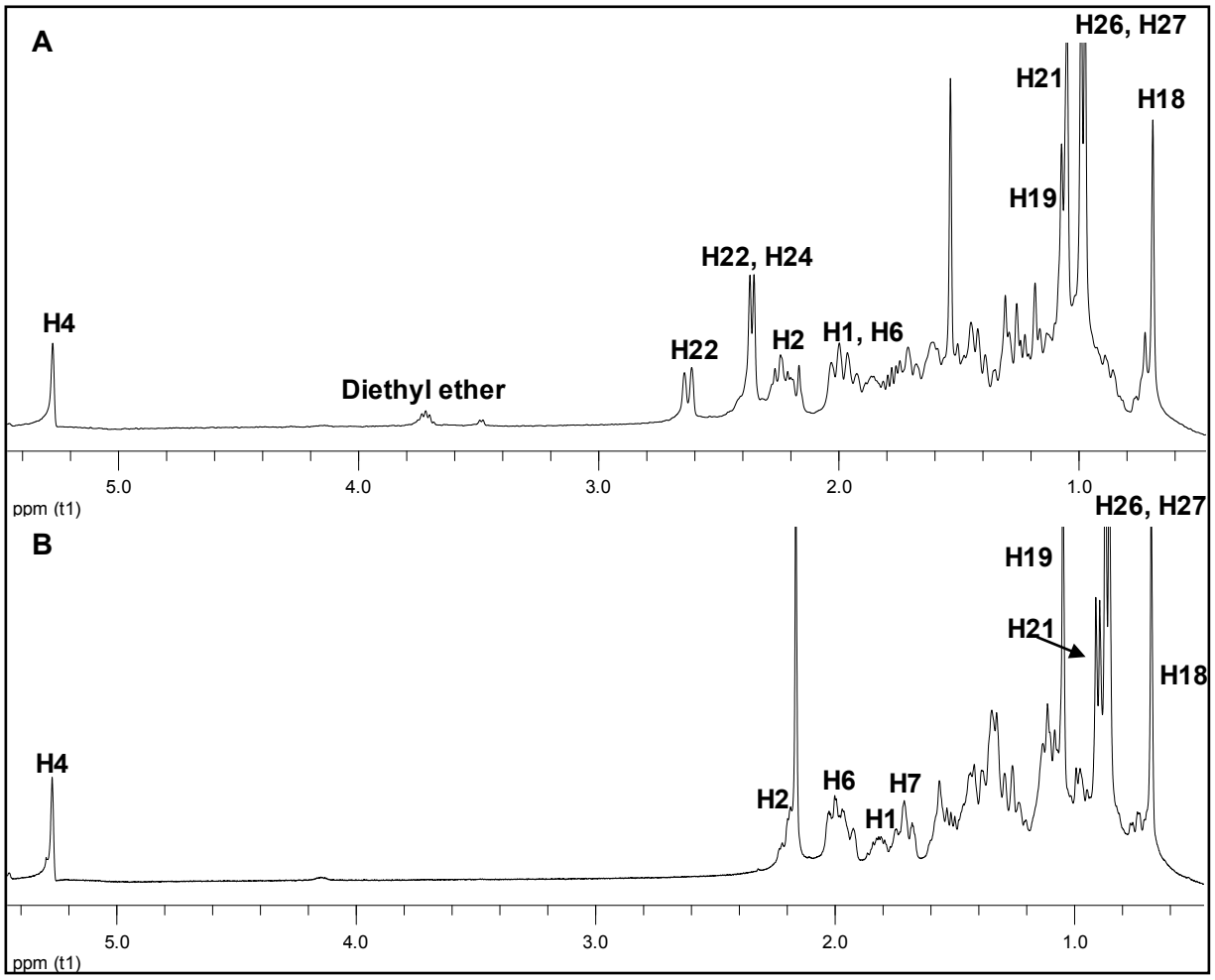

Figure 2.10: *^{1}H NMR of **A:** [3α-^{2}H]23-thiacholest-4-en-3β-ol (**8**) and **B:** [3α-^{2}H]cholest-4-en-3β-ol (**9**) in $CDCl_3$.*

In addition to the thia- and deuterium labeled cholesterol compounds, fluoro-cholesterol derivatives were prepared for use as possible biomarkers for the evaluation of cholesterol metabolism in M.tb. The fluoro-cholesterol compounds synthesized in this study include 3α-fluorocholest-5-ene (**10**) and 6β-fluoro-cholest-3β,5α-diol (**12**).

2.3. Fluoro-cholesterol derivatives

2.3.1. Synthesis of 3α-fluorocholest-5-ene (10)

3α-Fluorocholest-5-ene (**10**) was formed using the method reported by Liu *et al*.[18] Diethylaminosulfur trifluoride (DAST) was added to a solution of cholesterol in dry dichloromethane as shown in Scheme 2.14. The solution was allowed to stir at room temperature for 4 hours and the resulting residue purified using silica column chromatography to afford a white solid in low yield.

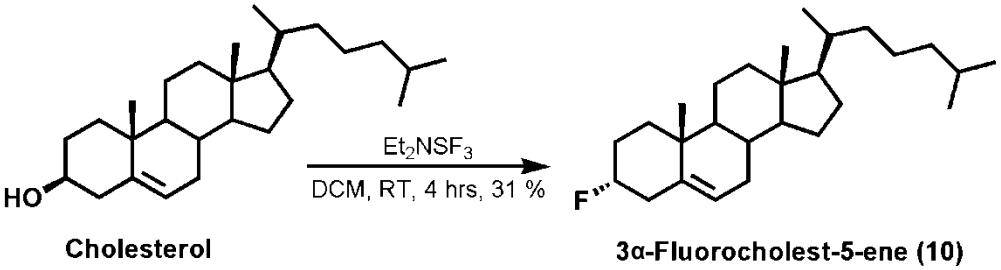

Scheme 2.14: *Synthesis of* 3α*-fluorocholest-5-ene (**10**).*

*^{1}H NMR and ^{13}C NMR spectroscopy analysis of 3α-fluorocholest-5-ene (**10**)*

The ^{1}H NMR spectrum (Figure 2.11) of (**10**) showed a distinct shift in the signal assigned to H3 from 3.52 ppm in cholesterol to 4.37 ppm and appeared as a broad doublet due to coupling with the fluorine atom. This change in chemical shift confirms the successful synthesis of (**10**) due to the presence of a more electron withdrawing fluoride at C3 as compared to the alcohol group in native cholesterol. H6 appeared as a doublet at 5.33 ppm with a *J* value of 3.7. A triplet at 2.37 ppm was assigned to H2 while H4 appeared as a multiplet at 1.94 ppm. H1 and H7 resonated at 1.62 ppm and 1.79 ppm, respectively. A profile similar to cholesterol was observed for the other ring and methyl protons. A doublet could be seen in the ^{13}C NMR spectrum of (**10**) due to the coupling effects of the fluorine with carbon and was assigned to C3. This further confirms the successful synthesis of (**10**).

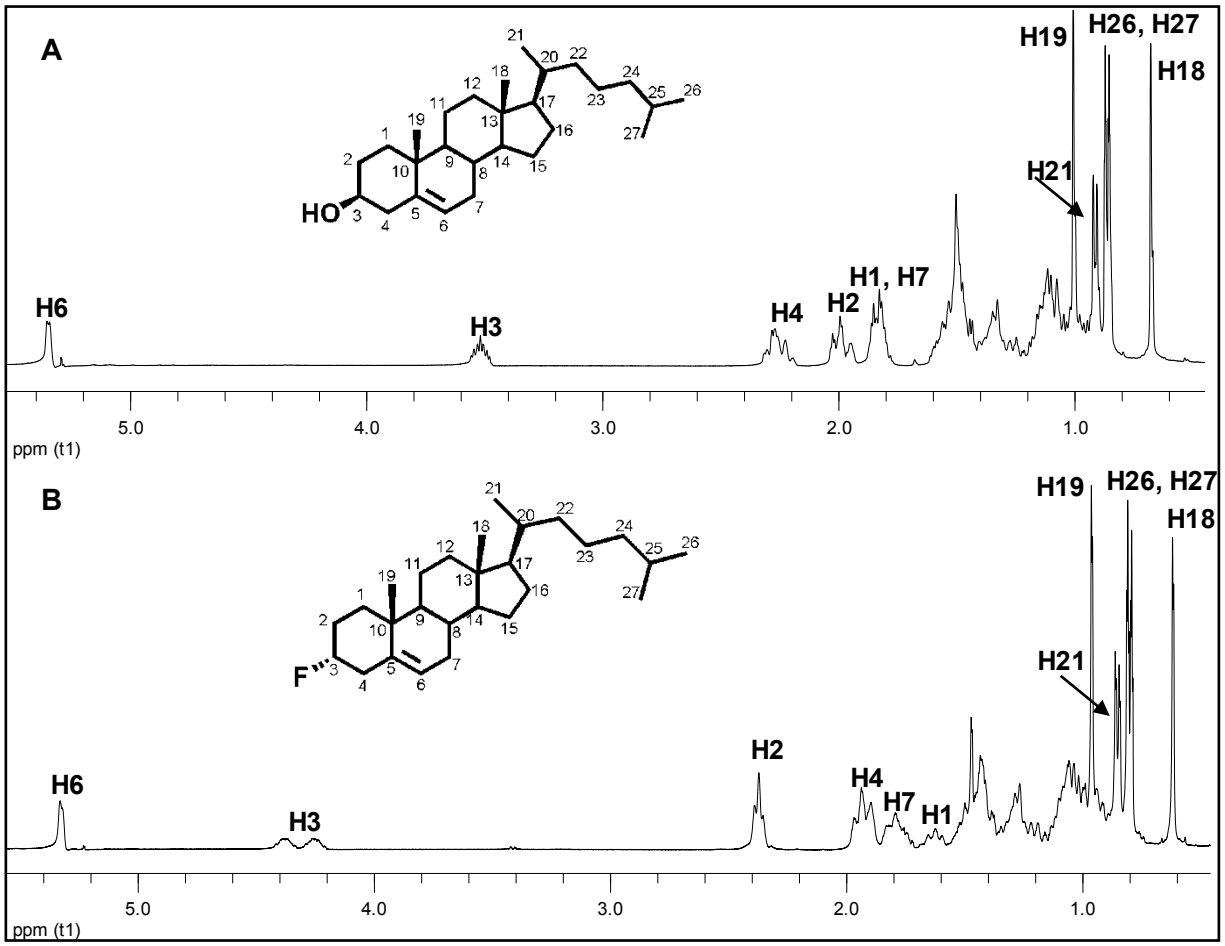

Figure 2.11: *^{1}H NMR spectra of **A:** cholesterol and **B:** 3α-fluorocholest-5-ene (**10**) in $CDCl_3$.*

2.3.2. 6β-Fluorocholestan-3β,5α-diol (12)

In order to synthesize 6β-fluorocholestan-3β,5α-diol (**12**), 5α,6α-epoxycholesterol (**11**) was prepared from cholesterol and the resulting epoxide opened using boron trifluoride etherate to afford (**12**) as shown in Scheme 2.15.

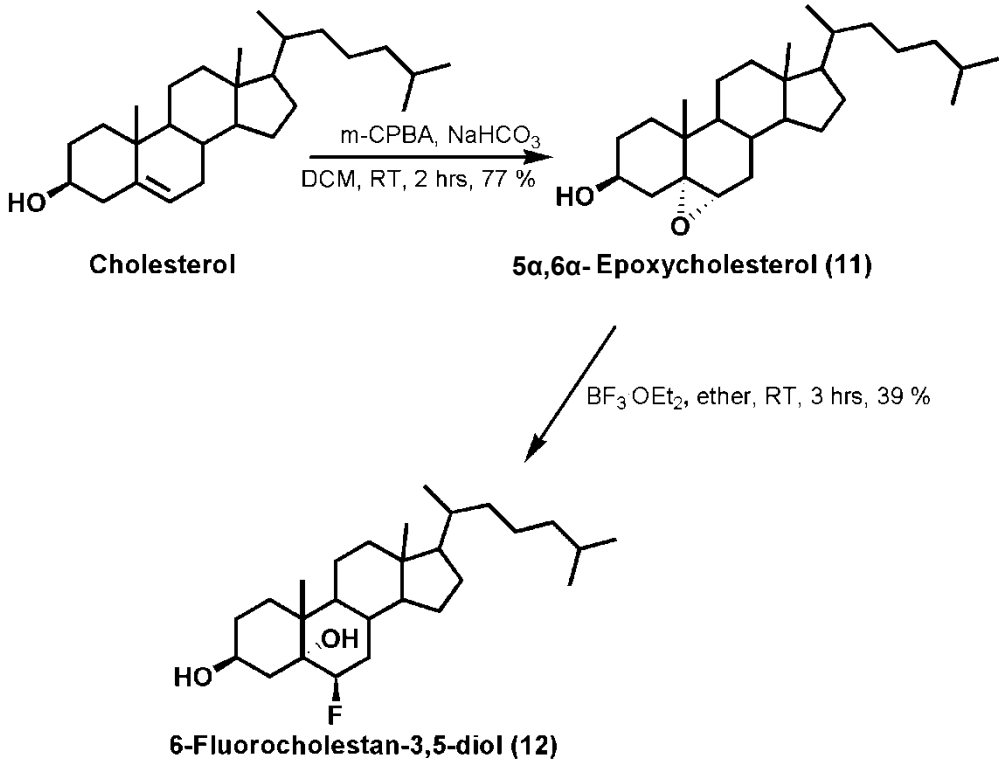

Scheme 2.15: *Synthesis of* 6β-*fluorocholestan-3β,5α-diol (**12**).*

The one-step cycloaddition of m-CPBA to cholesterol to form 5α,6α-epoxycholesterol (**11**) was prepared in dry dichloromethane following the procedure described by Ma *et al*.[19] After stirring for 2 hours, the mixture was quenched with aqueous $NaBH_4$ and the resulting residue purified by column chromatography to produce a white crystalline solid in a yield of 77 %.

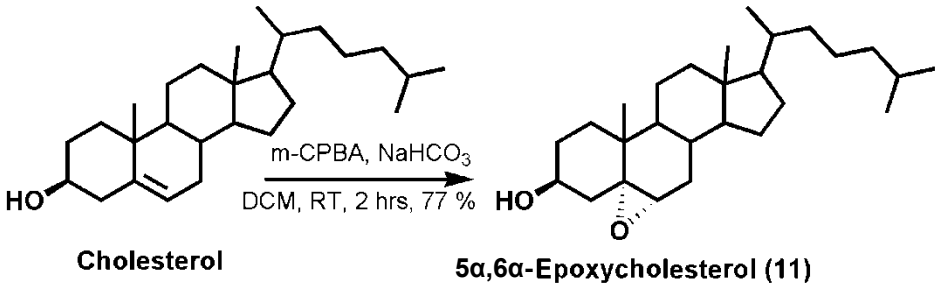

Scheme 2.16: *Synthesis of* 5α,6α-*epoxycholesterol, (**11**).*

Stereospecific epoxidation of cholesterol

In this experiment, cholesterol is stereospecifically converted to the 5α,6α-epoxide (Scheme 2.17). The presence of the angular methyl groups prevents attack on the double bond from the top. Thus, the epoxide forms exclusively on the back side (or α side) of the molecule.

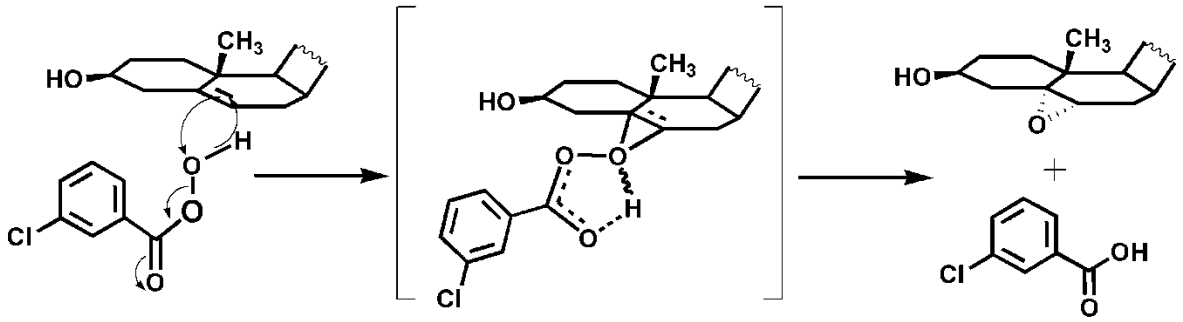

Scheme 2.17: *Formation of 5α,6α-epoxycholesterol (**11**).*

*^{1}H NMR and ^{13}C NMR spectroscopy analysis of 5α,6α-epoxycholesterol (**11**)*

In 5α,6α-epoxycholesterol (**11**), H3 now becomes the most deshielded proton due to the absence of an alkene proton and can be seen by the multiplet at 3.84 ppm in the ^{1}H NMR spectrum of (**11**) (Figure 2.12). A doublet at 2.83 ppm was assigned to H6 having a *J* value of 4.2 Hz. A triplet at 2.00 ppm was assigned to one of the protons of H2. A multiplet at 1.84 ppm integrated for three protons and was assigned to H4 and the other H2 proton, while H7 appeared as a multiplet at 1.72 ppm. 27 Carbon signals were observed in ^{13}C NMR spectrum which further confirms the formation of (**11**).

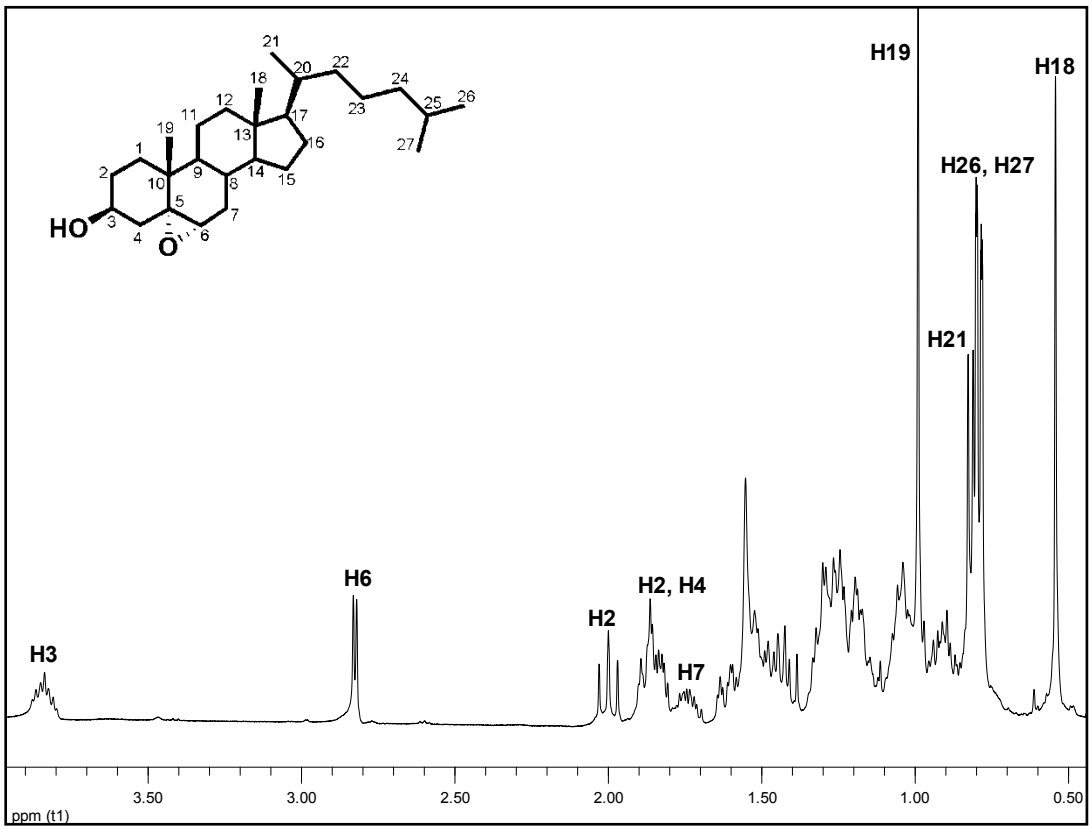

Figure 2.12: *^{1}H NMR 5α,6α-epoxycholesterol (**11**) in $CDCl_3$.*

6β-Fluorocholestan-3β,5a-diol (**12**) was synthesized from 5α,6α-epoxycholesterol (**11**) and boron trifluoride etherate. The solution was stirred under anhydrous conditions to afford (**12**) as a white solid.

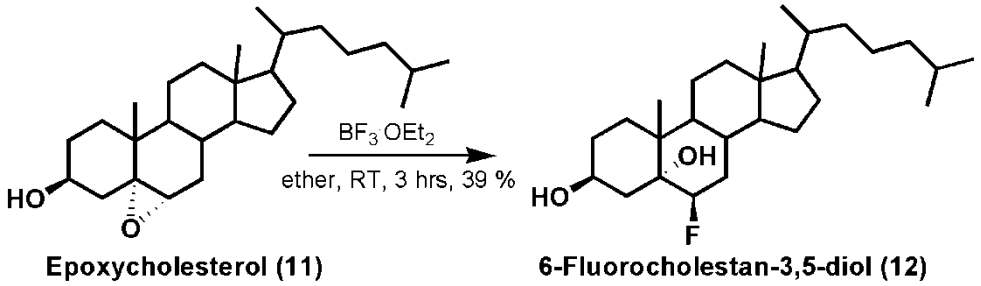

Scheme 2.18: *Synthesis of 6β-fluorocholestan-3β,5a-diol (**12**).*

Selective fluorination of epoxycholesterol

Steroidal epoxides have selectively been fluorinated with boron trifluoride complexed with diethyl ether.[20] Due to the formation of the epoxide forming exclusively from the bottom face, the only nucleophilic attack possible is from the top face to form the trans diaxial product 6β-fluorocholestan-3β,5α-diol (**12**).

*^{1}H NMR and ^{13}C NMR spectroscopy analysis of 6β-fluorocholestan-3β,5a-diol (**12**)*

The ^{1}H NMR spectrum of (**12**) revealed H6 a broad doublet between 4.32 ppm and 4.44 ppm with a *J* value of 48.8 Hz due to the coupling with the fluorine atom. H3 was observed as a multiplet at 3.72 ppm. H4 now becomes more deshielded due to the neighbouring alcohols and fluorine and shifted from 1.82 ppm to 2.06 ppm. A multiplet at 1.84 ppm integrated for four protons and was assigned to H2 and H7. In the ^{13}C NMR, C6 appeared as two distinct peaks at 92.0 ppm and 93.7 ppm due the coupling with fluorine which further confirms the synthesis of (**12**).

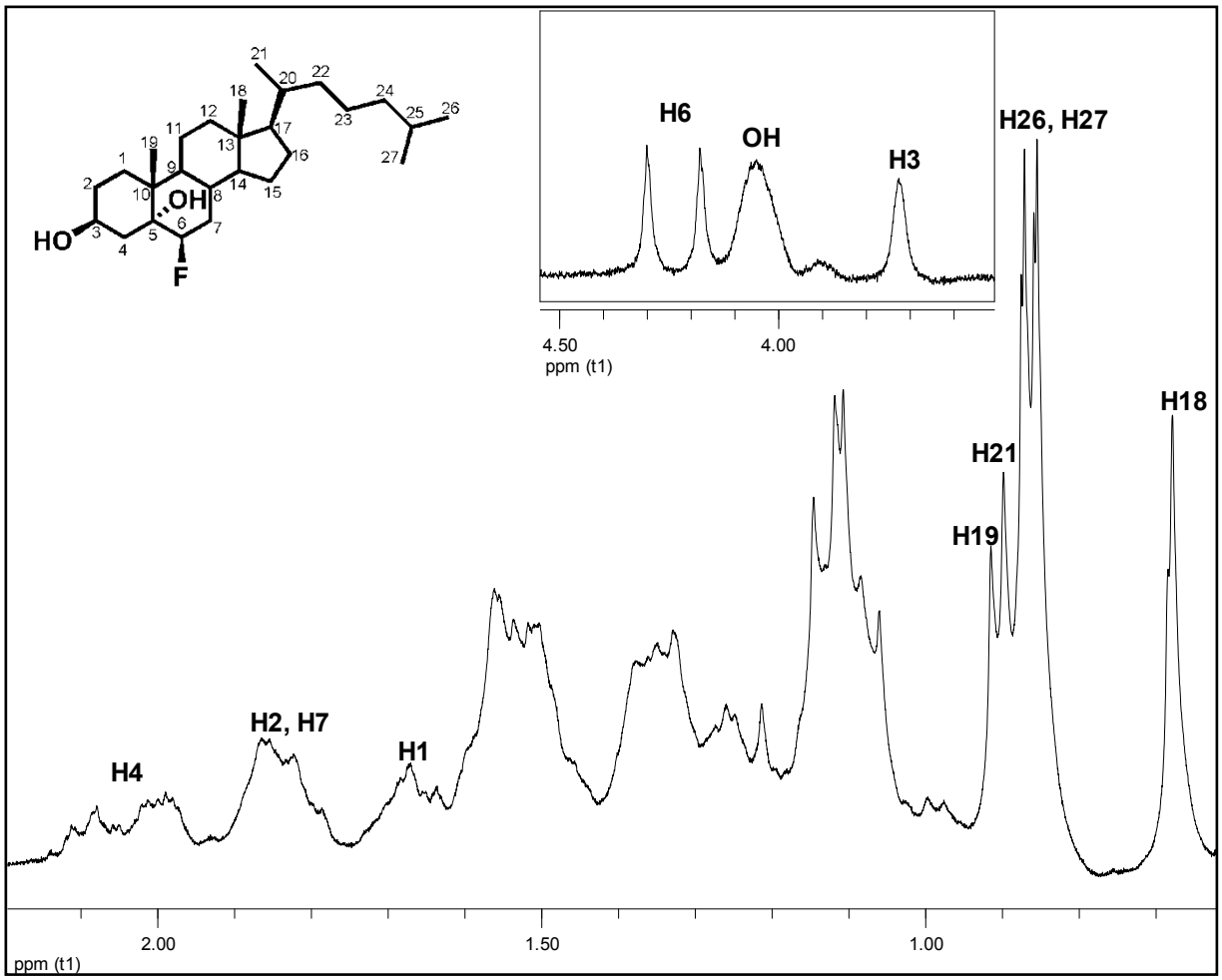

Figure 2.13: *^{1}H NMR 6β-Fluorocholestan-3β,5a-diol (**12**).*

Thia-, fluoro- and deuterium labeled cholesterol compounds have been synthesized and fully characterized to be evaluated as carbon sources for M.tb and M.smeg, respectively.

2.4. References

1. M. Ibrahim-Ouali and L. Rocheblave, *Steroids*, 2010, **75**, 701–709.

2. J. B. Johnston, A. Singh, A. A. Clary, C. K. Chen, P. Y. Hayes, S. Chow, J. J. De Voss and P. R. Ortiz de Montellano, *Bioorg. Med. Chem.*, 2012, **20**, 4064–4081.

3. E. Miao, S. R. Wilson and N. B. Javitttl, *Biochem. J.*, 1988, **255**, 1049–1052.

4. M. D. Rahman and R. A. Pascal, *J. Biol. Chem.*, 1990, **265**, 4989–4996.

5. H. Ouellet, J. B. Johnston and P. R. O. de Montellano, *Trends Microbiol.*, 2011, **19**, 530–539.

6. X. Yang, E. Dubnau, I. Smith and N. S. Sampson, *Biochemistry*, 2008, **46**, 9058–9067.

7. M. J. Armstrong and M. C. Carey, *J. Lipid Res.*, 1987, **28**, 1144–1155.

8. A. Ternay, *Organosulfur Compounds as ChemDefense Agents - Mustard*, 20030122 064, Colorado, 2001.

9. A. Bajaj, P. Kondaiah and S. Bhattacharya, *Bioconjug. Chem.*, 2008, **19**, 1640–1651.

10. J. W. Ralls, R. M. Dodson and B. Riegel, *J. Am. Chem. Soc*, 1949, **785**, 3320–3325.

11. R. M. Dodson and B. Riegel, *J. Org. Chem*, 1948, **13**, 424–437.

12. R. G. Pearson, L. Carroll and H. Langer, *J. Am. Chem. Soc*, 1951, **73**, 4149–4152.

13. M. D. Rahman and A. Pascal, *J. Biol. Chem.*, 1990, **265**, 4989–4996.

14. R. Kanagasabai, W. Zhou, J. Liu, T. T. M. Nguyen, P. Veeramachaneni and W. D. Nes, *Lipids*, 2004, **39**, 737–746.

15. H. Jungyeob and C. Jungwook, Patent, WO 2004/ 094450 A1, 2004.

16. E. Stastná, I. Cerný, V. Pouzar and H. Chodounská, *Steroids*, 2010, **75**, 721–725.

17. P. Ferraboschi, A. Fiecchi, P. Grisenti, E. Santaniello and S. Trave, *Synth. Commun.*, 1987, **17**, 1569 – 1575.

18. J. Liu, PhD Thesis, Texas Tech University, 2008.

19. E. Ma, H. Kim and E. Kim, *Steroids*, 2005, **70**, 245–250.

20. G. Haufe, *Thieme*, http://www.thieme-chemistry.com/fileadmin/Thieme/HW-100/pdf/march/wm_34_9_Haufe.pdf, 2005, (Accessed: August 2012).

Chapter 3

Synthesis and characterization of thiastearic acids

3.1. Introduction

As discussed in chapter 1, fatty acids (FAs) play an integral part in the survival of M.tb. FAs are incorporated into the mycobacterial cell wall which aid in protection and assist in the functioning of the pathogen.[1,2] Thia-fatty acids are FAs comprising of sulfur and are chemically similar to normal FAS, though thia-fatty acids can produce various metabolic effects depending on the position of sulfur within the FA chain.[3] The current study required the synthesis of thiastearic acids as well as evaluation of the metabolic effects these compounds have on both M.tb and M.smeg.

The synthesis of the thiastearic acids were carried out utilizing the protocol described by Rahman *et al*.[4] The bromo-carboxylic acid was reacted with an alkylthiol of the appropriate chain length to produce thiastearic acid derivatives containing sulfur in positions 9, 10 and 11. In the event of the suitable bromo-carboxylic acid not being commercially available, the bromo-alcohol was purchased and oxidized to the corresponding carboxylic acid as shown in Scheme 3.1.

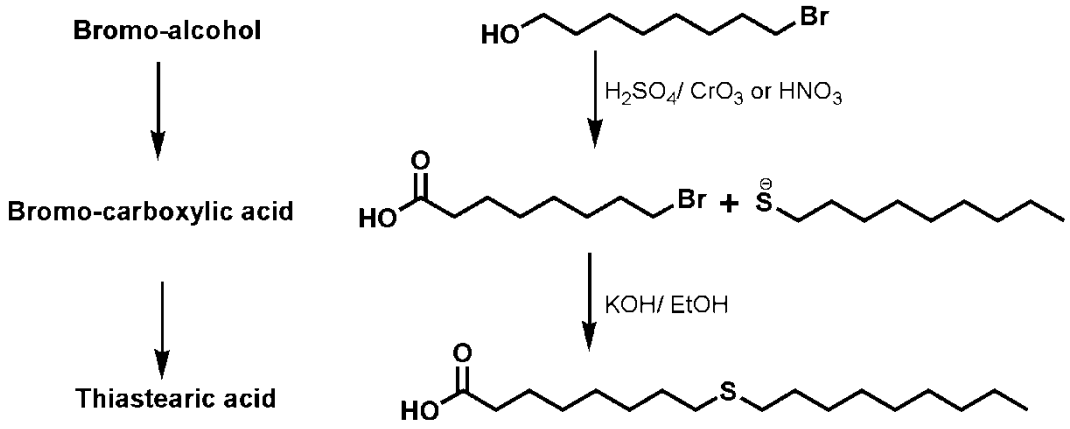

Scheme 3.1: *Synthesis of thiastearic acid.* [4]

3.2. Bromo-carboxylic acids

3.2.2. Synthesis and physical properties of the bromo-carboxylic acid

The synthesis of the bromo-carboxylic acid was carried out according to two different procedures described by Buchanan *et al.* and Meijler *et al.*, respectively.[1,5] In this study,

9-bromononanol was oxidized to the corresponding carboxylic acid using either nitric acid or chromium trioxide as shown in Scheme 3.2.

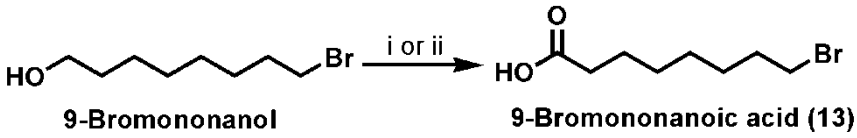

9-Bromononanol **9-Bromononanoic acid (13)**

i: CrO_3, H_2SO_4, H_2O, 0 °C, 2 hrs, RT, 16 hrs, 77 %. ii: HNO_3, RT, 4 hrs, 80 °C, 1 hr, 60 %.

Scheme 3.2.: *Synthesis of 9-bromononanoic acid (**13**).*[1,5]

The procedure using concentrated nitric acid was carried out by stirring the acid with the alcohol at room temperature for 4 hours followed by stirring at 80 °C for an additional hour. After extracting with diethyl ether, the solvent was evaporated to yield the carboxylic acid as a white solid.

The technique by Meijler *et al*. followed a Jones oxidation method whereby the alcohol was allowed to stir at 0 °C for 2 hours followed by stirring at room temperature for 16 hours with a solution of chromium trioxide, concentrated sulfuric acid and water.[1,5] Upon completion, an extraction with diethyl ether was carried out and the resulting residue purified using column chromatography to produce a colourless oil in a greater yield as compared to using nitric acid. In addition, a colourless oil was obtained as product and not a solid as in the case described above.

3.2.3. Characterization of 9-bromononanoic acid (13)

^{1}H NMR and ^{13}C NMR spectroscopy

The ^{1}H NMR spectrum of 9-bromononanoic acid (**13**) is shown in Figure 3.1. All proton signals were observed between 1.34 ppm and 3.44 ppm. No signal in the region of 11.0 ppm was observed for the carboxylic acid proton due to possible exchange with a deuterium atom. The most deshielded proton is H9 due to the adjacent bromide and was detected as a triplet at 3.34 ppm due to coupling with H8 and a *J* value of 6.9 Hz was observed. H2 appeared as a triplet at 2.28 ppm while a multiplet at 1.79 ppm was assigned to H8. A multiplet at 1.57 ppm was allocated to H3 while the most shielded protons (H4 – H7) occurred at 1.34 ppm as a multiplet. The ^{1}H NMR spectra agrees well with those described by both Buchanan *et al.* and Meijler *et al.*[1,5] The ^{13}C NMR spectrum displayed a signal at 180.1 ppm due to carboxylic acid carbon and 7 carbon signals were observed due to possible overlap of C4 – C7 signals.

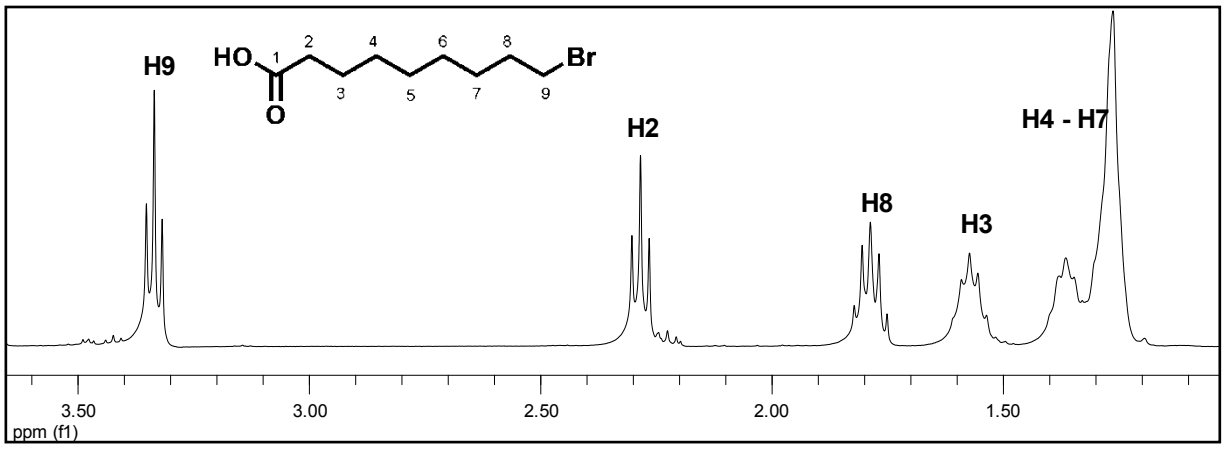

Figure 3.1: *^{1}H NMR 9-bromononanoic acid (**13**) in $CDCl_3$.*

3.3. Thiastearic acids

Synthesis and physical properties of thiastearic acids

Thiastearic acids were prepared by substituting sulfur in position 9, 10 and 11 (Figure 3.2). The synthesis was carried out from bromo-carboxylic acids and a 1:1 molar ratio of the corresponding alkylthiol using the method described by Rahman *et al*.[6] Potassium hydroxide was added to the acid and the mixture refluxed in absolute ethanol for 2 hours. After acidifying with glacial acetic acid, the product was extracted with dichloromethane and washed with water. Recrystallization of the resulting residue from acetone resulted in solids of low to moderate yields. Low yields could possibly be due to the formation of volatile elimination products. The physical appearance, yield and melting points are listed in Table 3.1.

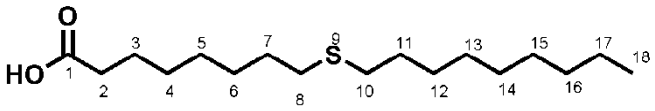

Figure 3.2.: *Chemical structure of 9-thiastearic acid (**14**).*

Table 3.1.: *Physical appearance, yield and melting points of thiastearic acids.*

Compound	Physical appearance	Yield (%)	Melting point (°C)	Literature melting point (°C)
14	white solid	35	43 – 45	51 – 52[7]
15	Light pink solid	78	40 – 42	46 – 47[7]
16	white solid	32	47 – 49	45 – 46[4]

9-Thiastearic acid (14**), 10-thiastearic acid (**15**) and 11-thiastearic acid (**16**)*

3.3.1. Characterization of thiastearic acids

^{1}H NMR and ^{13}C NMR spectroscopy

The synthesis of the thiastearic acids were confirmed using ^{1}H and ^{13}C NMR spectroscopy. The ^{1}H NMR spectrum of 10-thiastearic acid is shown in Figure 3.3 and was synthesized from 9-bromononanoic acid (Section 3.2). An upfield shift of H9 was observed from 3.34 ppm to 2.49 ppm since the bromide is no longer present in the thiastearic acid. Due to the presence of the carboxylic acid, a triplet at 2.34 ppm was assigned to H2 while a multiplet at 1.58 ppm integrating for six protons was assigned to H3, H8 and H12. The most shielded protons, H18, appeared as a triplet at 0.88 ppm. The additional protons (H4 – H7, H13 – H17) appeared as a multiplet at 1.31 ppm. A similar ^{1}H NMR spectrum was observed for the other thiastearic acids. The ^{13}C NMR spectrum showed the carboxylic acid carbon in the region of 180.0 ppm and the carbons adjacent to the sulfur in the region of 29.0 ppm as a single peak.

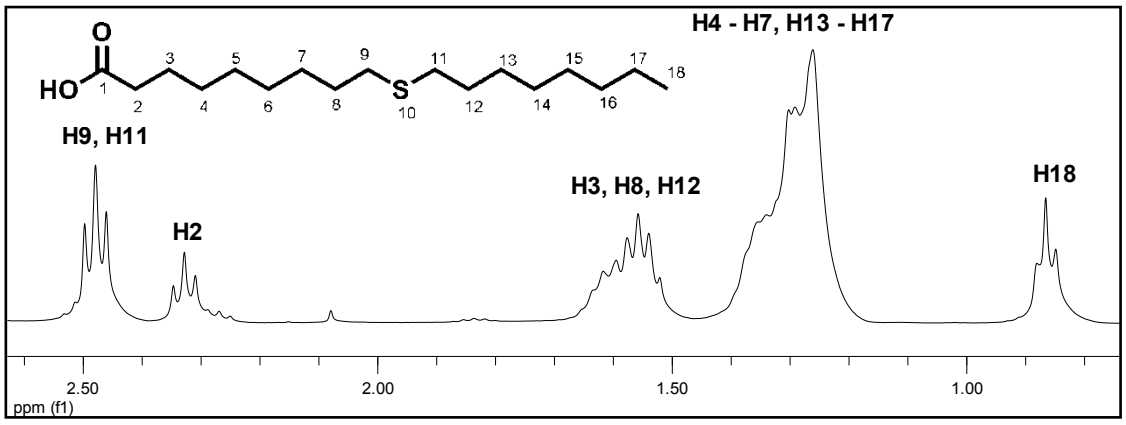

Figure 3.3: *^{1}H NMR 10-thiastearic acid (**15**) in $CDCl_3$.*

3.4. Thiastearic sulfoxides

Due to the possible desaturation (Section 1.3.4) of the thiastearic acids, the sulfur atom is expected to become oxidized. For this reason, the thiastearic acids were oxidized to the sulfoxide to be utilized as standards for GC-MS analysis to assess whether oxidation of the thiastearic acids was carried out by M.tb and M.smeg, respectively. The sulfoxides were prepared by stirring the thiastearic acid in the presence of hydrogen peroxide. White solids were obtained as products with moderate yields. The physical appearances, yields and melting points are shown in Table 3.2.

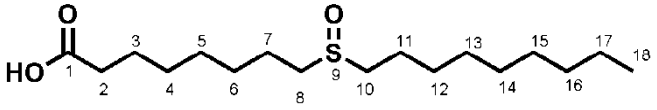

Figure 3.4.: *Chemical structure of 8-(nonylsulfinyl)octanoic acid (**17**).*

Table 3.2.: *Physical appearance, yield and melting points of thiastearic sulfoxides.*

Compound	Physical appearance	Yield (%)	Melting point (°C)	Literature melting point (°C)
(**17**)	white solid	42	81 – 82	78 – 80[7]
(**18**)	white solid	42	76 – 77	77 – 79[7]
(**19**)	white solid	50	78 – 70	–

** 8-(Nonylsulfinyl)octanoic acid (**17**), 9-(octylsulfinyl)nonanoic acid (**18**) and 10-(heptylsulfinyl)decanoic acid (**19**)*

3.4.1. Characterization of thiastearic sulfoxides

^{1}H NMR and ^{13}C NMR spectroscopy

The ^{1}H NMR spectra of 11-thiastearic acid (**16**) and its corresponding sulfinyl acid are shown in Figure 3.3. In the ^{1}H NMR spectrum of (**16**), H18, the most shielded protons appeared as a multiplet at 0.87 ppm. H10 and H12 resonated at 2.49 ppm due to the adjacent sulfur atom while H2 appeared as a triplet at 2.34 ppm. A multiplet at 1.59 ppm integrated for 6 protons and was assigned to H3, H9 and H13. The rest of the protons on the chain appeared as a multiplet between 1.29 – 1.37. A similar profile was observed for the sulfinyl derivative with a slight downfield shift of H10 and H12 due to the presence of the sulfoxide. The peaks for (**19**) generally appeared broader in the ^{1}H NMR spectrum.

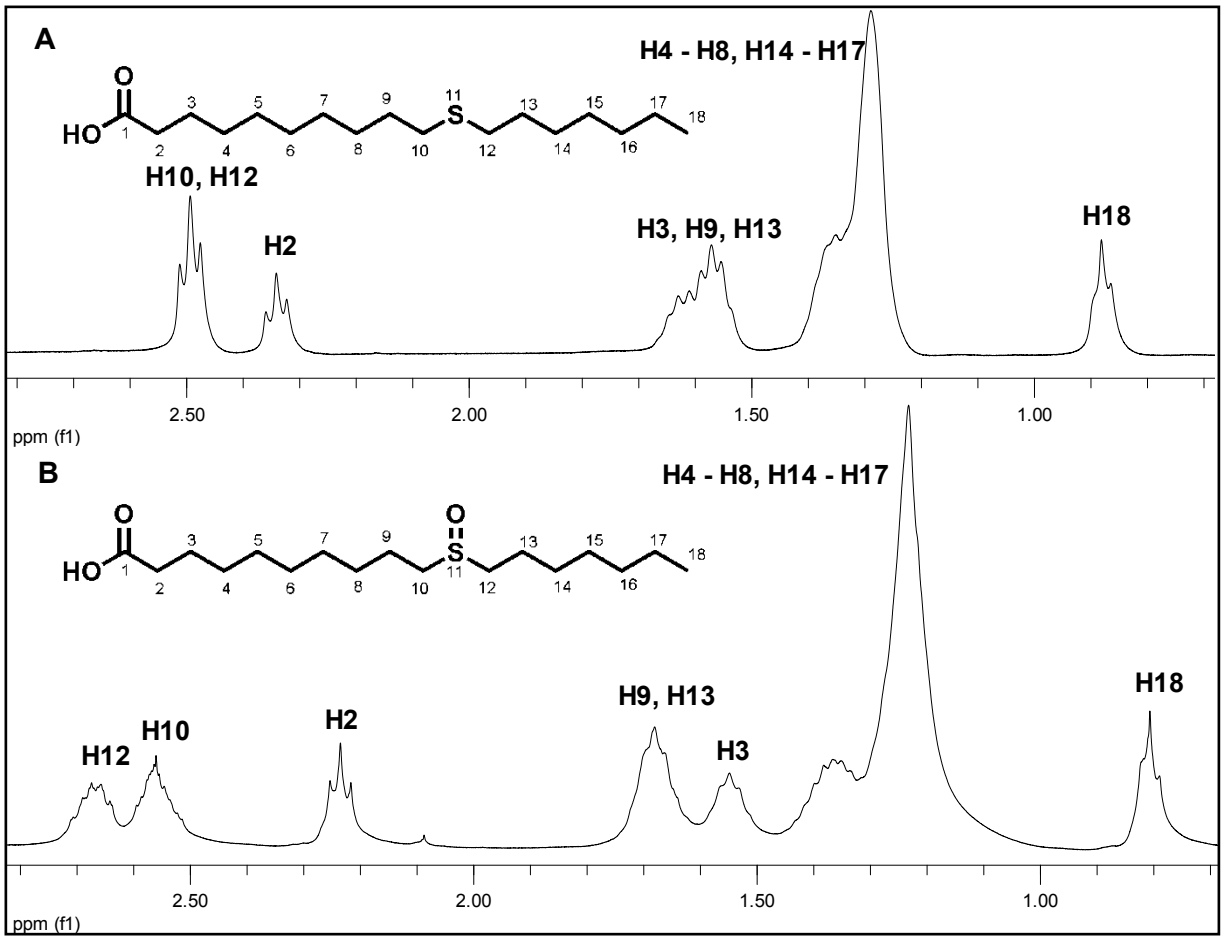

Figure 3.5: *^{1}H NMR of **A:** 11-thiastearic acid (**16**) and **B:** 10-(heptylsulfinyl)decanoic acid (**19**) in $CDCl_3$.*

The successful synthesis of the sulfoxy-acids was further confirmed by the use of mass spectroscopy. A [M+H] was determined to be 319.2 as expected.

The compounds synthesized were further evaluated as possible carbon sources for M.tb and M.smeg and the metabolism of the compounds analyzed by GC-MS.

3.5. References

1. M. M. Meijler, N. Amara and J. Rayo, Patent, 2011001419 A1, 2011.

2. V. Briken, S. A. Porcelli, G. S. Besra and L. Kremer, *Mol. Microbiol.*, 2004, **53**, 391–403.

3. S. Skrede, H. N. Sorensen, L. N. Larsen, H. H. Steineger, K. Hovik, O. S. Spydevold, R. Horn and J. Bremer, *Biochim. Biophys. Acta.*, 1997, **1344**, 115–131.

4. M. D. Rahman, D. L. Ziering, S. J. Mannarelli, K. L. Swartz, D. S. Huang and R. A. Pascal, *J. Med. Chem.*, 1988, **31**, 1656–1659.

5. G. W. Buchanan, R. Smits and E. Munteanu, *J. Fluor. Chem*, 2003, **123**, 255–259.

6. M. D. Rahman, H. M. Seidel and R. A. Pascal, *J. Lipid Res.*, 1988, **29**, 1543–1548.

7. R. A. Pascal and D. L. Ziering, *J. Lipid Res.*, 1986, **27**, 221–224.

Chapter 4

Growth response of M.tb and M.smeg to various cholesterol and stearic acid derivatives

4.1. Introduction

As covered in chapter 1, M.tb catabolizes lipids such as cholesterol and fatty acids.[1] As a result, the catabolic pathways are excellent drug targets for the development of novel and more efficient antitubercular drugs. Biomarkers that can indicate the presence or effect of lipid metabolic pathway inhibitors would be indispensable in biological studies and drug discovery efforts.

Numerous thiacholesterol and thia-fatty acids such as thiastearic acid have been synthesized before and utilized to probe the CYP450 enzymes responsible for lipid metabolism. Miao *et al.* used crude CYP450 enzymes isolates to evaluate the metabolism of (20*S*)-22-thiacholesterol.[2] The study confirmed that oxidation took place and that the S-oxidized product formed. The oxidized product prevented further catabolism from taking place and hence, could be considered as a competitive inhibitor of the CYP450 enzymes. Other thiacholesterol derivatives include 24-thiacholesterol, which showed moderate inhibition of *C.albicans* growth while 23-thiacholestanol had little inhibitory effect on the growth of *C.fasciculata*.[3,4] Due to the low inhibitory effect of 23-thiacholestanol, it can possibly be used to probe the CYP450 mediated catabolism since bacterial growth can be expected. The effect of thiacholesterol derivatives on bacterial growth has been evaluated in several microorganisms. However, the growth of M.tb in the presence of such compounds remains to be determined. Examples of other thia-lipids include thiastearic acids which were used to probe the Δ^9-desaturase (Section 1.5). Alloatti *et al.* studied the impact on the growth of *T.cruzi* in response to various thiastearic acids and established that 9-thiastearic acid had little effect whereas 10-thiastearic acid produced complete inhibition.[5] The growth of other microorganisms such as *C.fasciculata*, *T.brucei* and *S.cerevisiae* have also been assessed in the presence of several thiastearic acids with differences in growth brought about as a result of the placement of a sulfur atom along the stearic acid chain.[6–8] The growth of M.tb has however not yet been evaluated in the presence of thia-fatty acids such as thiastearic acids. For this reason, cholesterol and stearic acid were modified to include a sulfur atom to establish its effect on the growth of M.tb and M.smeg and to determine whether the synthesized compounds can be utilized as alternative carbon sources to the natural substrates, cholesterol and stearic acid. Fluorine and deuterium labeled compounds have also been synthesized and the growth of M.tb and M.smeg monitored in the presence of these compounds. The results obtained are discussed below.

4.2. Evaluation of cholesterol derivatives as carbon sources

4.2.1. Effect on growth of M.tb in the presence of cholesterol derivatives

M.tb growth curves were obtained by growing the culture in a medium containing 0.1 % cholesterol or cholesterol derivative and the optical density monitored at 600 nm (OD_{600}) over 28 days. From the growth curves obtained (Figure 4.1), the growth with cholesterol was observed to be significantly greater compared to the synthesized compounds as noted by the higher OD_{600} readings. A longer lag phase was observed with the cholesterol analogs. From the compounds synthesized, 23-thiacholest-4-en-3-one was observed to be the best substrate with a steeper growth curve and higher OD readings obtained between 9 – 16 days. 6β-fluorocholestan-3β,5α-diol was found to be the least favored substrate with a lag phase of 9 days and lowest OD readings obtained for the first 16 days.

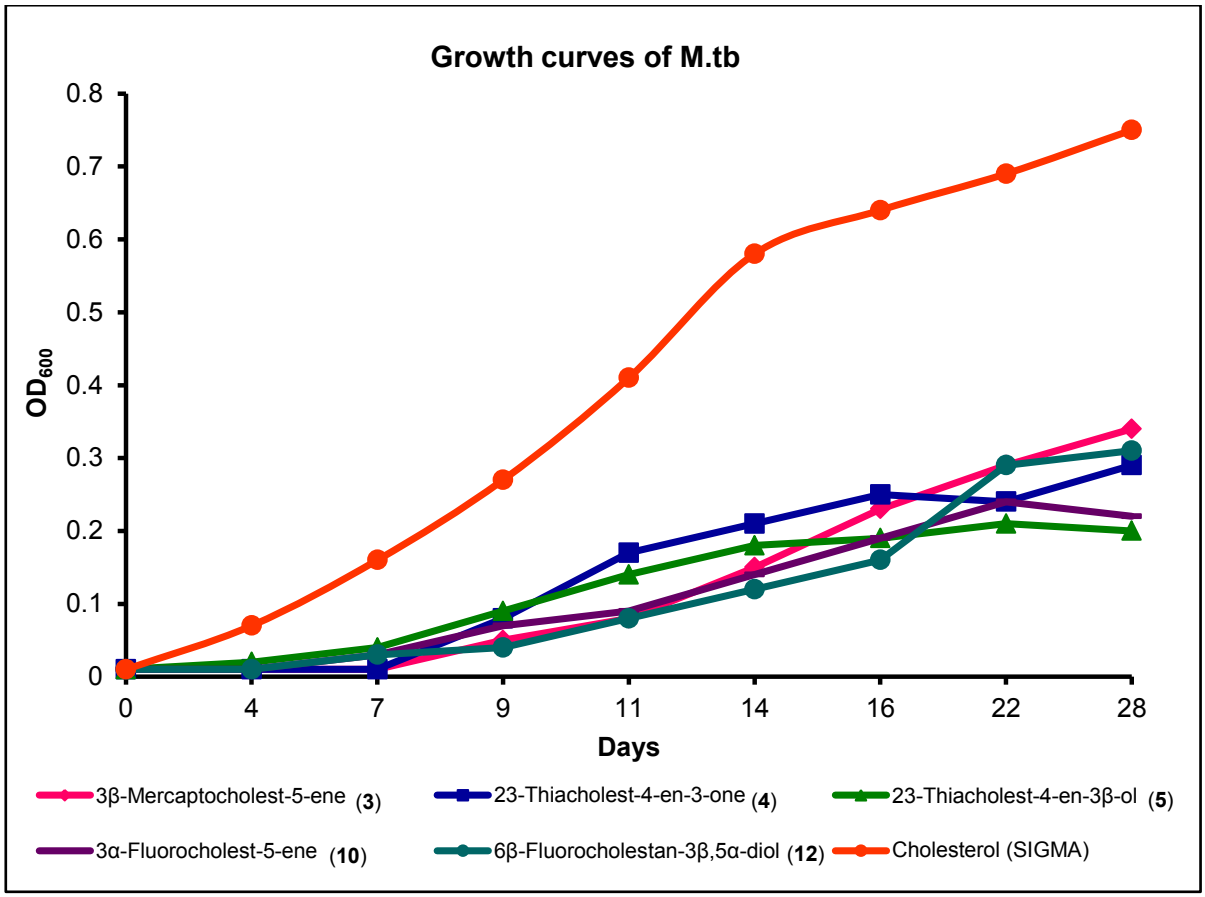

Figure 4.1: *Growth curves of M.tb with cholesterol and cholesterol analogs as carbon sources.*

4.2.2. Effect on growth of M.smeg in the presence of cholesterol derivatives

The growth of M.smeg on cholesterol is well established and documented.[9,10] In the current study, M.smeg was grown in several stages as described by Wang *et al*.[11] The culture was streaked out on agar containing Middlebrook 7H9 broth, glycerol, NaCl, Tween® 80 and water and incubated at 37 °C for 4 days. The culture was subsequently grown in stages with increasing dependency on cholesterol as the carbon source (Scheme 4.1). The effectiveness of the synthesized compounds as carbon sources were then evaluated by incubating with a final concentration of 0.1 % of each compound and monitoring the OD_{595} readings over 4 days. All growth curves were performed in triplicate.

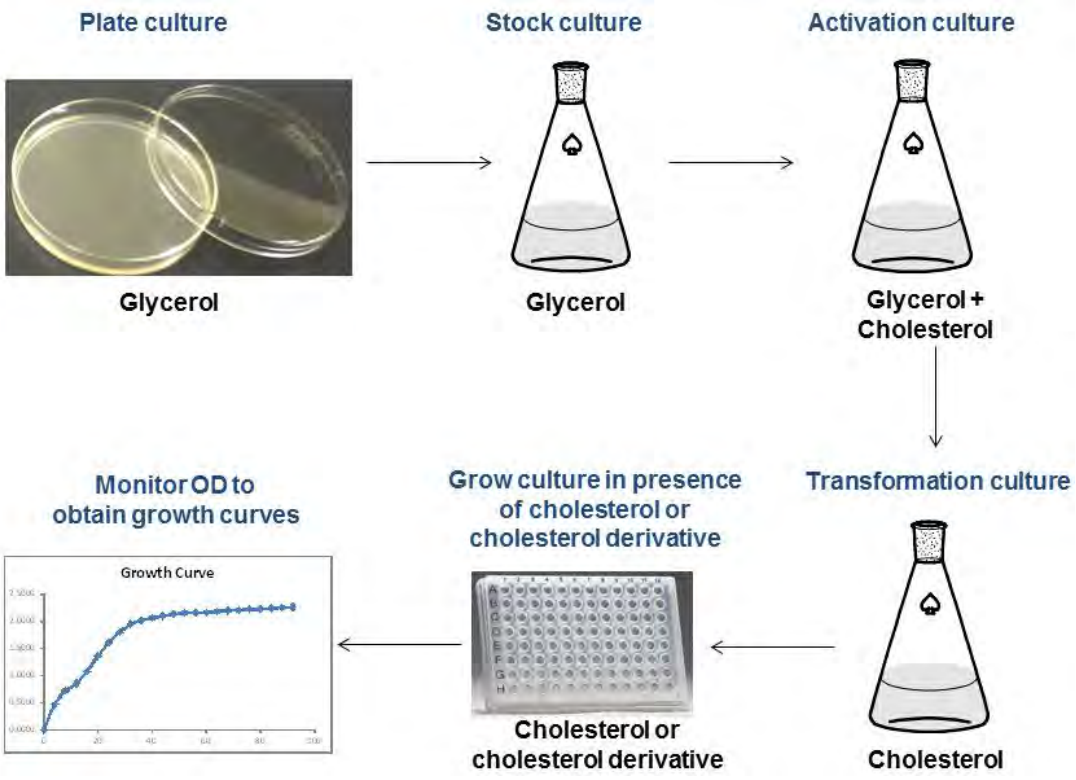

Scheme 4.1: *Growth conditions of M.smeg and determination of growth curves. The carbon source is throughout each growth stage is indicated* [11-13]

Cholesterol catabolism is initiated by the conversion to cholest-4-en-3-one by the enzyme 3β-HSD (Section 1.7.4) in which the presence of the 3β-substituent plays a significant role in the binding to the enzyme. By inhibiting the action of 3β-HSD, bacterial growth can be monitored to establish whether or not side-chain degradation can still occur. To this end, in both 3β-mercaptocholest-5-ene (**3**) and 3α-fluorocholest-5-ene (**10**), the C3-positions have been modified. The growth of M.smeg was monitored in the presence of these compounds and the growth curves are shown in Figure 4.2. Within the first 4 hours a similar growth pattern was observed with cholesterol and (**3**). For the time interval 8 – 20 hours, (**3**) was utilized as the favoured substrate while (**10**) was utilized as the least effective carbon source.

After 20 hours, the growth in the presence of (**3**) has reached a stationary state while steady growth was observed with (**10**). The positive growth of M.smeg in the presence of (**3**) and (**10**) suggests that side-chain degradation can occur independent of 3β-HSD activity.

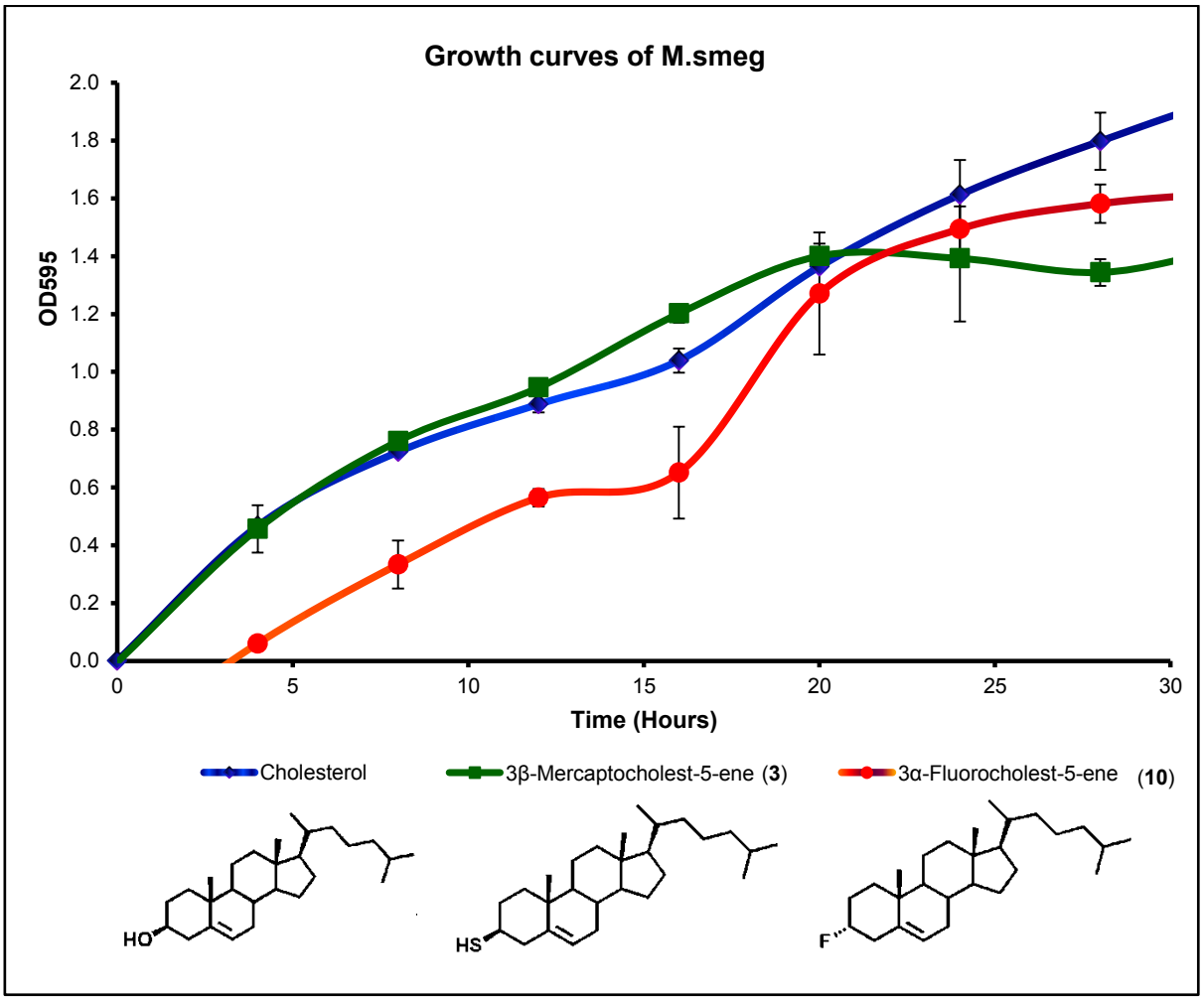

Figure 4.2: *Growth curves of M.smeg with cholesterol, 3β-mercaptocholest-5-ene (**3**) and 3α-fluorocholest-5-ene (**10**) as carbon sources.*

Studies on the effect of side-chain modification of cholesterol on the growth of M.smeg were also performed. M.smeg was grown in the presence of cholesterol analogs with a sulfur atom placed in position C23. These compounds include 23-thiacholest-4-en-3-one (**4**), which is a sulfur derivative of the first cholesterol catabolic product, cholest-4-en-3-one. For the first 16 hours, the rate of growth with (**4**) was the same as for cholesterol after which cholesterol becomes the favoured substrate. During the catabolism of (**4**), sulfur is not expected to be oxidized as the sulfur atom is present in an odd numbered carbon position. This can be seen by the cholesterol catabolic pathway published by Quellet *et al.*[12] Thus, since no S-oxidation is expected to occur, the growth reduction is most likely not due to the presence of S-oxidized products which could possibly hinder further degradation from taking place. The

potential of 23-thiacholest-4-en-3β-ol (**5**) and its deuterium labeled derivative have also been assessed as carbon sources for M.smeg. A similar growth pattern was expected with these two compounds as a result of the similarity in structures, which was observed for the first 12 hours. After 12 hours, (**5**) becomes the favoured substrate with higher OD readings. In the presence of the deuterium labeled derivatives, [3α-^{2}H]23-thiacholest-4-en-3β-ol (**8**) and [3α-^{2}H]cholest-4-en-3β-ol (**9**), similar growth was bserved for the first 16 hours after which (**8**) becomes the favored substrate. The growth curves are shown in Figure 4.3.

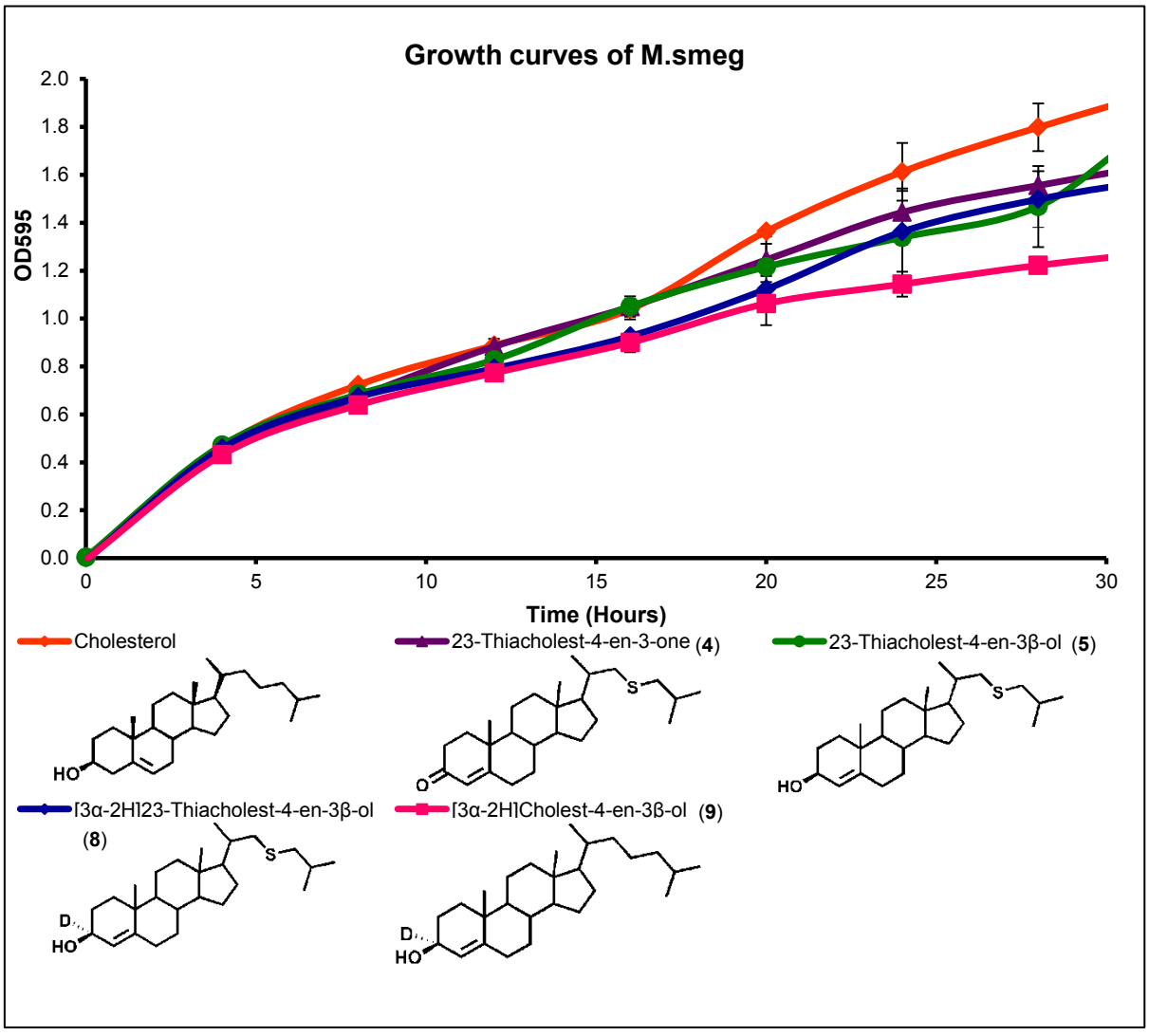

Figure 4.3: *Growth curves of M.smeg with cholesterol, 23-thiacholest-4-en-3-one (**4**), 23-thiacholest-4-en-3β-ol (**5**), [3α-^{2}H]23-thiacholest-4-en-3β-ol (**8**) and [3α-^{2}H] cholest-4-en-3β-ol (**9**) as carbon sources.*

6β-Fluoro-steroids have previously been evaluated as inhibitors in various organisms.[14,15] In this study 6β-fluorocholestan-3β,5α-diol (**12**) was assessed as a substrate for growth of M.smeg. Within the first 4 hours, cholesterol becomes the favoured substrate although growth was observed in the presence of (**12**) and after 28 hours a stationary phase was obtained. The growth curves are shown in Figure 4.4.

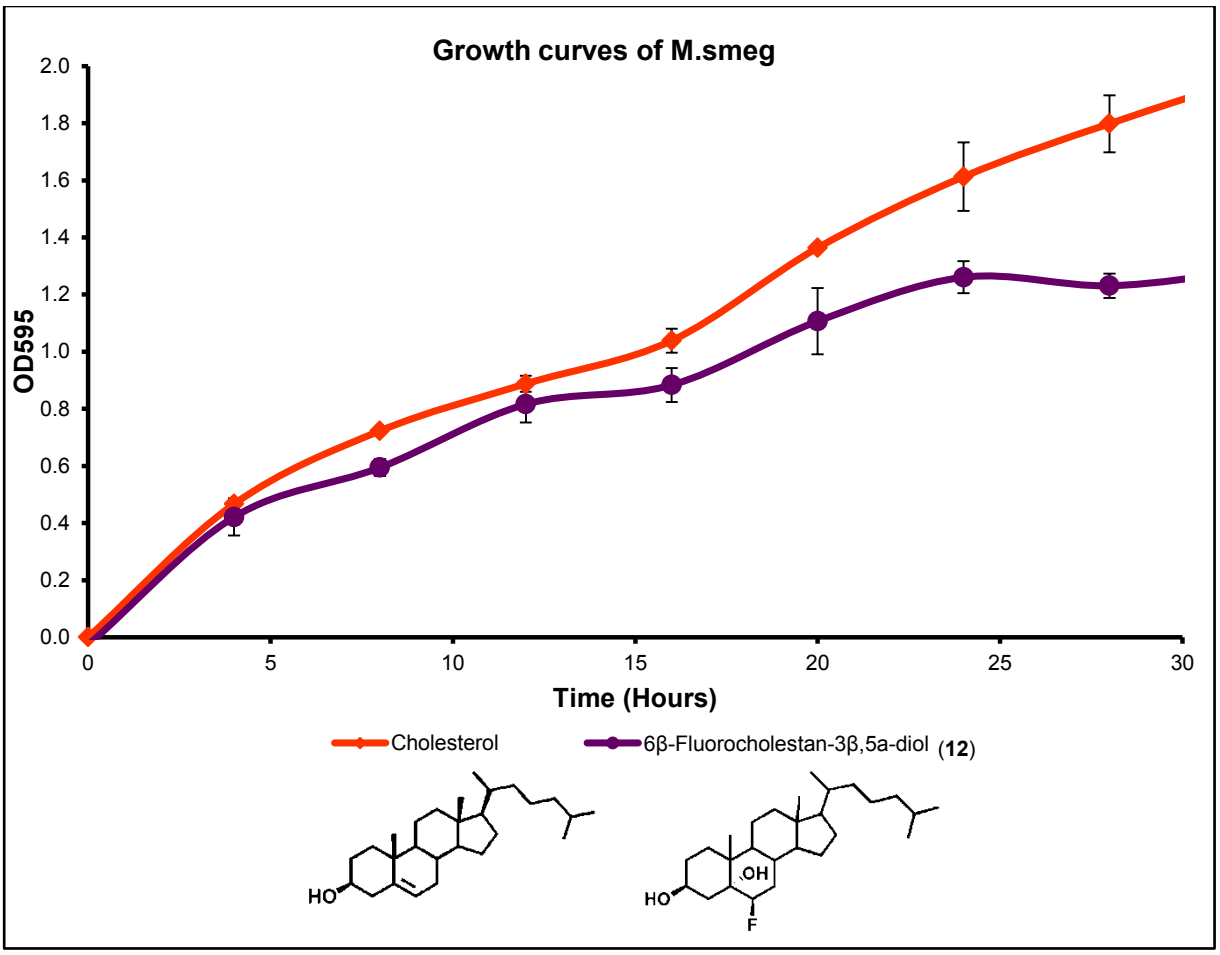

Figure 4.4: *Growth curves of M.smeg with cholesterol and 6β-fluorocholestan-3β,5α-diol* (**12**) *as carbon sources.*

4.3. Utilization of the thiastearic acid derivatives as carbon sources

4.3.1. Effect on growth of M.tb in the presence of thiastearic acid derivatives

M.tb was cultured in the presence of 0.1 % thiastearic acid derivatives. The growth curves are shown in Figure 4.5. These curves suggest that the stearic acid derivatives are more favorable substrates for mycobacterial growth compared to the cholesterol analogs as shown by the steeper growth curves and higher OD readings.

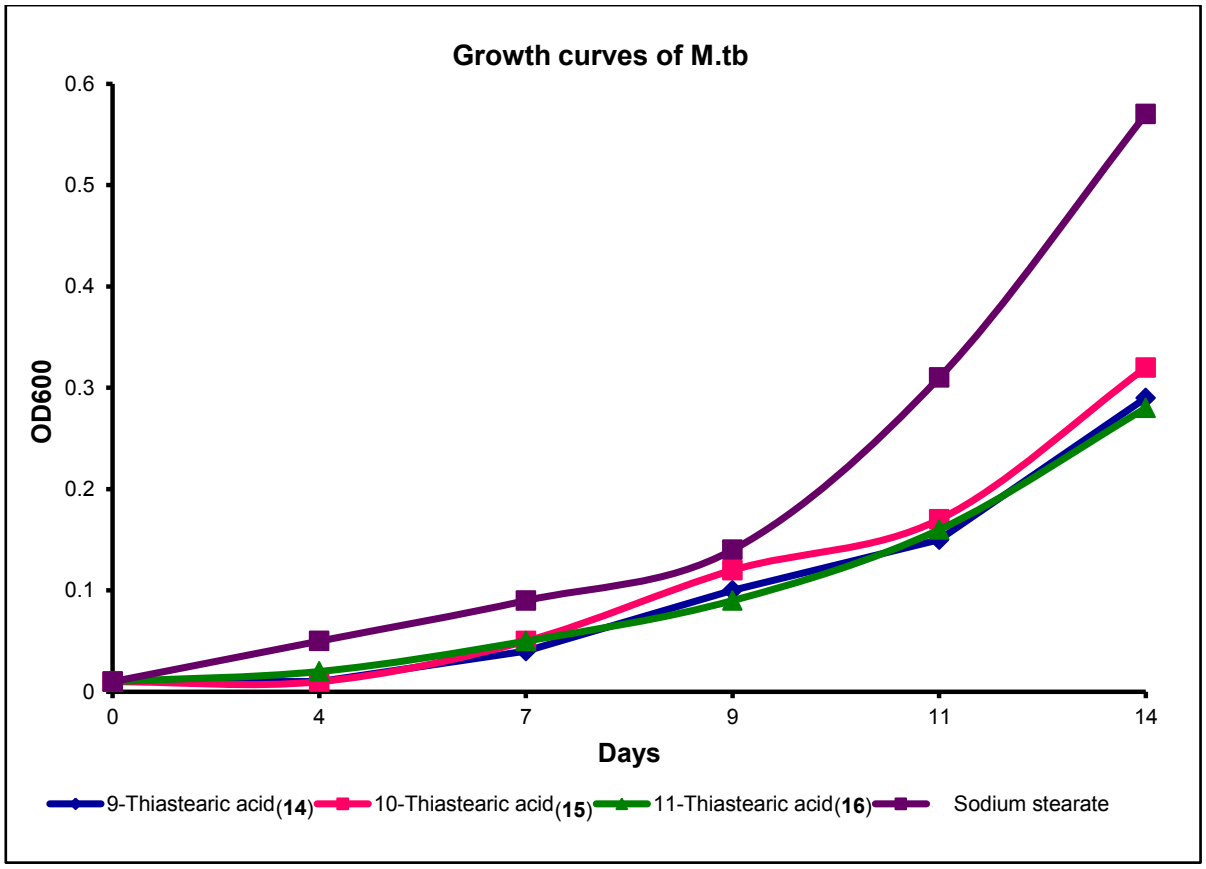

Figure 4.5: *Growth curves of M.tb with thiastearic acid as carbon sources.*

4.3.2. Effect on growth of M.smeg in the presence of thiastearic acid derivatives

To determine whether or not M.smeg can utilize the thiastearic acids as carbon sources, a culture was grown in 0.1 % thiastearic acid and the OD_{595} readings monitored over 4 days (Figure 4.6). All growth curves were performed in triplicate. Depending on the position of sulfur within the carbon chain of thiastearic acid, the fatty acids are expected to be S-oxidized *via* the action of Δ^9-desaturase. To determine whether or not the S-oxidized compounds will act as inhibitors and prevent further desaturation from occurring, the S-oxidized derivatives were also evaluated as possible carbon sources. From the growth curves obtained it can be seen that M.smeg utilizes the thiastearic acids as the favored substrates compared to the S-oxides, with 9- and 10-thiastearic acid being the most favored

substrate. Growth in the presence of the S-oxides was observed, indicating that these compounds can also be utilized as a carbon source by M.smeg.

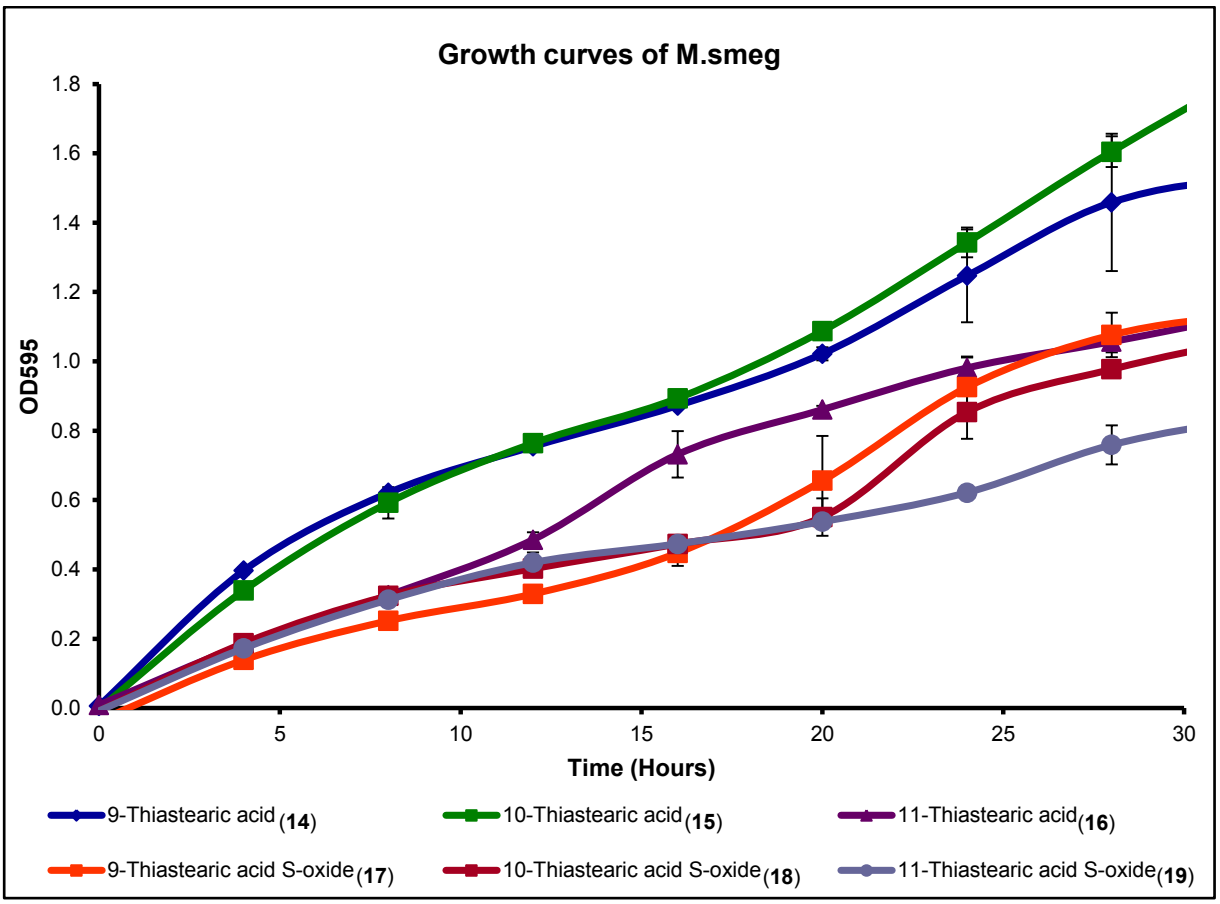

Figure 4.6: *Growth curves of M.smeg with thiastearic acid derivatives as carbon sources.*

The various growth curves obtained demonstrate that both M.tb and M.smeg are able to utilize the synthesized compounds as carbon sources. Though little growth was observed when M.tb was grown in the presence of the cholesterol derivatives, more encouraging results were obtained with the thiastearic acids. The lower growth observed with the synthesized compounds indicate that they might serve better as internal standards rather than molecular biomarkers. The fast-growing M.smeg adapted more favorably to the compounds synthesized with higher OD readings obtained compared to M.tb. The fate of the compounds as a result of catabolism and hence their suitability as biomarkers for lipid catabolism was the next step to be evaluated.

4.4. References

1. S. T. Thomas, B. C. VanderVen, D. R. Sherman, D. G. Russell and N. S. Sampson, *J. Biol. Chem.*, 2011, **286**, 43668–43678.

2. E. Miao, S. Joardar, C. Zuo, N. J. Cloutier, A. Nagahisa, C. Byon, S. R. Wilson and W. H. Orme-Johnson, *Biochemistry*, 1995, **34**, 8415–8421.

3. M. A. Ator, S. J. Schmidt, J. L. Adams, R. E. Dolle, L. I. Kruse, C. L. Frey and J. M. Barones, *J. Med. Chem.*, 1992, **35**, 100–106.

4. M. Rahman and R. Pascal, *J. Biol. Chem.*, 1990, **265**, 4989–4996.

5. A. Alloatti, S. A. Testero and A. D. Uttaro, *Int. J. Parasitol.*, 2009, **39**, 985–993.

6. A. E. Tremblay, N. Tan, E. Whittle, D. J. Hodgson, B. Dawson, P. H. Buist and J. Shanklin, *Org. Biomol. Chem.*, 2010, **8**, 1322–1328.

7. A. Alloatti, S. Gupta, M. Gualdrón-López, M. Igoillo-Esteve, P. A. Nguewa, G. Deumer, P. Wallemacq, S. G. Altabe, P. A. M. Michels and A. D. Uttaro, *PLoS One*, 2010, **5**, 1–10.

8. D. J. Hodgson, K. Y. Y. Lao, B. Dawson and P. H. Buist, *Helv. Chim. Acta*, 2003, **86**, 3688–3697.

9. A. Brzostek, T. Sliwiński, A. Rumijowska-Galewicz, M. Korycka-Machała and J. Dziadek, *Microbiology*, 2005, **151**, 2393–402.

10. I. Uhía, B. Galán, S. L. Kendall, N. G. Stoker and J. L. García, *Environ. Microbiol. Rep.*, 2012, **4**, 168–182.

11. Z. Wang, F. Zhao, X. Hao, D. Chen and D. Li, *J. Mol. Catal. B Enzym.*, 2004, **27**, 147–153.

12. H. Ouellet, J. B. Johnston and P. R. O. de Montellano, *Trends Microbiol.*, 2011, **19**, 530–539.

13. A. Bowers and H. J. Ringold, *J. Am. Chem. Soc.*, 1958, **80**, 4423–4424.

14. A. Bowers, L. C. Ibanez and H. J. Ringold, *J. Am. Chem. Soc.*, 1959, **81**, 5991–5993.

Chapter 5

GC-MS evaluation of thia and fluoro-cholesterol derivatives

5.1. Introduction

Cholesterol plays a significant role in the pathogenesis and survival of M.tb, especially as a carbon and energy source.[1] For this reason, metabolic profiling of cholesterol and its metabolites holds great value in pathology of health and disease. The initial degradation stages of cholesterol in M.tb is well established in the literature, however, downstream metabolite investigations are still ongoing.[2] Labeled cholesterol analogs will therefore serve as ideal biomarkers to follow the metabolism downstream. The cholesterol derivatives synthesized in this study were modified with sulfur or fluorine and tested as possible biomarkers for cholesterol catabolism in M.smeg. Depending on their metabolic stability, the potential value of these cholesterol derivatives is to serve as internal standards for analytical quantification techniques such as GC-MS and LC-MS. Cholesterol remains a major problem in diseases such as hypercholesterolemia and is quantified on a daily basis in biological fluids such as blood serum. Internal standards for such practises are useful for accurate quantification. The compounds synthesized are chemically similar to the natural substrate, cholesterol, yet significantly different with respect to the molecular weight. This makes them ideal candidates for use as internal standards. The simultaneous evaluation process of the compounds as either biomarkers or internal standards is summarized in Scheme 5.1.

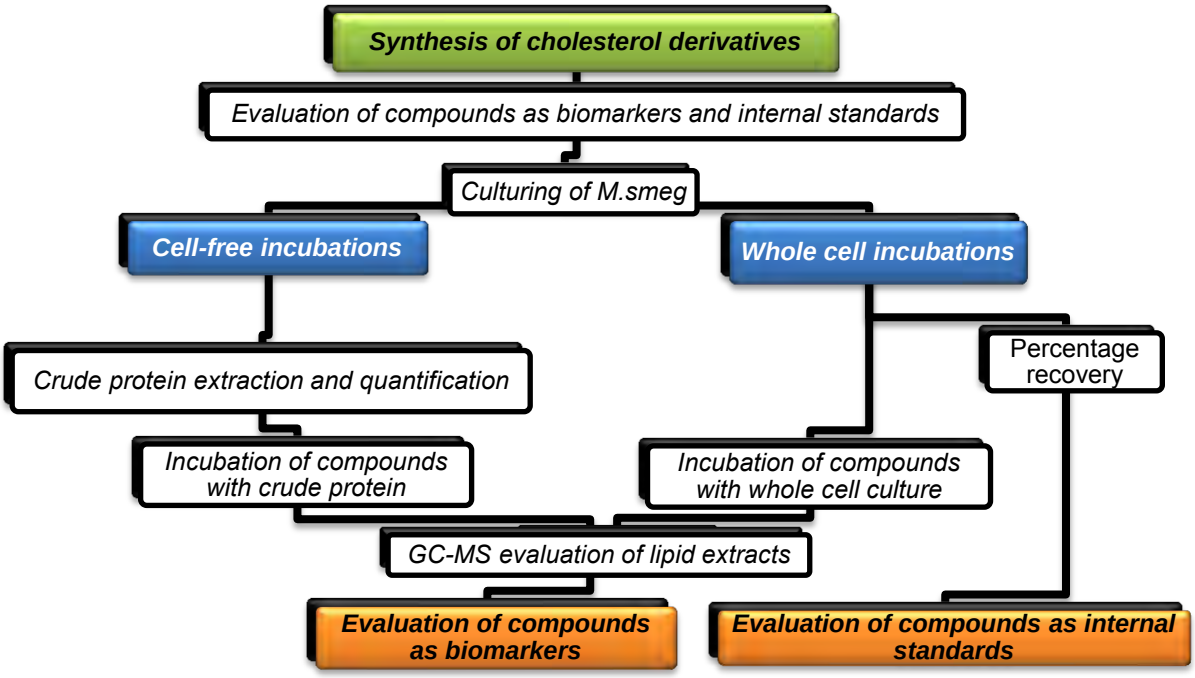

Scheme 5.1: *Evaluation process of cholesterol and its synthesized derivatives.*

The compounds synthesized were analyzed by GC-MS and utilized as standards for the incubation experiments.

5.2. Gas Chromatography

GC-MS remains one of the most favorable techniques for the analysis of lipid substances. Applications include drug detection, fire retardation and explosive examinations and pesticide analysis.[3] When developing and employing a new analytical method for regulatory control, a full method validation is required.[4] An analytical method validation consists of all the processes necessary to demonstrate that a particular method is reliable for the proposed application. These processes include:

- Selectivity (To be able to identify and quantify the analyte in the biological matrix)
- Accuracy
- Precision (To be able to accurately and precisely determine known concentrations of the analyte in the biological matrix)
- Sensitivity
- Recovery (Extraction efficiency)
- Reproducibility and
- Stability

In the current study, focus was placed on creating a program that is selective, accurate and precise. Furthermore, the recovery of these compounds in a biological matrix was also determined.

5.2.1. Column selection and GC conditions

Phase:

Columns for GC are selected based on phase and column dimensions. The column used for the current analysis was the Agilent HP-5ms (0.25 mm x 30 m x 0.25 µm). This is an all-purpose column used for the analysis of pesticides, drugs of abuse and halogenated compounds. This non-polar column consists of 5 % diphenyl- and 95 % dimethylpolysiloxane that has been bonded and crosslinked. The stationary phase of the column contributes greatly to the selectivity of the GC program. The molecules of interest will interact differently with the stationary phase depending on the polarity of the compounds. A greater retention of analytes is observed when using columns of a similar polarity. Due to the hydrophobic nature of the compounds being analyzed, a non-polar column was chosen which generally also allow for analyses at higher temperatures.

Dimensions:

The length, diameter and film thickness of the column are significant parameters to consider when choosing a column. The diameter of the column affects the efficiency and retention of the analytes. A high efficiency will produce narrow peaks and hence increase the selectivity. The efficiency is inversely proportional to the diameter and a diameter range of 0.18 – 0.25 mm is generally used when a high efficiency is required to increase selectivity. The length of the column is directly proportional to the efficiency. A greater column length will increase the efficiency while at the same time increasing the run time as well as column bleed. The film thickness influences the temperature limit for which thinner films are generally used for high boiling or high molecular weight compounds. An average film thickness of 0.25 µm was selected for the current study.

Temperature program:

The initial oven temperature was set to 290 °C at which it was held for 20 minutes. A temperature gradient of 0.5 °C/min was employed until 300 °C was achieved at which point it was held at this temperature for 3 minutes.

5.3. GC-MS analysis of standards

The synthesized steroids were evaluated by GC-MS. Standard samples of 1 mg/mL were prepared in whole cell medium and 1.5 µL injected for the analysis. The EICs of the standards are overlaid in Figure 5.1. Under the current temperature program, cholesterol eluted at 5.822 minutes as shown in Table 5.1. The cholesterol analogs evaluated eluted between 4 – 11 minutes. The retention times and the abundance of the molecular ions are shown in Table 5.1, together with other abundant fragments for each standard.

Table 5.1: *Retention times and abundance of molecular ions and other significant mass fragments of standards.*

Retention Time (min)	Compound	Molecular Mass (Abundance, %)	Other molecular fragments (Abundance, %)
4.259	3α-Fluorocholest-5-ene (**10**)	388.3 (62.84)	275.2 (100.00), 233.1 (71.12)
5.822	Cholesterol	386.2 (60.39)	145.1 (100.00), 368.3 (86.88)
6.871	3β-Mercaptocholest-5-ene (**3**)	402.3 (100.00)	247.2 (48.27), 387.3 (44.67)
7.342	Cholestenone	384.3 (30.08)	124.1 (100.00)
8.609	23-Thiacholest-4-en-3β-ol (**5**)	404.3 (11.58)	272.2 (100.00)
9.141	6β-Fluorocholestan-3β,5α-diol (**12**)	422.3 (6.10)	44.1 (26.5), 207.0 (100)
11.334	23-Thiacholest-4-en-3-one (**4**)	402.3 (31.71)	270.7 (100.00)

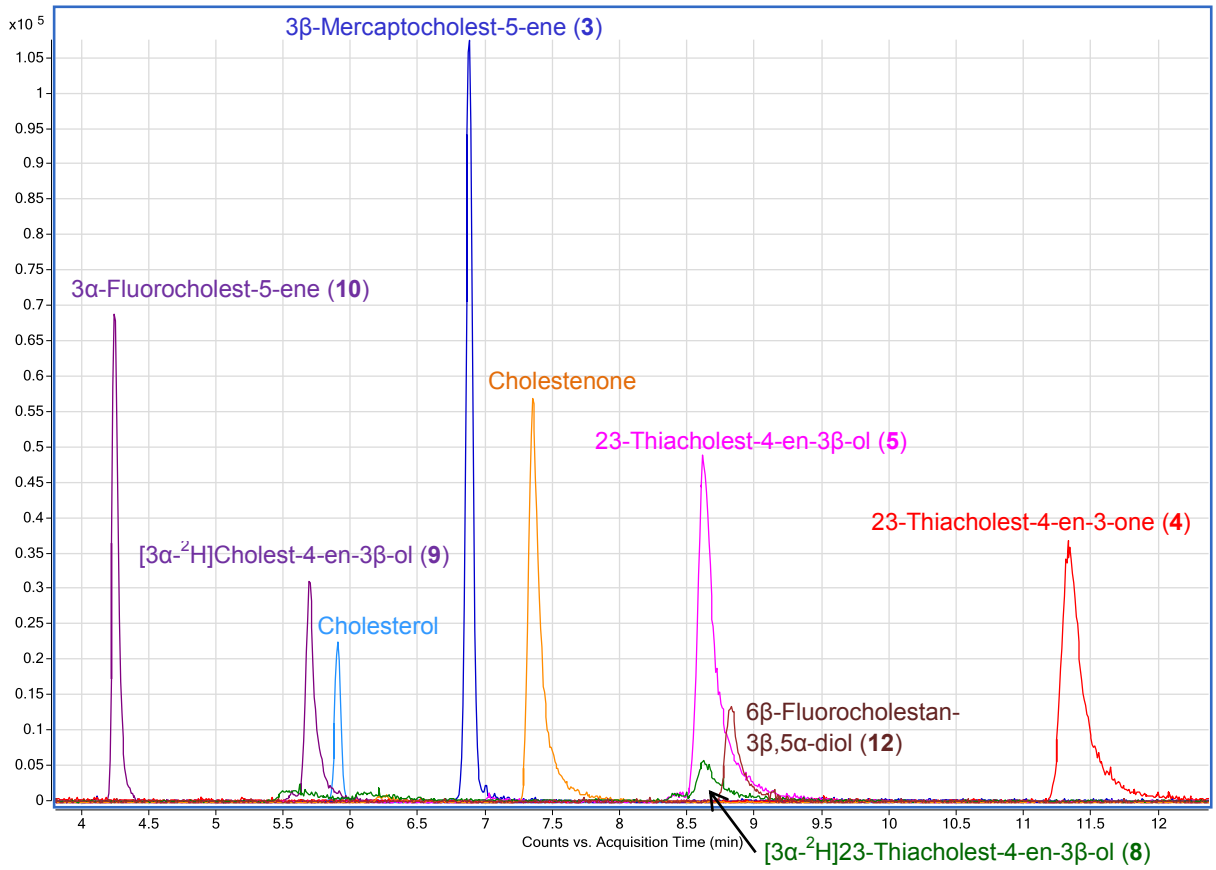

Figure 5.1: *EICs of standard compounds.*

Relatively efficient (narrow) peaks were obtained for cholesterol, 3β-mercaptocholest-5-ene (**3**) and 3α-fluorocholest-5-ene (**10**) with good to moderate response factors. Tailing was observed for the other steroids which suggest that the column chosen could possibly not be the most suitable for the analysis of these compounds. The tailing of peaks was observed for the more polar compounds which can be seen by broadening of peaks with an increase in retention time.

The primary enzymatic metabolic step in cholesterol metabolism is the action of cholesterol oxidase or 3β-hydroxy-Δ(5)-steroid dehydrogenase (3β-HSD) to produce cholestenone. Cholesterol oxidase is responsible for the oxidation of cholest-5-en-3β-ol to cholest-5-en-3-one and the subsequent isomerization to cholest-4-en-3-one (Scheme 5.1).[5] Various biomedical and industrial applications of cholesterol oxidase have been discussed in Section 1.7.6.1. Instead of utilizing synthetic chemistry, enzymes such as cholesterol oxidase can be exploited as alternative methods for producing 3-ketosteroids. As previously stated, 6-fluoro-steroids display good biological activity that can be developed into drugs such as hormones and contraceptive agents.[6] The formation of such compounds *via* cholesterol oxidation would therefore be of great interest.

5.4. Enzymatic oxidation of 3β-hydroxy steroids *via* cholesterol oxidase

The 3β-hydroxy steroids synthesized in this study were assessed in the presence of cholesterol oxidase and the sensitivity of the enzyme evaluated in the presence of sulfur (23-thiacholest-4-en-3β-ol (**5**)) and fluorine (6β-fluorocholestan-3β,5α-diol (**12**)). The expected outcome of this experiment is shown in Scheme 5.2. The study was accomplished by the addition of cholesterol oxidase to the steroid (1 mg) in a phosphate buffer and incubating at 37 °C for 45 minutes. The reaction was terminated by extracting with chloroform prior to analyzing by GC-MS. All experiments were performed in duplicate.

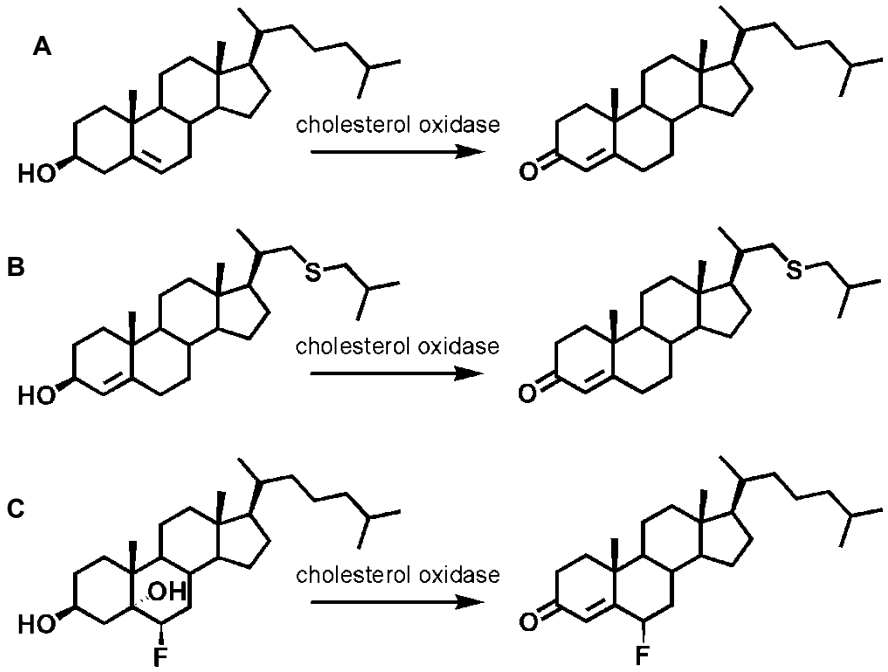

Scheme 5.2: *Enzymatic oxidation of* ***A:*** *cholesterol to cholestenone,* ***B:*** *23-thiacholest-4-en-3β-ol (**5**) to 23-thiacholest-4-en-3-one and* ***C:*** *6β-fluorocholestan-3β,5α-diol (**12**) to 6β-fluorocholest-4-en-3-one.*

Cholesterol was incubated with cholesterol oxidase and the resulting TIC of the extract displayed in Figure 5.2.B. The action of cholesterol oxidase could be observed by the presence of an additional peak at 7.272 minutes which can be attributed to the oxidation product, cholestenone. This was confirmed by comparing the retention time and molecular mass fragmentation pattern to a cholestenone standard (Figure 5.2.C). Residual cholesterol was observed which suggests that a longer incubation period should be adopted or a higher concentration of enzyme be added in future studies.

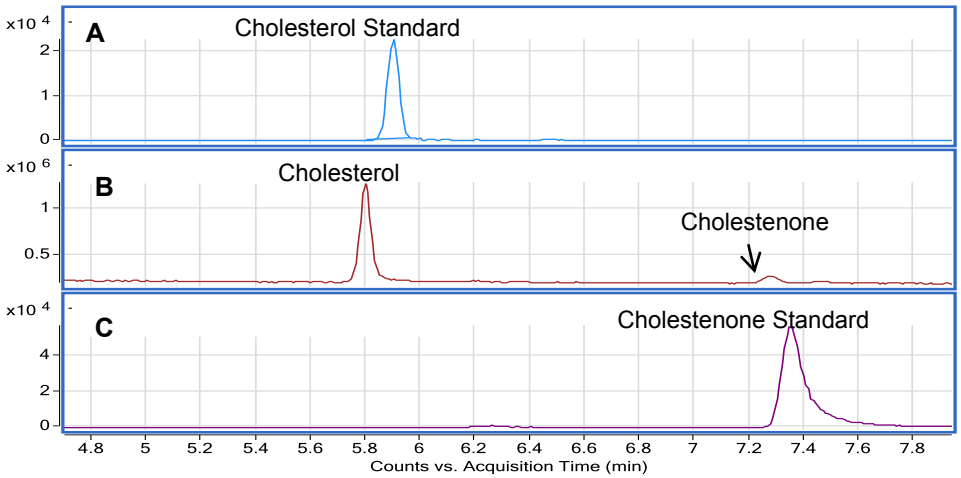

Figure 5.2: A: *EIC of cholesterol standard,* ***B:*** *TIC of cholesterol oxidase experiment with cholesterol and* ***C:*** *EIC of cholestenone standard.*

Cholesterol oxidase experiments were also performed on 23-thiacholest-4-en-3β-ol (**5**). The TIC of the extract is shown in Figure 5.3.B. The outcome of this experiment can be seen by the appearance of a new peak at 11.151 minutes which was confirmed to be 23-thiacholest-4-en-3-one (**4**).

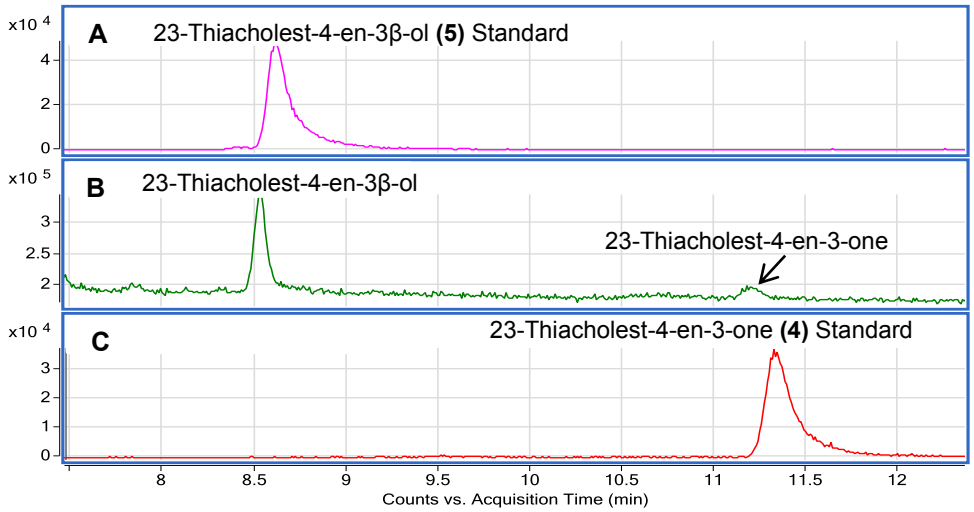

Figure 5.3: A: *EIC of 23-thiacholest-4-en-3β-ol (**5**),* ***B:*** *TIC of extract of cholesterol oxidase experiment of 23-thiacholest-4-en-3β-ol (**5**) and* ***C:*** *EIC of 23-thiacholest-4-en-3-one.*

6β-Fluorocholestan-3β,5α-diol (**12**) was incubated with cholesterol oxidase and the TIC of the resulting extract displayed in Figure 5.4.B. The standard sample of (**12**) revealed three peaks in the GC-MS trace. At 9.045 minutes, (**12**) could be identified by its molecular mass of 422.3. The peaks at 8.914 minutes and 7.438 minutes both corresponded to a molecular mass of 404.3 which could possibly be due to the elimination of water. This can result in the production of 6β-fluorocholest-4-en-3β-ol or 3,5-epoxy,6β-fluorocholestane (Figure 5.5). These compounds could possibly have formed during the purification process when the compound was synthesized. The aim was to establish whether (**12**) can be enzymatically oxidized to 6β-fluorocholest-4-en-3-one which holds significance in applications within the medicinal field (Section 1.17.1). The mass spectra of these peaks are shown in Figure 5.6. The TIC of the cholesterol oxidase experiment revealed an additional peak at 12.536 minutes which is most likely 6β-fluorocholest-4-en-3-one due to the oxidation *via* cholesterol oxidase. This is yet to be confirmed through the use of synthetic standards.

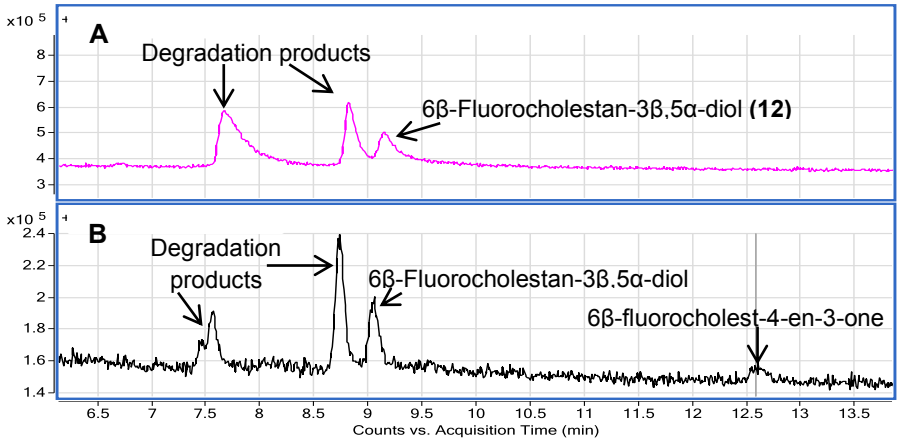

Figure 5.4: A: *TIC of 6β-fluorocholestan-3β,5α-diol (**12**) standard and **B:** TIC of extract of cholesterol oxidase 6β-fluorocholestan-3β,5α-diol (**12**).*

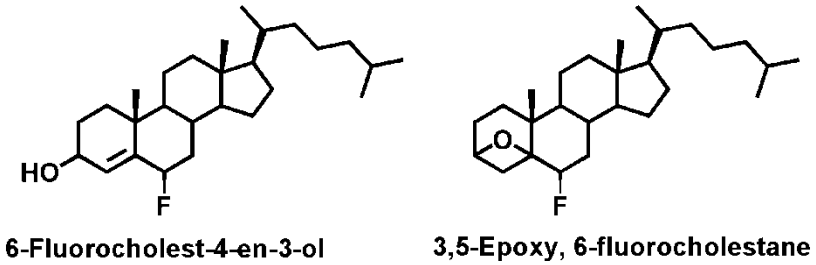

Figure 5.5: *Possible by-products of 6β-fluorocholestan-3β,5α-diol (**12**) synthesis.*

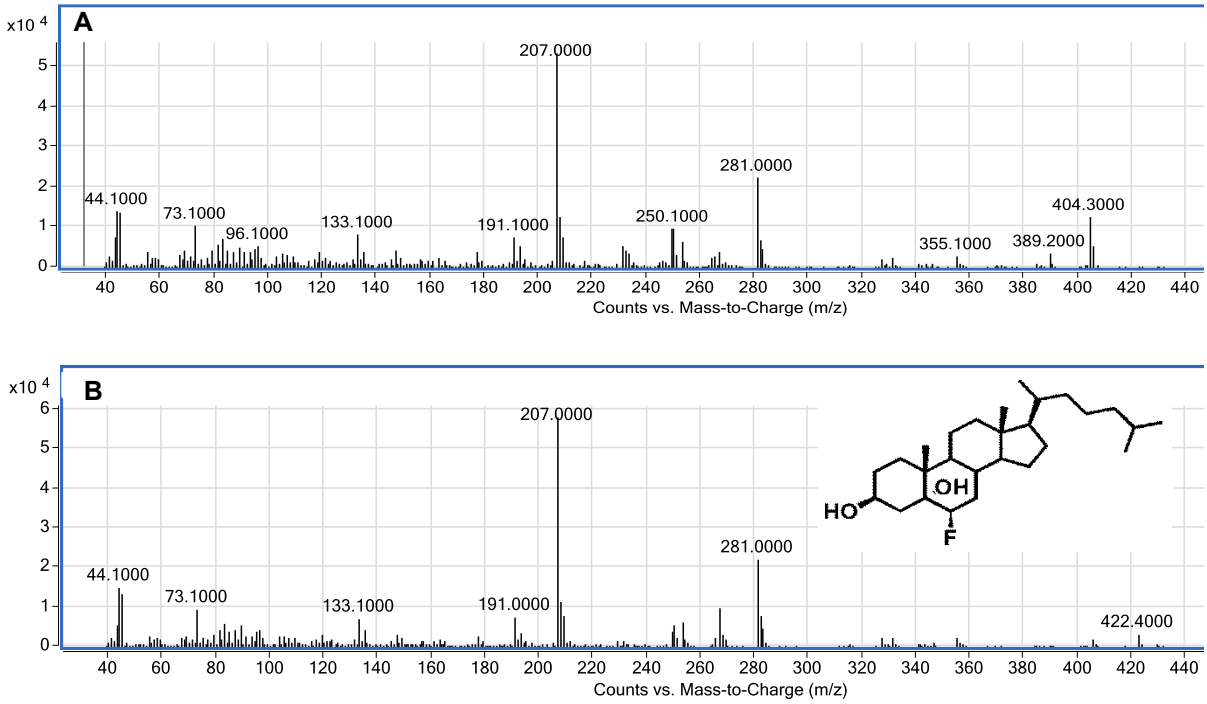

Figure 5.6: *Molecular mass fragmentation of **A:** 6β-fluorocholest-4-en-3-one and **B:** 6β-fluorocholestan-3β,5α-diol (**12**).*

From the cholesterol oxidase results obtained it can be concluded that the enzyme is not specific to cholesterol and that the sulfur and fluorine present in the cholesterol backbone (23-thiacholest-4-en-3β-ol (**5**) and 6β-fluorocholestan-3β,5α-diol (**12**)) act as substrates for cholesterol oxidase. It should also be noted that (**5**) is a α,β-unsaturated ketone with the double bond at C4 instead of at C5 as present in cholesterol and good oxidation results were achieved. The concentrations determined for the final products are shown in Table 5.2.

Table 5.2: *Cholesterol oxidase results for 3β-hydroxy steroid experiments.*

Experiment	Compound	Retention Time (min)	Starting concentration (mg/mL)	Final concentration (mg/mL)
Cholesterol	Cholesterol	5.797	1.10	0.47 (± 0.09)
	Cholestenone	7.272	0.00	0.10 (± 0.00)
23-Thiacholest-4-en-3β-ol (**5**)	23-Thiacholest-4-en-3β-ol	8.531	0.96	0.62 (± 0.00)
	23-Thiacholest-4-en-3-one	11.151	0.00	0.10 (± 0.00)

Now that it has been established that the 3β-hydroxy steroids can be enzymatically oxidized to their 3-keto counter parts, incubations of M.smeg was carried out in the presence of the compounds synthesized to evaluate the possible degradation products as a result of CYP450 enzyme activity. The possible metabolism of the compounds was investigated following two distinct protocols; cell-free incubations and whole cell incubations.

5.5. Evaluation of thia- and fluoro-cholesterol derivatives as metabolic markers in M.smeg

Cell-free incubations

Cell-free incubations were prepared by the addition of 1 mg/mL crude protein extract of M.smeg to a Tris-HCl buffer containing 1 mg/mL cholesterol or synthesized cholesterol derivative. The crude protein was obtained by sonicating the resulting pellet of M.smeg from a transformation culture (Section 7.22). The isolation of the crude protein was performed in a Tris-HCl buffer containing a protease inhibitor cocktail. The crude protein was isolated from the pellet and the concentration determined using a Bradford assay.[7]

Determination of crude protein concentration

The crude protein concentration was determined *via* Bradford's method.[7] A standard curve (Figure 5.7) was obtained using bovine serum albumin (BSA) as the reference protein and the absorbance read at 595 nm. The absorbance reading of the crude protein extract sample was determined to be 0.3253, which led to a concentration of 7.6 µg/µL.

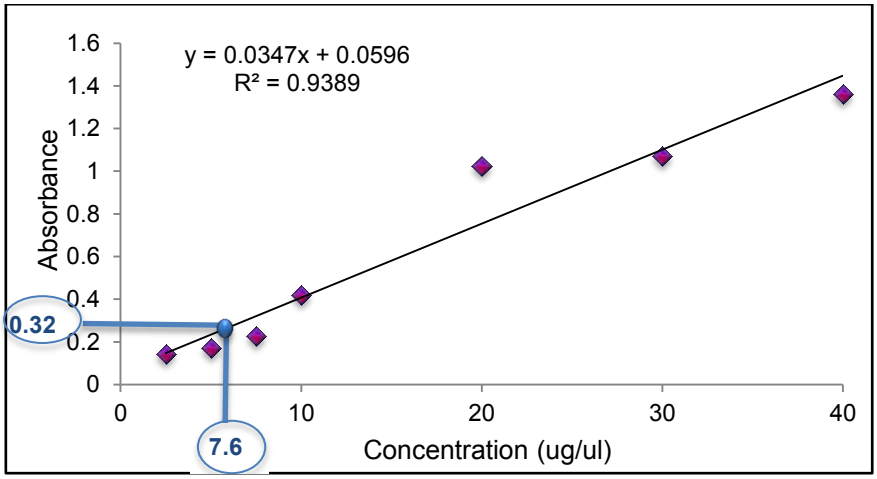

Figure 5.7: *Standard curve for Bradford protein determination.*

Whole cell incubations

Whole cell incubations were prepared by inoculating approximately 2 mg/mL cholesterol or cholesterol derivative with M.smeg and incubating at 37 °C for 24 hours. The reaction was terminated by the addition of KOH, extracted with chloroform and analyzed by GC-MS.

5.5.2. GC-MS analysis of cholesterol extracts

In the cell-free extract, cholesterol was observed at a retention time of 5.857 minutes and the internal standard, [3α-^{2}H]cholest-4-en-3β-ol (**9**), at 5.683 minutes, as shown in Figure 5.8.B. The EICs for the cholesterol and cholestenone standards are shown in Figure 5.8.A and Figure 5.8.D, respectively. According to the cholesterol catabolic pathway, cholesterol is converted to cholestenone followed by sequential side-chain oxidation as stated in Section 1.7.4. In the cell-free extract, cholestenone was detected at 7.325 minutes and a clear trend in increase in polarity was observed over with a concomitant increase in retention time. The C26-OH metabolite was identified at 8.478 minutes while the C26-aldehyde could be seen at 9.901 minutes with a molecular mass of 400.3. The C26-OH could not be identified based on its molecular mass, however, daughter fragmentations (44.1, 191.0, 281.0) identical to that of cholesterol were observed. Oxidized product C26-aldehyde was identified and, it is likely that the peak at 8.478 minutes is due to C26-OH based on the retention time due to its polarity. The GC-MS trace of the extract from the whole cell incubation is shown in Figure 5.8.C. Cholesterol can be seen at 5.884 minutes and the presence of cholestenone was

confirmed when a molecular weight of 384 that corresponds to the cholestenone standard. Unlike the cell-free incubation, cholestenone was the only catabolic product detected in the whole cell incubation extract.

Table 5.3: *Quantitation results of cell-free and whole cell incubations of M.smeg with cholesterol.*

Experiment	Compound	Retention Time (min)	Starting Concentration (mg/mL)	Final Concentration (mg/mL)
Cell-free	Cholesterol	5.857	1.00	0.49 (± 0.09)
	Cholestenone	7.325	0.00	0.10 (± 0.00)
Whole cell	Cholesterol	5.884	2.12	1.29 (± 0.10)
	Cholestenone	7.316	0.00	0.10 (± 0.00)

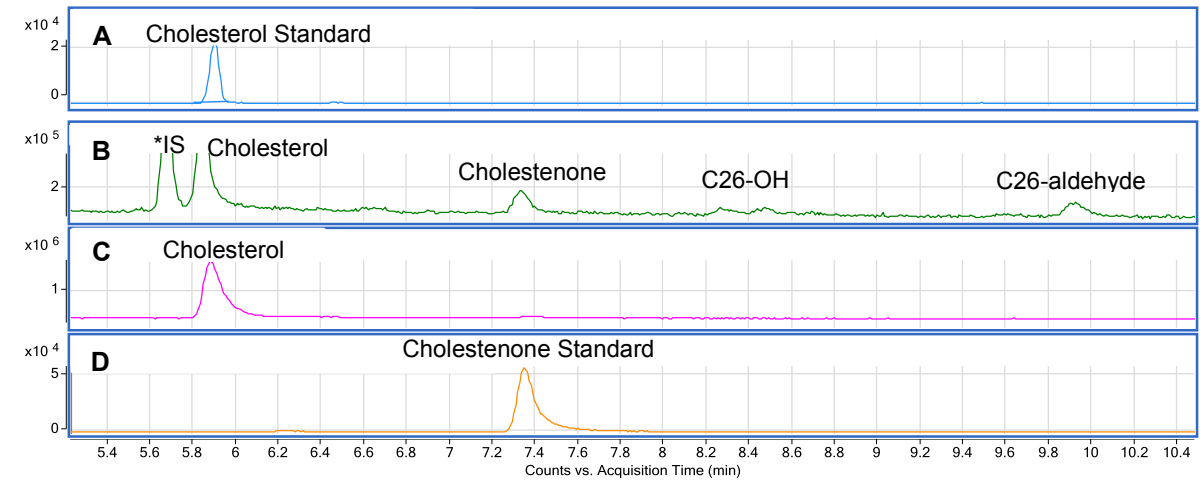

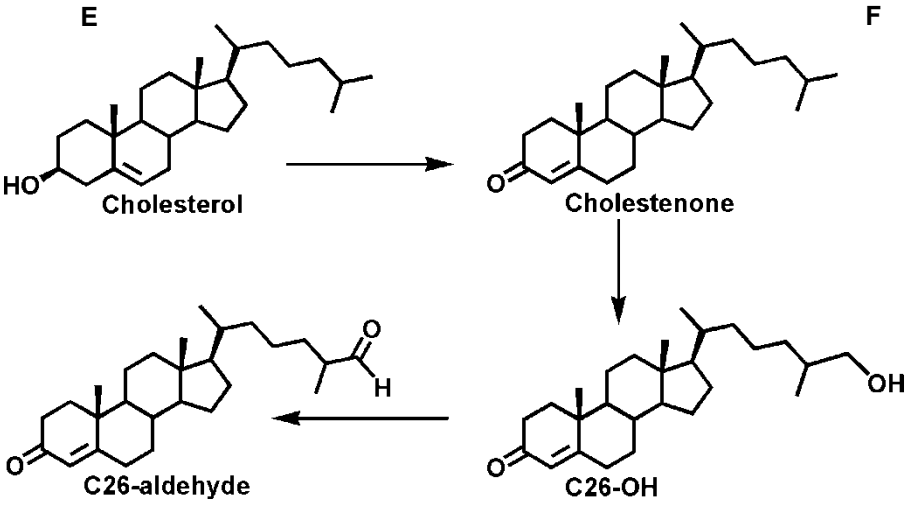

F

Retention time (min)	*Molecular mass*
Cholesterol 5.857	*386.3*
Cholestenone 7.325	*384.2*
C26-OH 8.478	*400.2*
C26-aldehyde 9.901	-

Figure 5.8: A: *EIC of cholesterol standard,* ***B:*** *TIC of cholesterol cell-free incubation extract,* ***C:*** *TIC of cholesterol whole cell incubation extract,* ***D:*** *EIC of cholestenone standard,* ***E:*** *Cholesterol catabolic pathway and* ***F:*** *Retention time and molecular mass data for peaks identified for cell-free incubation extract. *IS: Internal standard*

5.5.2. GC-MS analysis of 3β-mercaptocholest-5-ene (3) extracts

Previous evaluation of 3β-mercaptocholest-5-ene (**3**) by Armstrong *et al.* revealed that no oxidation is obtained due to the activity of cholesterol oxidase.[8] This outcome was further confirmed in this study as no S-oxidation products could be observed by GC-MS analysis. As a result, possible side-chain degradation can be monitored in the absence of cholesterol oxidase activity which is considered as the initiation of cholesterol metabolism. The TIC profiles of the cell-free and the whole cell incubations were similar after a 24 hour incubation period. From the whole cell incubation it can be seen that (**3**) was retained for 6.888 minutes. The internal standard was the only other peak present in the cell-free incubation with no other metabolites observed in either incubation systems. The low quantity of (**3**) recovered, suggests that the catabolic products formed were not appropriately extracted as suggested by the positive growth curves obtained with (**3**) as the sole carbon source for M.smeg (Chapter 4).

Table 5.4: *Quantitation results of cell-free and whole cell incubations of M.smeg with 3β-mercaptocholest-5-ene* ***(3)****.*

Experiment	Compound	Retention Time (min)	Starting Concentration (mg/mL)	Final Concentration (mg/mL)
Cell-free	3β-mercaptocholest-5-ene (**3**)	6.836	0.98	0.13 (± 0.00)
Whole Cell	3β-mercaptocholest-5-ene (**3**)	6.888	2.03	0.13 (± 0.00)

5.5.3. GC-MS analysis of 23-thiacholest-4-en-3-one (4) and 23-thiacholest-4-en-3β-ol (5) extracts

The cell-free and whole cell metabolism of 23-thiacholest-4-en-3-one (**4**) could not be evaluated under the current incubation and GC-MS protocols. No additional peaks could be observed in the GC-MS trace. However, a reduction in the concentration of 23-thiacholest-4-en-3-one (**4**) was noted after the 24 hour incubation time. A positive growth curve was obtained with (**4**) as the carbon source which proposes that the extraction protocol or the GC-MS program should be modified to improve the detection of the possible catabolic products or LC-MS should be considered for the more polar products.

An enhanced growth curve for M.smeg with (**5**) was noted as compared to (**4**). From the cholesterol oxidase results acquired, it was observed that 23-thiacholest-4-en-3β-ol (**5**) became oxidized to 23-thiacholest-4-en-3-one (**4**). This outcome could be seen for both the

cell-free and whole cell incubations of (**5**) where (**4**) was observed in the region of 11.212 minutes. The TIC of the whole cell incubation extract is shown in Figure 5.9. No further oxidation products could be observed. The concentrations as a result of the incubations are shown in Table 5.5.

Table 5.5: *Quantitation results of cell-free and whole cell incubations of M.smeg with 23-thiacholest-4-en-3-one (**4**) and that 23-thiacholest-4-en-3β-ol (**5**).*

	Experiment	Compound	Retention Time (min)	Starting Concentration (mg/mL)	Final Concentration (mg/mL)
23-thiacholest-4-en-3-one (**4**)	Cell-free	23-thiacholest-4-en-3-one (**4**)	11.308	1.02	0.81 (± 0.78)
	Whole cell	23-thiacholest-4-en-3-one (**4**)	11.229	2.05	0.40 (± 0.00)
23-thiacholest-4-en-3β-ol (**5**)	Cell-free	23-thiacholest-4-en-3β-ol (**5**)	8.609	1.02	0.99
		23-thiacholest-4-en-3-one (**4**)	11.989	0.00	0.02
	Whole cell	23-thiacholest-4-en-3β-ol (**5**)	8.277	2.05	0.50
		23-thiacholest-4-en-3-one (**4**)	11.212	0.00	0.42

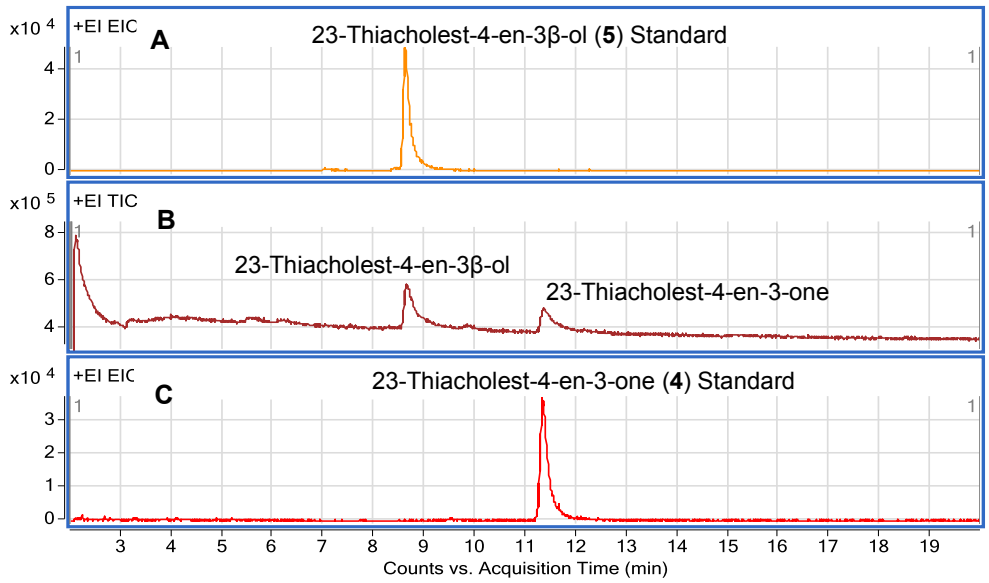

Figure 5.9: A: *EIC of 23-thiacholest-4-en-3β-ol (**5**) standard,* ***B:*** *TIC of whole cell incubation extract of 23-thiacholest-4-en-3β-ol (**5**) and* ***C:*** *EIC of 23-thiacholest-4-en-3-one (**4**) standard.*

5.5.4. GC-MS analysis of 3α-fluorocholest-5-ene (10)

Previous evaluation of 3α-fluorocholest-5-ene (**10**) by Armstrong *et al.* revealed that the presence of fluorine in position C3 inhibited the activity of cholesterol oxidase.[8] Thus, the metabolic activity on the side-chain of cholesterol was determined in the absence of 3β-HSD activity using (**10**). The TIC of the resulting whole cell incubation extract is shown in Figure 5.9. An additional peak at 5.877 minutes was observed with a M^+ of 386.3 which is consistent with that of cholesterol. This result is consistent with the results obtained for the growth curve of M.smeg with (**10**). Slow growth of M.smeg is initially observed with steady growth after 15 hours after which comparable growth to cholesterol is observed. Thus, 3α-fluorocholest-5-ene (**10**) is first converted to cholesterol before further degradation can occur.

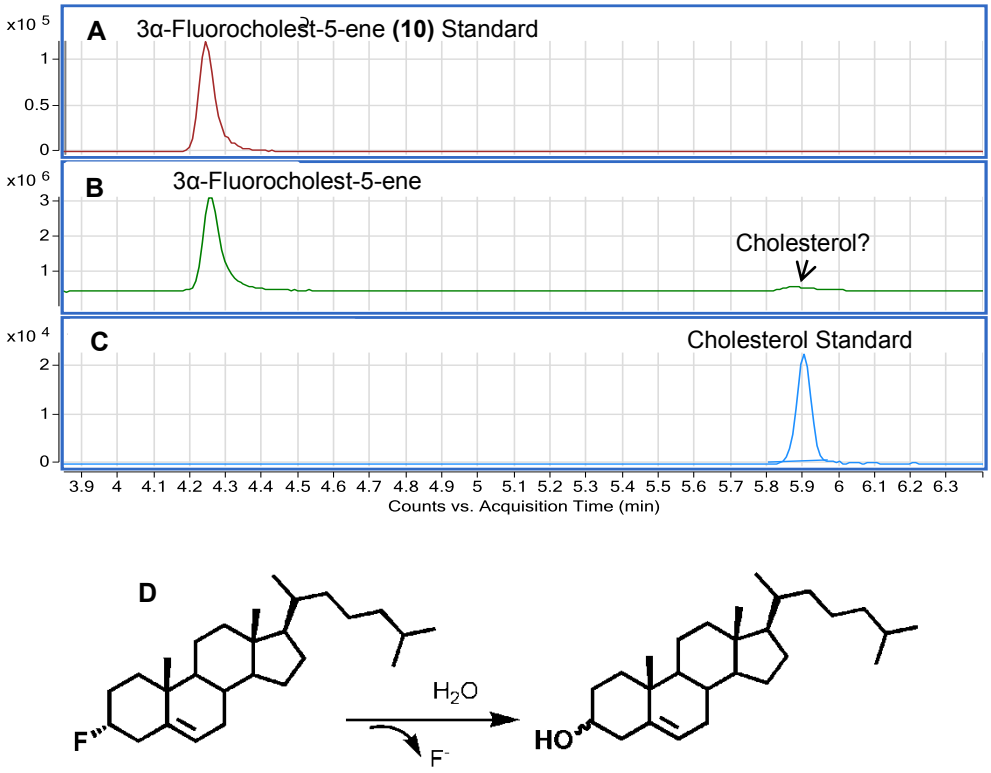

***Figure 5.10: A:** EIC of 3α-fluorocholest-5-ene (**10**), **B:** TIC of whole cell incubation extract of 3α-fluorocholest-5-ene (**10**), **C:** EIC of cholesterol and **D:** Cholesterol formation from (**10**).*

The cell-free incubation of 6β-fluorocholestan-3β,5α-diol (**12**) indicated no visible catabolic products. Due to the production of 6β-fluorocholest-4-en-3-one during the cholesterol oxidase experiment, it can be concluded that a longer incubation period is required or the crude protein concentration be increased to evaluate (**12**) as a biomarker.

In Chapter 4, the growth of M.smeg was discussed with respect to utilizing the compounds as carbon sources. The catabolism of these compounds was monitored and evaluated by GC-MS. Econazole is a known antimycobacterial drug that is speculated to inhibit the P450 enzymes (CYP125, CYP142 and CYP124) responsible for side-chain degradation. The incubations as described above were repeated in the presence of econazole to assess whether it affected the catabolism of the steroid analogues.

5.6. Evaluation of thia- and fluoro-cholesterol derivatives in the presence of econazole in M.smeg

M.smeg was incubated in the presence of the synthesized compounds in a cell-free medium with the addition of econazole. As expected, the catabolism of cholesterol was inhibited which could be seen by the higher concentration of cholesterol (0.83 mg/mL) recovered after 24 hours of incubation. No other degradation products were observed as discussed for the incubation with cholesterol in the absence of econazole. Little effect of econazole could be observed on the concentration of 3β-mercaptocholest-5-ene (**3**) and 3α-fluorocholest-5-ene (**10**) after the incubation. The initial and final concentrations with and without econazole is presented in Table 5.6 and displayed in Figure 5.11.

Table 5.6: *Intitial and final concentrations of compounds incubated with M.smeg with and without econazole.*

Incubation	**Whithout econazole**		**With econazole**	
Compound	*Initial Concentrate (mg/mL)*	*Final Concentration (mg/mL)*	*Initial Concentrate (mg/mL)*	*Final Concentration (mg/mL)*
Cholesterol	1.00	0.49	1.00	0.83 (± 0.02)
3β-Mercaptocholest-5-ene (**3**)	0.98	0.13	1.00	0.13 (± 0.00)
3α-Fluorocholest-5-ene (**10**)	1.04	1.05	1.06	1.05 (± 0.03)

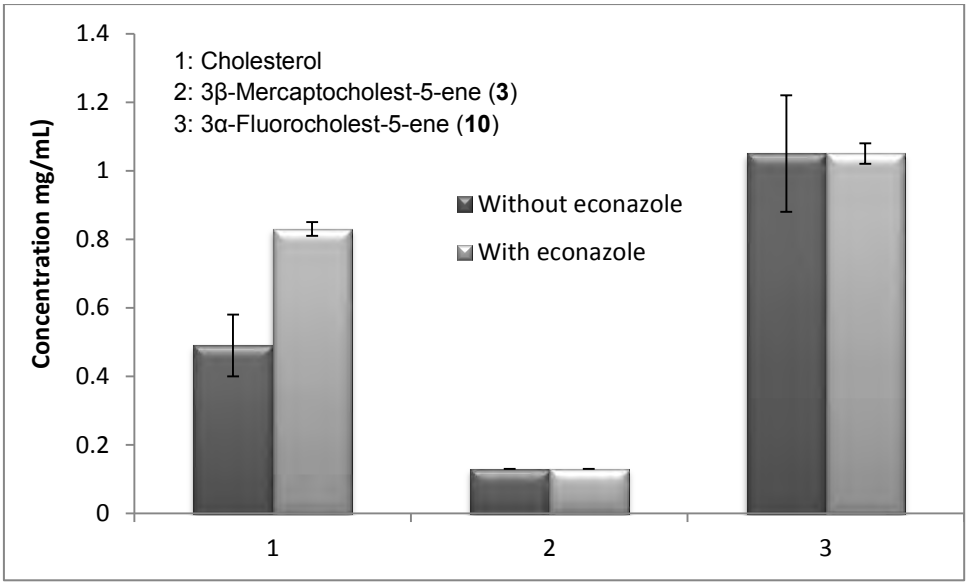

Figure 5.11: *Final concentrations of synthesized compounds incubated with M.smeg with and without econazole*

The catabolic metabolites produced on account of the incubation of the compounds with M.smeg were evaluated by means of GC-MS. Cholesterol degradation products could be identified and quantified in both the cell-free and whole cell medium. This GC-MS program provided a platform for the analysis of the steroids synthesized. Cholesterol oxidase was able to oxidize all of the 3β-hydroxy steroids synthesized albeit the presence of sulfur or fluorine in the cholesterol back-bone.

The cholesterol derivatives synthesized in this study were evaluated as potential biomarkers for the metabolic pathway in M.smeg. Under the current experimental conditions, little can be concluded about the catabolic products of these compounds. Thus, the compounds evaluated will probably have more value as internal standards for the quantitation of steroids such as cholesterol due to their similar chemical nature. The percentage recovery of the compounds was determined to assess their potential as internal standards.

The value of the compounds was also evaluated as internal standards.

5.7. Percentage recovery of cholesterol compounds in whole cell medium

Recovery is determined by the extraction efficiency of an analytical procedure, quantified as a percentage of a known quantity of an analyte carried through the sample extraction.[4] The extraction efficiency or percentage recovery was determined by immediate extraction of whole cell medium containing known amounts of steroids which have been inoculated with M.smeg. The concentrations recovered from these experiments were determined by utilizing a calibration curve. The calibration curve was established by spiking whole cell medium with steroid of concentrations in the range of 0.27 mg/mL - 2.00 mg/mL. In this concentration

range, six calibration samples were analyzed with two replicates at each calibration point. The calibration curves of cholesterol and its analogs are shown in Figure 5.11 and the percentage recovery summarized in Table 5.6. All experiments were performed in duplicate.

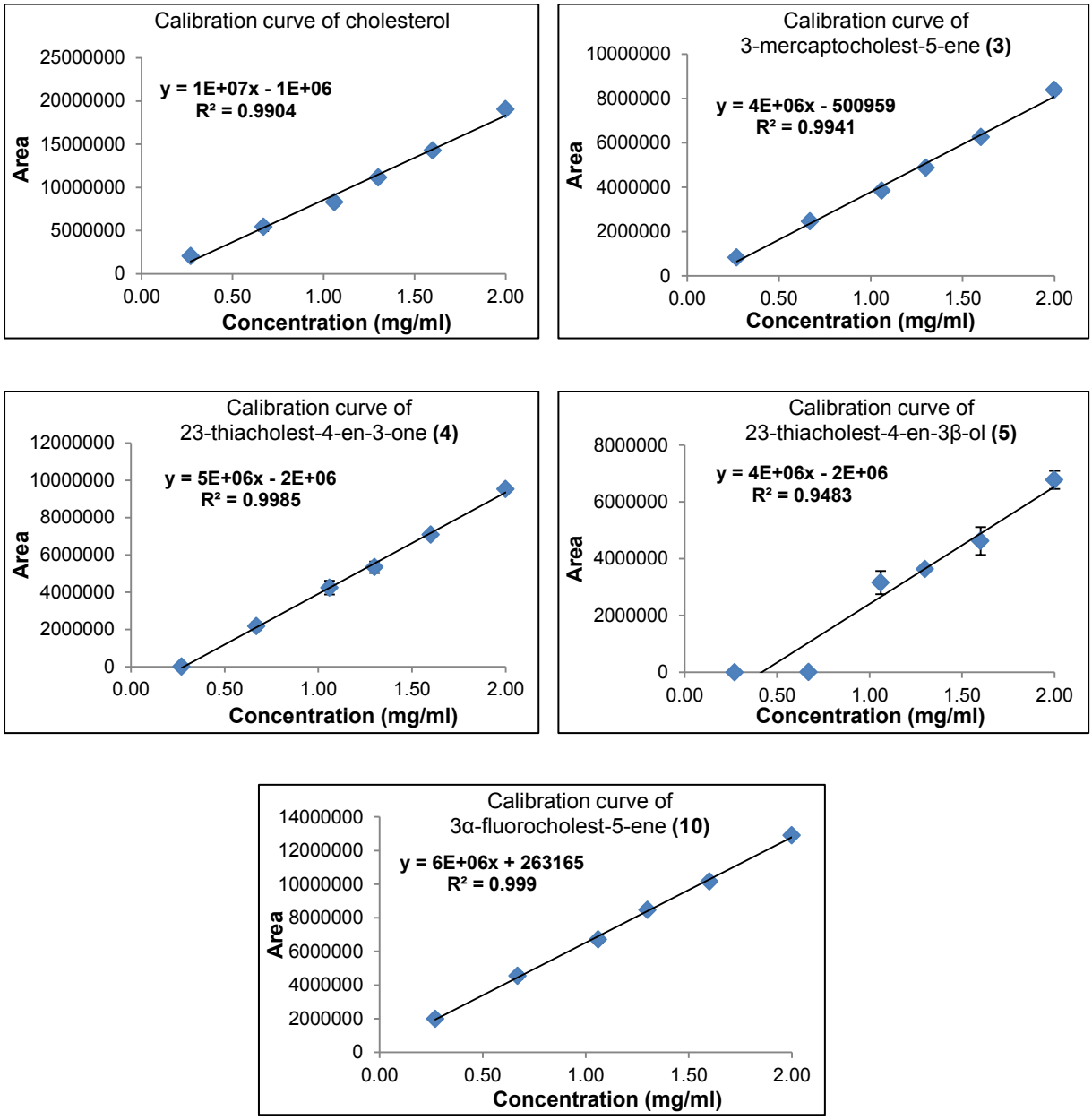

Figure 5.11: *Calibration curves for standard compounds.*

Table 5.6: *Recovery % of cholesterol and cholesterol derivatives*

Compound	Retention Time (min)	Recovery (%)	Standard Deviation (%)
Cholesterol	5.866	87	5.9
3β-Mercaptocholest-5-ene (**3**)	6.853	83	0.0
23-Thiacholest-4-en-3-one (**4**)	11.308	105	4.1
23-Thiacholest-4-en-3β-ol (**5**)	8.600	84	0.0
3α-Fluorocholest-5-ene (**10**)	4.241	107	1.0

The percentage recovery of cholesterol was determined to be 87 %. 3β-Mercaptocholest-5-ene (**3**) and 23-thiacholest-4-en-3β-ol (**5**) displayed similar recoveries to cholesterol whereas 23-thiacholest-4-en-3-one (**4**) and 3α-Fluorocholest-5-ene (**10**) displayed recoveries just above 100 %.

5.8. References

1. W. Lee, B. C. Vanderven, R. J. Fahey and D. G. Russell, *J. Biol. Chem.*, 2013, **288**, 6788–6800.

2. H. Ouellet, J. B. Johnston and P. R. O. de Montellano, *Trends Microbiol.*, 2011, **19**, 530–539.

3. L. HimaBindu, A. Parameswari and C. Gopinath, *Int. J. Pharm. Qual. Assur.*, 2013, **4**, 42–51.

4. V. P. Shah, K. K. Midha, J. W. Findlay, H. M. Hill, J. D. Hulse, I. J. McGilveray, G. McKay, K. J. Miller, R. N. Patnaik, M. L. Powell, A. Tonelli, C. T. Viswanathan and A. Yacobi, *Pharm. Res.*, 2000, **17**, 1551–1557.

5. X. Yang, E. Dubnau, I. Smith and N. S. Sampson, *Biochemistry*, 2008, **46**, 9058–9067.

6. A. Bowers, L. C. Ibanez and H. J. Ringold, *J. Am. Chem. Soc.*, 1959, **81**, 5991–5993.

7. M. M. Bradford, *Anal. Biochem.*, 1976, **72**, 248–54.

8. M. J. Armstrong and M. C. Carey, *J. Lipid Res.*, 1987, **28**, 1144–1155.

Chapter 6

GC-MS evaluation of thiastearic acids

6.1. Introduction

Long chain fatty acids such as stearic acid are unique components of mycobacterial cells.[1] It is utilized as both a carbon source and starting material for mycolic acid synthesis. Thiastearic acid has broadly been used as a biomarker and inhibitor in various organisms.[2,3] However, thiastearates have not been evaluated as biomarkers or internal standards for the study of M.tb catabolism. It is largely accepted that several metabolic effects can be achieved depending on the position of sulfur within the fatty acid chain.[4] Desaturases are responsible for introducing a double bond into the fatty acid chain that serves as precursors for mycolic acid synthesis. Depending on the position of sulfur within the stearic acid backbone, the desaturases can either be inhibited or the thiastearic acid can be utilized as a biomarker to follow the catabolism of stearic acid further downstream. As discussed in Section 1.5, desaturation at position C9 is significant as substitution of sulfur at this position leads to the oxidation of sulfur and formation of a sulfoxide.[5] In this study, 9, 10 and 11-thiastearic acids were synthesized and the metabolic effect as a result of the position of sulfur determined in M.smeg.

6.2. GC-MS analysis of thiastearic acids

The thiastearic acids synthesized were evaluated by GC-MS (Figure 6.1.A). Standard samples of 1 mg/mL were prepared in cell-free medium and 1.5 µL injected for the analysis. Due to the similar chemical nature of these compounds, similar retention times of 10.8 – 10.9 minutes were observed. Because of the weak molecular ion in the mass spectra of these compounds, the mass fragmentation patterns of the daughter fragments were analyzed. The mass spectrum of 9-thiastearic acid is shown in Figure 6.1.C and the mass fragmentation associated with the masses observed displayed in Figure 6.1.B.

A

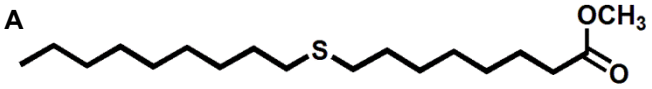

B

Fragment	Calculated mass	Actual mass	Abundance (%)
$CH_3(CH_2)_8S^+(CH_2)_7COCH_3$	318.0	Not detected	-
$CH_3(CH_2)_8S^+(CH_2)_7$	257.5	255.1	27.0
$CH_3(CH_2)_8S^+(CH_2)_3$	200.9	199.1	28.3
$CH_3(CH_2)_8S^+$	159.3	159.1	5.12
$CH_3(CH_2)_6$	9.0	101.1	24.3
$CH_3(CH_2)_5$	8.0	84.9	52.6
$CH_3(CH_2)_4$	71.0	71.0	26.9
$CH_3(CH_2)_3$	57.0	57.0	46.5
$CH_3(CH_2)_2$	43.0	43.4	71.4

C

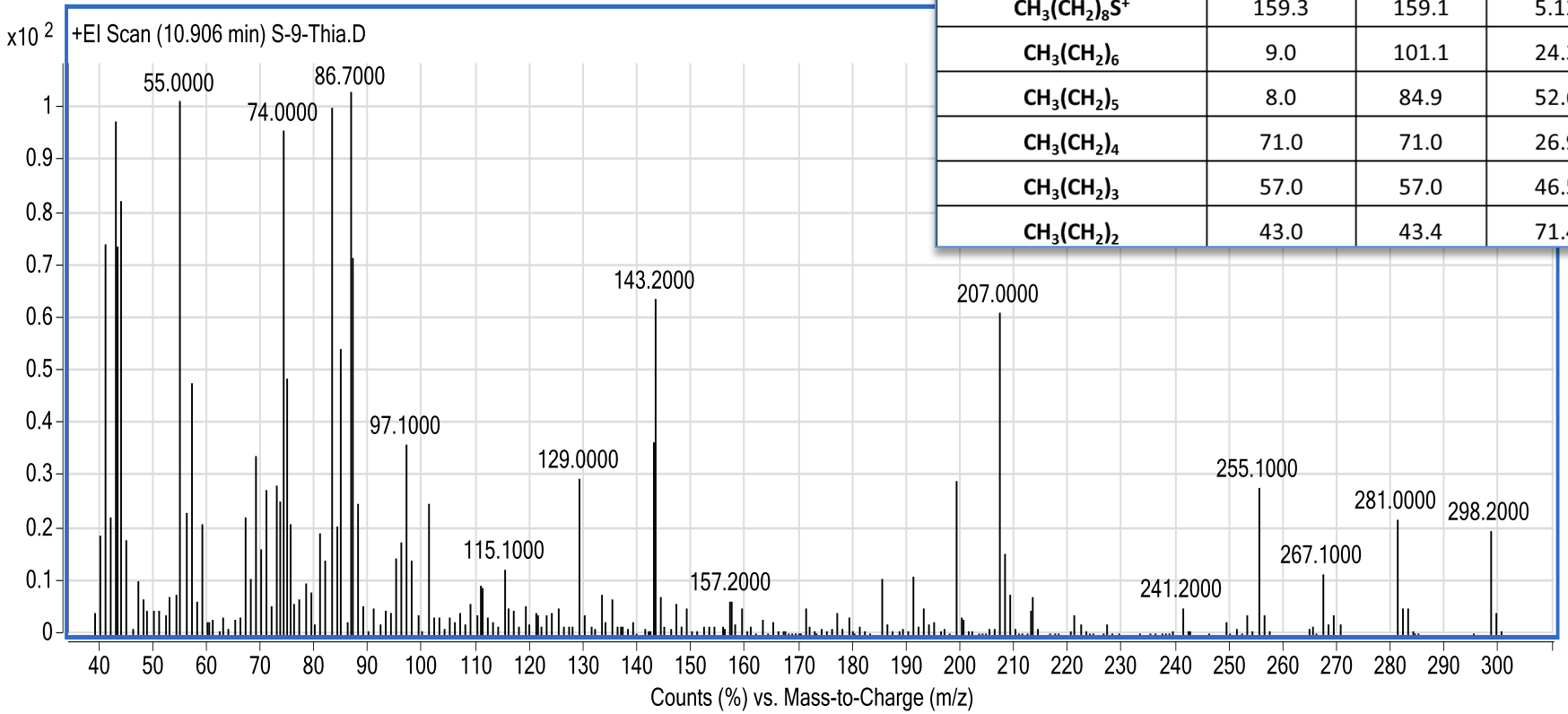

Figure 6.1: A: *Chemical structure of 9-thiastearic acid (**14**),* ***B:*** *Mass fragmentation of 9-thiastearic acid (**14**) and* ***C:*** *Mass spectrum of 9-thiastearic acid (**14**).*

Due to the possible oxidation of sulfur to the corresponding sulfoxide, the sulfoxide derivatives of 9, 10 and 11-thiastearic acids were also synthesized and evaluated by GC-MS. Under the current program, S-oxidation was not detected and therefore the production of the sulfoxide not monitored. The change in concentration of the individual thiastearic acids was however, examined.

The thiastearic acid derivatives synthesized were incubated with M.smeg for 24 hours at 37 °C. The reactions were terminated by the addition of KOH and extracted with chloroform. The resulting extracts were analyzed by GC-MS and the change in concentration of acids determined.

The initial and final concentrations of the thiastearic acids are shown in Table 6.1. Reactions were initiated with approximately 1 mg/mL fatty acid and the final concentration after an incubation period of 24 hours recorded. The percentage of thiastearic acid degraded ranged from 13 – 37 % with the least amount of 11-thiastearic acid (**16**) catabolized. This result is further confirmed by the growth curves as the lowest growth of M.smeg was observed with (**16**).

Table 6.1: *Initial and final concentrations of M.smeg incubations.*

	Initial conc. (mg/mL)	Final conc. (mg/mL)
9-Thiastearic acid (14)	1.02	0.64
10-Thiastearic acid (15)	1.08	0.74
11-Thiastearic acid (16)	1.06	0.92

6.3. Percentage recovery of thiastearic acids

The extraction efficiency or percentage recovery was determined by immediate extraction of cell-free medium containing known amounts of thiastearic acids which have been inoculated with crude protein extract. The concentrations recovered from these experiments were determined by utilizing calibration curves of the standard thiastearic acids in the cell-free medium. The calibration curve was established by spiking cell-free medium with fatty acid concentrations in the range of 0.37 mg/mL – 1.09 mg/mL. All experiments were performed in duplicate. The percentage recovery of the thiastearic acids obtained had an acceptable range of 74 – 105 % with 9-thiastearic acid displaying the lowest recovery percentage.

Table 5.6: *Recovery % of thiastearic acid derivatives*

Compound	Recovery (%)
9-Thiastearic acid	74
10-Thiastearic acid	83
11-Thiastearic acid	105

6.4. References

1. T. I. Mayakova, E. E. Kuznetsova, M. G. Kovaleva and S. A. Plyusnin, *J. Chromatogr. B. Biomed. Appl.*, 1995, **672**, 133–137.

2. R. A. Pascal, S. J. Mannarelli and D. L. Ziering, *J. Biol. Chem.*, 1986, **261**, 12441–12443.

3. M. D. Rahman, D. L. Ziering, S. J. Mannarelli, K. L. Swartz, D. S. Huang and R. A. Pascal, *J. Med. Chem.*, 1988, **31**, 1656–1659.

4. K. E. Hovik, O. S. Spydevold and J. Bremer, *Biochim. Biophys. Acta*, 1997, **1349**, 251–256.

5. A. E. Tremblay, N. Tan, E. Whittle, D. J. Hodgson, B. Dawson, P. H. Buist and J. Shanklin, *Org. Biomol. Chem.*, 2010, **8**, 1322–1328.

Chapter 7

Conclusion

7.1. General conclusions

In this study, M.tb lipid substrates were modified with substitution of carbon by sulfur or hydrogen by fluorine or deuterium. In addition, substitution of the hydroxyl group by sulfur or fluorine was carried out. The position of substitution was decided based on the position of oxidation on the lipid molecule in the catabolic pathway. Cholesterol catabolism is initiated by the conversion of cholesterol to cholestenone by cholesterol oxidase or 3β-hydroxy-Δ(5)-steroid dehydrogenase (3β-HSD).[1] The importance of the 3β-hydroxy moiety is well established in the literature for this reaction.[2] For this reason the 3β-hydroxy group was deliberately altered and 3β-mercaptocholest-5-ene (**3**) and 3α-fluorocholest-5-ene (**10**) synthesized to inhibit the enzymatic activity of cholesterol oxidase and 3β-HSD. The synthesis of these compounds is well-known and literature procedures were followed. The value of these compounds as biomarkers and internal standards however has not yet been determined.

Cholesterol was successfully converted to 3β-mercaptocholest-5-ene (**3**) *via* the tosylation of cholesterol and subsequent substitution to cholesterylisothiouronium tosylate (**2**). The final substitution of this synthesis was performed *via* a base mediated elimination of isothiouronium tosylate to form (**3**). Novel side-chain thia cholesterol compounds, 23-thiacholest-4-en-3-one (**4**) and 23-thiacholest-4-en-3β-ol (**5**) were successfully synthesized *via* hydroxymethylprogesterone tosylate (delta-4-HMP) and 2-methyl-1-propanethiol and subsequent reduction to form (**5**). In addition, the deuterium labeled 23-thia analog, [3α-^{2}H]23-thiacholest-4-en-3β-ol (**8**) was synthesized and used as an internal standard for GC-MS analysis. The presence of the hydroxyl group in (**5**), together with the sulfur at C23 provides a method for testing the relative reactivity of this substrate towards cholesterol oxidase. In addition to (**5**), 6β-fluorocholestan-3β,5a-diol (**12**) was synthesized and the cholesterol oxidase activity on this compound determined. The existence of fluorine at C6 of keto-steroids has good biological activity as hormones and contraceptive agents. The synthesis of such compounds often requires several steps with little to moderate yield. Enzymatic oxidation of the hydroxyl steroid can be exploited as an alternative synthetic method. In addition to the cholesterol compounds, thiastearic acid derivatives were synthesized. These fatty acids were synthesized by substitution reactions of bromo-alcohols with thioalkyls. The synthesized compounds were characterized by ^{1}H, ^{13}C, FT-IR and elemental analysis. The identity of the lipid molecules was established *via* molecular mass data as determined by GC-MS. The *in vitro* biological evaluation of the compounds was

carried out to establish the potential of the compounds to serve as carbon sources for M.tb and M.smeg. The value of the compounds as biomarkers or internal standards was evaluated.

The compounds were evaluated as carbon sources for both M.tb and M.smeg and the growth curves established in the presence of these compounds. The growth curves revealed that the steroid derivatives of cholesterol are not as good a substrate as cholesterol itself. However, the results confirmed that the compounds can be utilized as carbon sources by both M.tb and M.smeg. M.tb adapts to the host environment by switching its metabolic pathways from carbohydrates to lipids during infection.[1] During this process, transcriptional and metabolic adaptation is required for the mycobacterium to utilize cholesterol as a carbon source.[3] The lower affinity of the mycobacteria species to the modified cholesterol analogs suggests that the structural changes made to the cholestol analogs effects the growth of the bacteria which is possibly due to the variation in interactions with the CYP450 enzymes.

The mycobacterial species were grown with various thiastearic acids (**14** – **16**) and the growth curves evaluated. The growth of M.tb was only marginally affected in the presence of the thiastearic acids compared to the stearate standard. Overall, greater growth was noted with the thiastearic acids compared to the steroids. This can possibly be due to the higher solubility of the fatty acids which can imply that the thiastearic acids were more readily available to the mycobacteria or that the mycobacteria are better adapted to utilizing fatty acids compared to steroids evaluated.

In this study it was established that the compounds synthesized can be utilized as carbon sources by M.tb and M.smeg and the catabolic fate of the compounds were determined. Cholesterol catabolism is initiated by the formation of cholestenone *via* the action of cholesterol oxidase or 3β-HSD. The 3β-hydroxy steroids synthesized, 23-thiacholest-4-en-3β-ol (**5**) and 6β-fluorocholestan-3β,5α-diol (**12**), were enzymatically oxidized *via* cholesterol oxidase. Cholesterol was used as a reference and the change in concentration monitored after 45 minutes. Oxidation products could be observed for all three compounds at retention times higher than that of the original alcohol indicating the expected increase in polarity.

Due to the significance of the 3β-hydroxy moiety of cholesterol, the steroid was modified with sulfur (3β-mercaptocholest-5-ene (**3**)) or fluorine (3α-fluorocholest-5-ene (**10**)) at C3 to prevent the oxidation by cholesterol oxidase. In the absence of this initial oxidation, it was evaluated whether side-chain degradation still occurs. Extracts of cell-free and whole cell incubation results of (**3**) revealed no additional peaks in the TICs, thus no side-chain catabolic products were identified. This does not necessarily mean that side-chain degradation does not occur, but that under the current analytical conditions, it could not be

detected. This was further confirmed by the positive growth curves obtained for M.smeg grown in the presence of (**3**). LC-MS analysis would be a better method of evaluating the more polar metabolic products. No side-chain oxidation products were observed in the TICs for the incubation extracts of (**10**). A peak corresponding to cholesterol was detected which suggests that the fluorine gets substituted and cholesterol forms. Based on the results obtained, it cannot be concluded whether side-chain degradation occurs in the absence of cholesterol oxidase or 3β-HSD activity. Additional investigation is therefore required to establish whether side-chain degradation does occur in the absence of cholesterol oxidase activity.

The compounds synthesized were also evaluated as biomarkers for cholesterol catabolism in M.smeg. The cholesterol incubation extracts revealed cholestenone as one of the catabolic products together with two other side-chain oxidations products. This was identified based on the use of a cholestenone standard and molecular mass data. In the presence of econazole, almost 50 % less cholesterol was degraded which confirms the inhibition activity of econazole on the P450 enzymes. The synthesized compounds were tested in the same manner. 23-Thiacholest-4-en-3-one (**4**) and 23-thiacholest-4-en-3β-ol (**5**) were evaluated and the TICs of the incubations extracts of (**5**) showed clear oxidation of the compound taking place to form (**4**) as determined in the cholesterol oxidase experiments.

In addition to evaluating the compounds as biomarkers, the use of the compounds as internal standards was also determined. Due to the similar chemical nature of the synthesized compounds to that of cholesterol and stearic acid, the analogs make for excellent internal standards. It is known that substituting a methylene group (-CH_2-) with a sulfur atom (-S-) in the molecule does not perturb the shape of the molecule but increases the mass by 18 amu.[4] The subsequent S-oxidation due to catabolism causes a further mass shift of +16 amu, thus indicating its identity as a non-natural thia-derivative. Good recovery percentages and no visible degradation in the short term were observed which shows that the utility of the compounds as internal standards will allow for accurate quantification of the lipids in analytical procedures required for accurate quantification.

The thiastearic acids were incubated with M.smeg and the concentration of the compounds noted after a 24 hour period. A decrease in concentration after the incubation period was observed with 9-thiastearic acid (**14**) and 10-thiastearic acid (**15**) while little change was seen with 11-thiastearic acid (**16**). This was further perceived by the M.smeg growth curves which showed that (**14**) and (**15**) were better substrates and that less growth with (**16**) was observed. This could possibly be due to the significant olefination at C9 and C10 during

desaturation of fatty acids. The lower growth observed with (**11**) suggests that C11 in stearic acid can possibly be targeted for inhibition of stearic acid catabolism.

The evaluation of the compounds as inhibitors of downstream lipid catabolism requires further studies. The catabolic products obtained in this study were as a result of early side-chain degradation. This can be seen by the C26-OH and C26-aldehyde products obtained for the cholesterol incubations.

7.2. Future Aspects

Further *in vitro* studies will be required to determine whether side-chain degradation can occur when cholesterol oxidase activity is inhibited. The crude protein concentration can be increased or the duration of the cell-free incubations. The side-chain catabolic enzymes, CYP125 and CYP142 can be isolated and the binding of (**3**) and (**10**) with these enzymes assessed. The crystal structures of CYP125 and CYP125-cholesterol complex have been reported by McLean *et al* and will shed light on the substrate specificity of these enzymes and whether cholesterol side-chain is possible when the activity of 3β-HSD is blocked.[5]

In this study, a biological and analytical platform was established to evaluate lipid catabolism in M.tb and M.smeg. However further application prospects are possible. The value of the compounds as internal standards has been determined in a whole cell mycobacterial growth medium. Their use in quantification techniques for cholesterol quantification in pathology would be of great interest. Thus, further evaluation of the compounds as internal standards can be carried out in various media such as blood serum.

7.3. References

1. H. Ouellet, J. B. Johnston and P. R. O. de Montellano, *Trends Microbiol.*, 2011, **19**, 530–539.

2. B. L. Heyl, D. J. Tyrrell and J. D. Lambeths, *J. Biol. Chem.*, 1986, **261**, 2743–2749.

3. J. E. Griffin, A. K. Pandey, S. A. Gilmore, V. Mizrahi, J. D. McKinney, C. R. Bertozzi and C. M. Sassetti, *Chem. Biol.*, 2012, **19**, 218–227.

4. R. A. Pascal and D. L. Ziering, *J. Lipid Res.*, 1986, **27**, 221–224.

5. K. J. McLean, P. Lafite, C. Levy, M. R. Cheesman, N. Mast, I. A. Pikuleva, D. Leys and A. W. Munro, *J. Biol. Chem.*, 2009, **284**, 35524–35533.

Chapter 8

Experimental

8.1. General Materials and Methods

Materials

All chemicals and reagents were purchased from Merck and/or Sigma Aldrich and used as received. Reactions were monitored by thin-layer chromatography (TLC) using Merck F254 aluminium-backed pre-coated silica analytical plates. Detection was done using ultraviolet light at 245 nm and by heating the TLC plate after spraying with 1 % ceric ammonium sulphate in 3 M sulfuric acid. Column chromatography was carried out using silica gel (Merck Silica Gel 60, 70-230 mesh) and eluting with hexane, ethyl acetate.

Instrumentation

^{1}H nuclear magnetic resonance (NMR) spectra were obtained using a Varian Mercury (300 or 400 MHz) and/or Bruker (400 MHz) spectrometer at ambient temperatures using $CDCl_3$, unless otherwise stated. NMR shifts were recorded as δ in parts per million (ppm) with tetramethylsilyl (TMS) used as the internal standard. The spin multiplicities were recorded as: s, singlet; d, doublet; t, triplet; q, quartet and m, multiplet. ^{13}C NMR was recorded on a Bruker (100 MHz) using $CDCl_3$. Infrared (IR) spectra were recorded on a Jasco FT-IR 410 spectrometer using KBr pellets. Microanalysis for carbon, hydrogen, nitrogen and sulfur were recorded on an Elemental Analyzer CHNS-O. Melting points were determined using a Reichert-Jung Thermovar hot plate microscope and are uncorrected.

8.2. Cholesteryl tosylate (1)[1]

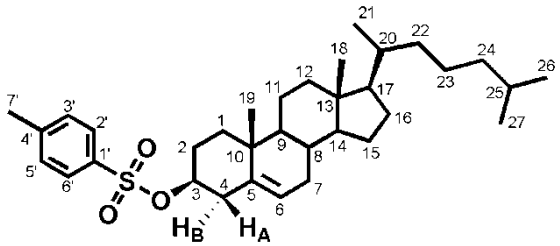

A catalytic amount of DMAP was added to an ice cooled solution of cholesterol (1.05 g, 2.71 mmol) in dry DCM (6 mL) and anhydrous pyridine (6 mL). Toluenesulfunylchloride (1.50 g, 7.89 mmol) was added to the solution and allowed to stir at 0 °C for 4 hours with additional stirring at room temperature for 12 hours. The solution was diluted with DCM (15 mL) and washed with 1 M HCl (2 x 20 mL), H_2O (20 mL) and brine (20 mL). The organic

layer was collected and dried over anhydrous $MgSO_4$. The solvent was reduced in vacuo and the residue recrystallized from a combination of DCM and MeOH to yield a white crystalline solid (0.97 g, 66 %).

M.p.: 132 – 133 °C. Lit.[1] m.p.: 132 – 133 °C. R_f (Hex:EtOAc, 5:5) 0.68. ^{1}H NMR (400 MHz, $CDCl_3$): ppm 0.66 (3H, s, H18), 0.85 (3H, d, *J* 1.5 Hz, H26), 0.87 (3H, d, *J* 1.4 Hz, H27), 0.90 (3H, d, *J* 6.5 Hz, H21), 0.97 (3H, s, H19), 0.99 – 1.75 (20H, m, H8 – H9, H11– H17, H20, H22 – H25), 1.81 (2H, m, H1), 1.81 (3H, m, H2, H7), 1.98 (2H, m, $H4_A$, H7), 2.27 (1H, dd, *J* 4.9 Hz, 13.1 Hz $H4_B$), 2.44 (3H, s, H7''), 4.33 (1H, m, H3), 5.31 (1H, d, *J* 4.8 Hz, H6), 7.32 (2H, d, *J* 8.1 Hz, H3'', H5''), 7.79 (2H, d, *J* 8.1 Hz, H2'', H6''). ^{13}C NMR (100 MHz, $CDCl_3$): ppm 11.8, 18.7, 19.1, 21.0, 21.6, 22.5, 22.8, 23.8, 24.2, 28.0, 28.2, 28.7, 31.8, 31.9, 35.8, 36.2, 36.4, 36.9, 38.9, 39.5, 39.7, 42.3, 49.9, 56.2, 56.7, 82.4, 123.5, 127.6 (2C), 129.7 (2C), 134.9, 138.9, 144.4. *FT-IR* (KBr): *v* (cm^{-1}) 1599, 1470 (Aromatic C=C stretch), 2943 (Aromatic C-H stretch). Elemental Analysis (%): Calc. For $C_{34}H_{52}O_3S$: C, 75.5 %; H, 9.7 %; S, 5.0 %. Anal. Found: C, 74.4 %; H, 9.7 %; S, 5.0 %.

8.3. Cholesterylisothiouronium tosylate (2)[2]

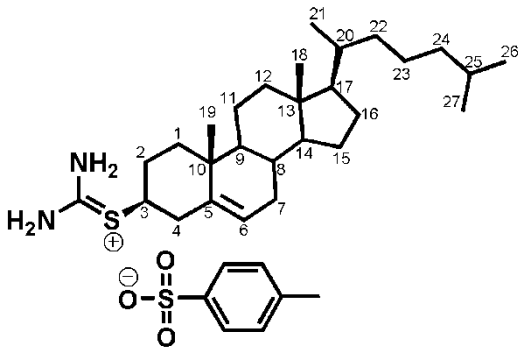

A suspension of cholesteryl tosylate (**1**) (4.74 g, 8.76 mmol), thiourea (8.13 g, 106.80 mmol) and dry isopropanol (40 mL) was allowed to reflux for 4 hours. H_2O (20 mL) was added to the refluxing solution and the resulting suspension cooled to room temperature and allowed to stand at 4 °C overnight. The resulting precipitate was collected by filtration, washed with acetone and dried to afford the product as a white crystalline solid (5.00 g, 93 %).

M.p.: 237 – 239 °C. Lit.[2] m.p.: 237 – 239 °C. R_f (Hex:EtOAc, 5:5) 0.86. *FT-IR* (KBr): *v* (cm^{-1}) 3492, 3430 (N-H stretch), 1657 (N-H bend), 1653 (Aromatic C=C stretch), 1383 and 1183 (S=O stretch), 1208 (C-N stretch). Elemental Analysis (%): Calc. For $C_{35}H_{56}O_3N_2S_2$: C, 68.1 %; H, 9.2 %; N, 4.5 %; S, 10.4 %. Anal. Found: C, 67.5 %; H, 9.2 %; N, 4.1 %; S, 9.4 %.

8.4. 3β-Mercaptocholest-5-ene (3)[2]

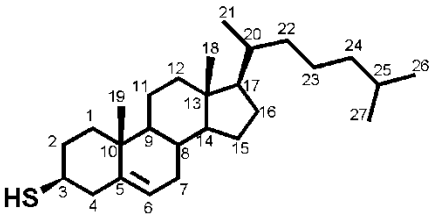

NaOH (10.10 g, 252.50 mmol) was added to a mixture of cholesterylisothiouronium tosylate (**2**) (4.82 g, 7.81 mmol) in absolute EtOH (30 mL) which was allowed to reflux under nitrogen until the mixture became homogeneous (approximately 30 minutes). H_2O (10 mL) was added and the solution was refluxed for a further 2 hours. After cooling to room temperature, the solution was poured into iced H_2O (50 mL) followed by the addition of glacial acetic acid (2 mL). The resulting precipitate was collected by filtration and recrystallized from EtOH to afford a yellow solid (1.11 g, 40 %).

M.p.: 93 – 95 °C. Lit.[2] m.p.: 94 – 96 °C. R_f (Hex:EtOAc, 5:5) 0.90. ^{1}H NMR (400 MHz, $CDCl_3$): ppm 0.65 (3H, s, H18), 0.83 (3H, d, *J* 1.6 Hz, H26), 0.84 (3H, d, *J* 1.6 Hz, H27), 0.88 (3H, d, *J* 6.6 Hz, H21), 0.97 (3H, s, H19), 1.01 – 1.99 (22H, m, H1, H8 – H9, H11– H17, H20, H22 – H25), 1.83 (1H, m, SH), 1.90 – 2.04 (4H, m, H2, H7), 2.28 (2H, m, H4), 2.67 (1H, m, H3), 5.29 (1H, d, *J* 4.6 Hz, H6). ^{13}C NMR (100 MHz, $CDCl_3$): ppm 11.9, 18.7, 19.3, 20.9, 22.6, 22.8, 23.8, 24.3, 28.0, 28.2, 29.3, 31.8, 34.1, 35.8, 36.2, 37.5, 39.4, 39.5, 39.7, 39.9, 42.3, 44.2, 50.3, 56.2, 56.7, 121.0, 141.9. *FT-IR* (KBr): *v* (cm^{-1}) 2897 (S-H stretch). Elemental Analysis (%): Calc. For $C_{27}H_{46}S$: C, 80.5 %; H, 11.5 %; S, 7.9 %. Anal. Found: C, 80.6 %; H, 11.6 %; S, 6.0 %. M/Z 402.3 (100 % [M^+])

8.5. 23-Thiacholest-4-en-3-one (4)

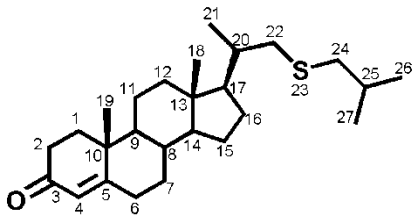

Solid NaOH (0.38 g, 9.52 mmol) was added to 2-methyl-1-propanethiol (1.00 mL, 9.38 mmol) and stirred at room temperature for 1 hour. The resulting mixture was added to a suspension of hydroxymethylprogesterone tosylate (delta-4-HMP-tosylate) (1.03 g, 2.45 mmol) in absolute EtOH and allowed to stir at room temperature for 30 minutes followed by refluxing for 4 hours. Concentrated HCl (3 mL) and H_2O (3 mL) were added at room temperature and the mixture further refluxed overnight. The resulting solution was cooled to room temperature, poured into diethyl ether (50 mL) and washed with 1 M NaOH (2 x 50 mL) and

H_2O (50 mL). The organic layer was dried over anhydrous $MgSO_4$ and the solvent evaporated. Recrystallization from MeOH and H_2O afforded a white crystalline solid (0.28 g, 29 %).

M.p.: 101 – 103 °C. R_f (Hex:EtOAc, 6:4) 0.69. ^{1}H NMR (400 MHz, $CDCl_3$): ppm 0.72 (3H, s, H18), 0.98 (6H, d, *J* 6.6 Hz, H26, H27), 1.06 (3H, d, *J* 7.8 Hz, H21), 1.18 (3H, s, H19), 1.81 – 1.22 (16H, m, H7 – H9, H11 – H12, H14 – H17, H20, H25), 2.01 (2H, m, H1), 2.26 (2H, m, H6), 2.36 (4H, m, H22, H24), 2.63 (2H, dd, *J* 2.9 Hz, 12.3 Hz, H2), 5.72 (1H, m, H4). ^{13}C NMR (100 MHz, $CDCl_3$): ppm 12.0, 17.4, 18.8, 21.0, 22.0, 22.1, 22.2, 28.1, 28.8, 32.0, 32.9, 34.0, 35.6, 35.7, 36.8, 38.6, 39.5, 40.5, 42.5, 42.6, 53.8, 55.4, 55.8, 123.8, 171.4, 199.5. *FT-IR* (KBr): *v* (cm^{-1}) 1669 (C=O). Elemental Analysis (%): Calc. For $C_{26}H_{42}OS$: C, 77.6 %; H, 10.5 %; S, 7.9 %. Anal. Found: C, 77.2 %; H, 10.5 %; S, 7.0 %. M/Z 402.3 (26.7 % [M^+])

8.6. 23-Thiacholest-4-en-3β-ol (5)

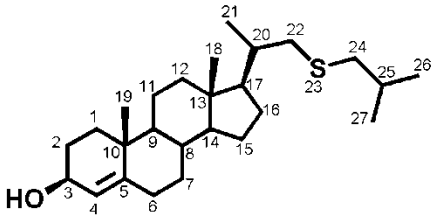

$NaBH_4$ (0.39 g, 10.31 mmol) was added to a solution of 23-thiacholest-4-en-3-one (**4**) (0.51 g, 1.27 mmol) and $CeCl_3 \cdot 7H_2O$ (0.43 g, 1.15 mmol) in MeOH (20 mL) at 0 °C in one portion. The solution was allowed to stir at 0 °C for 2 hours before quenching with H_2O (10 mL). The resulting solution was poured into 5 % HCl (15 mL) and extracted with DCM (2 x 20 mL). The organic layers were collected and washed sequentially with brine (3 x 20 mL) and H_2O (20 mL) then dried over anhydrous $MgSO_4$. The solvent was reduced under vacuum and the resulting residue recrystallized from diethyl ether to yield (**5**) as a white solid (0.39 g, 76 %).

M.p.: 76 – 78 °C. R_f (Hex:EtOAc, 5:5) 0.51. ^{1}H NMR (400 MHz, $CDCl_3$): ppm 0.69 (3H, s, H18), 0.97 (6H, d, *J* 6.6 Hz, H26, H27), 1.05 (3H, m, H21), 1.07 (3H, s, H19), 1.81 – 1.22 (16H, m, H7 – H12, H14 – H17, H20, H25), 2.01 (4H, m, H1, H6), 2.26 (1H, m, H2), 2.36 (3H, d, *J* 6.8 Hz, H22, H24), 2.62 (1H, dd, *J* 2.9 Hz, 12.3 Hz, H22), 3.48 (1H, m, H3), 4.15 (1H, broad s, OH), 5.27 (1H, m, H4). ^{13}C NMR (100 MHz, $CDCl_3$): ppm 12.0, 18.8, 18.9, 21.0, 22.0, 22.2, 24.2, 28.2, 28.8, 29.5, 32.2, 33.1, 35.4, 36.0, 36.9, 37.4, 40.0, 40.5, 42.5, 42.7, 54.4, 55.5, 56.0, 68.0, 123.4, 147.7. *FT-IR* (KBr): *v* (cm^{-1}) 3402 (OH). Elemental Analysis (%): Calc. For $C_{26}H_{44}OS$: C, 77.1 %; H, 11.0 %; S, 7.9 %. Anal. Found: C, 74.4 %; H, 11.0 %; S, 7.0 %. M/Z 386.3 (35.0 % [M^+])

8.7. 22-(Isothiouronium)-20-methylpregna-4-en-3-one (6)[3]

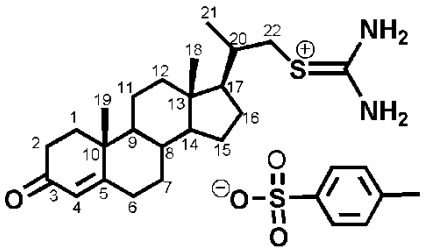

A suspension of delta-4-HMP-tosylate (0.49 g, 1.03 mmol), thiourea (0.90 g, 12.99 mmol) and dry isopropanol (10 mL) was allowed to reflux for 4 hours. H_2O (5 mL) was added to the refluxing solution and the resulting suspension cooled to room temperature and allowed to stand at 4 °C overnight. The resulting precipitate was collected by filtration, washed with acetone and dried to afford the product as a white solid (0.55 g, 95 %).

M.p.: 227 – 230 °C. Lit.[3] m.p.: 158 – 160 °C. R_f (Hex:EtOAc, 5:5) 0.38. *FT-IR* (KBr): *v* (cm^{-1}) 3376 and 3270 (N-H stretch), 1673 (N-H bend), 1446 (Aromatic C=C stretch), 1212 (C-N stretch). Elemental Analysis (%): Calc. For $C_{30}H_{44}N_2O_4S_2$: C, 64.2 %; H, 8.0 %; N, 5.0, S, 11.4 %. Anal. Found: C, 63.3 %; H, 8.0 %; N, 4.0 %; S, 11.3 %.

8.8. 22-mercapto-20-methylpregna-4-en-3-one (7)[4]

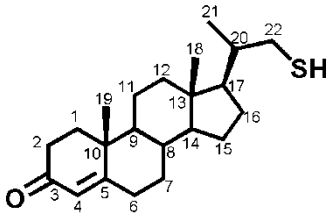

NaOH (1.18 g, 29.50 mmol) was added to a mixture of pregna-4-en-3-one, 22-(isothiouronium)-20-methyl (**6**) (0.51 g, 0.92 mmol) in absolute EtOH (10 mL) which was allowed to reflux under nitrogen until the mixture became homogeneous (approximately 30 minutes). H_2O (5 mL) was added and the solution was refluxed for a further 2 hours. After cooling to room temperature, the solution was poured into iced H_2O (15 mL) followed by the addition of glacial acetic acid (0.2 mL). The resulting precipitate was collected by filtration and recrystallized from EtOH to afford an orange solid (0.18 g, 58 %).

M.p.: 189 – 192 °C. Lit.[4] m.p.: 150 – 154 °C. R_f (Hex:EtOAc, 5:5) 0.66. ^{1}H NMR (400 MHz, $CDCl_3$): ppm 0.68 (3H, s, H18), 1.02 (3H, m, H21), 1.12 (3H, s, H19), 1.15 – 2.63 (19H, m, H1, H6 – H9, H11, H12, H14 – H17, H20), 2.85 (2H, d, *J* 12.0 Hz H22), 3.65 (2H, m, H2), 5.64 (1H, m, H4). ^{13}C NMR (100 MHz, $CDCl_3$): ppm 11.9, 12.0, 17.4, 18.5, 21.0, 24.2, 28.2, 32.0, 32.9, 34.0, 35.6, 35.7, 36.4, 39.5, 42.8, 46.7, 46.8, 53.8, 55.2, 55.8, 123.8, 171.3.

Elemental Analysis (%): Calc. For $C_{22}H_{34}OS$: C, 76.2 %; H, 9.8 %; S, 9.2 %. Anal. Found: C, 71.9 %; H, 9.2 %; S, 8.0 %.

General procedure for the reduction of α,β-unsaturated ketones using $NaBD_4$.

$NaBD_4$ (1.00 mmol) was added to a solution of ketone (1.00 mmol) and $CeCl_3 \cdot 7H_2O$ (1.00 mmol) in absolute EtOH (20 mL) at 0 °C in one portion. The solution was allowed to stir at 0 °C for 2 hours before quenching with H_2O (10 mL). The resulting solution was poured into 5 % HCl (15 mL) and extracted with DCM (2 x 20 mL). The organic layers were collected and washed sequentially with brine (3 x 20 mL) and H_2O (20 mL) then dried over anhydrous $MgSO_4$. The solvent was reduced under vacuum and the resulting residue recrystallized from diethyl ether to yield the desired product.

8.9. [3α-^{2}H]23-Thiacholest-4-en-3β-ol (8)

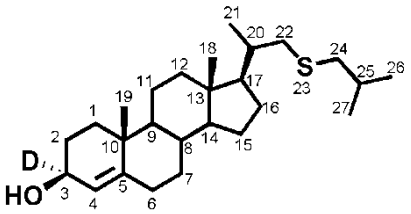

Compound (**8**) was obtained from 23-thiacholest-4-en-3-one (**4**) (0.10 g, 0.25 mmol), to yield a product as a white solid (79.70 mg, 79 %).

M.p.: 81 - 84 °C. R_f (Hex:EtOAc, 5:5) 0.75. ^{1}H NMR (400 MHz, $CDCl_3$): ppm 0.69 (3H, s, H18), 0.97 (6H, d, *J* 6.6 Hz, H26, H27), 1.05 (3H, m, H21), 1.07 (3H, s, H19), 1.13 – 2.04 (16H, m, H7 – H12, H14 – H17, H20, H25), 1.92 – 2.03 (4H,m, H1, H6), 2.26 (3H, m, H2, H22), 2.36 (2H, d, *J* 6.8 Hz, H24), 2.84 (1H, dd, *J* 2.9 Hz, 12.3 Hz, H22), 5.27 (1H, m, H4). ^{13}C NMR (100 MHz, $CDCl_3$): ppm 12.0, 18.8, 18.9, 21.0, 22.0, 22.2, 24.2, 28.2, 28.8, 29.4, 32.0, 32.3, 33.1, 35.4, 35.7, 35.9, 36.0, 36.9, 39.7, 40.5, 42.5, 42.7, 54.4, 55.5, 56.1, 123.4. *FT-IR* (KBr): *v* (cm^{-1}) 3437 (OH). M/Z 405.3 (10.9 % [M^+])

8.10. [3α-^{2}H]Cholest-4-en-3β-ol (9)[5]

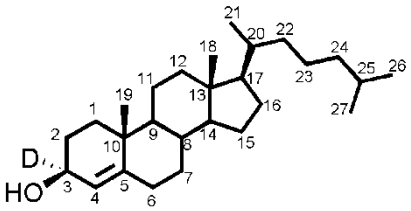

Compound (**9**) was attained from cholest-4-en-3-one (0.11 g, 0.27 mmol) to afford (**9**) as a white solid (61.00 mg, 57 %).

M.p.: 112 – 115 °C. Lit.[5] m.p.: 130 – 132 °C. R_f (Hex:EtOAc, 5:5) 0.64. ^{1}H NMR (400 MHz, $CDCl_3$): ppm 0.68 (3H, s, H18), 0.86 (3H, d, *J* 1.6 Hz, H26), 0.87 (3H, d, *J* 1.6 Hz, H27), 0.90 (3H, d, *J* 6.4 Hz, H21), 1.05 (3H, s, H19), 1.11 – 1.56 (20H, m, H8 – H12, H14 – 17, H20, H22 – H25), 1.69 (2H, m, H7), 1.82 (2H, m, H1), 1.98 (2H, m, H6), 2.18 (1H, m, H2), 5.27 (1H, m, H4). ^{13}C NMR (100 MHz, $CDCl_3$): ppm 12.0, 18.7, 19.0, 21.1, 22.6, 22.8, 23.9, 24.2, 28.0, 28.2, 29.5, 32.3, 33.2, 35.4, 35.7, 35.8, 36.0, 36.2, 37.4, 39.5, 39.9, 42.5, 54.5, 56.2, 56.3, 123.2, 147.9. Elemental Analysis (%): Calc. For $C_{27}H_{45}DO$: C, 83.2 %; H, 11.6 %. Anal. Found: C, 82.2 %; H, 11.4 %. M/Z 387.3 (45.4 % [M^+])

8.11. 3α-Fluorocholest-5-ene (10)[6]

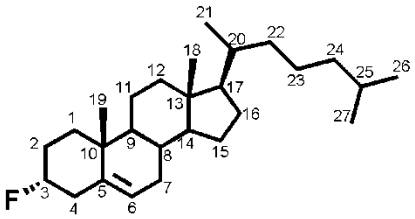

Diethylaminosulfur trifluoride (DAST) (85 µL, 6.45 mmol) was added to a solution of cholesterol (0.51 g, 1.29 mmol) in dry DCM (10 mL). The solution was allowed to stir at room temperature under nitrogen for 4 hours. Upon completion, the solution was diluted with DCM (15 mL) and washed with 5 % $NaHCO_3$ (2 x 15 mL). The organic layer was collected, dried over anhydrous $MgSO_4$ and evaporated. The resulting residue was purified by column chromatography and recrystallized from EtOH to yield a white solid (0.15 g, 31 %).

M.p.: 90 – 93 °C. R_f (Hex:EtOAc, 5:5) 0.88. ^{1}H NMR (400 MHz, $CDCl_3$): ppm 0.62 (3H, s, H18), 0.79 (3H, d, *J* 1.6 Hz, H26), 0.81 (3H, d, *J* 1.6 Hz, H27), 0.85 (3H, d, *J* 6.5 Hz, H21), 0.96 (3H, s, H19), 0.99 – 1.53 (20H, m, H8 – H12, H14 – 17, H20, H22 - H25), 1.62 (2H, m, H1), 1.79 (2H, m, H7), 1.94 (2H, m, H4), 2.37 (2H, m, H2), 4.24 and 4.37 (1H, m, H3), 5.33 (1H, d, *J* 3.7 Hz H6). ^{13}C NMR (100 MHz, $CDCl_3$): ppm 11.9, 18.7, 19.3, 21.1, 22.6, 22.8, 23.8, 24.3, 28.0, 28.2, 28.7, 28.9, 31.9, 32.0, 35.8, 36.2, 36.3, 36.4, 39.5, 39.8, 42.4, 50.1, 56.2, 56.8, 92.0 and 93.7 (C3), 123.0, 139.3. Elemental Analysis (%): Calc. For $C_{27}H_{45}F$: C, 83.4 %; H, 11.5 %. Anal. Found: C, 82.6 %; H, 11.6. M/Z 388.3 (58.9 % [M^+])

8.12. 5α,6α-Epoxycholest-3β-ol (11)[7]

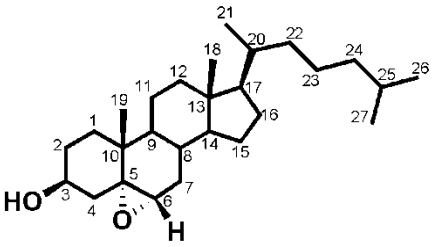

A mixture of $NaHCO_3$ (2.54 g, 30.28 mmol), m-CPBA (2.61 g, 16.88 mmol) and cholesterol (2.91 g, 7.53 mmol) in dry DCM (20 mL) was allowed to stir at room temperature for 2 hours. The resulting mixture was quenched with saturated aqueous $NaBH_4$ and diluted with DCM (20 mL). This was then washed with aqueous $NaHCO_3$ (2 x 30 mL) and brine (20 mL). The organic layer was dried over anhydrous $MgSO_4$ and the solvent evaporated to produce a yellow residue which was purified by column chromatography and recrystallized from acetone and H_2O to yield a white solid (0.99 g, 77 %).

M.p.: 143 – 146 ºC. Lit.[7] m.p.: 145 – 146 ºC. R_f (Hex:EtOAc, 5:5) 0.48. ^{1}H NMR (400 MHz, $CDCl_3$): ppm 0.56 (3H, s, H18), 0.78 (3H, d, *J* 1.7 Hz, H26), 0.80 (3H, d, *J* 1.7 Hz, H27), 0.82 (3H, d, *J* 6.4 Hz, H21), 0.85 – 0.93 (6H, m, H22 – H24), 0.99 (3H, s, H19), 1.04 – 1.60 (14H, m, H8 – H9, H11 – H12, H14 – H17, H20, H25), 1.74 (2H, m, H7), 1.84 (3H, m, H2, H4), 2.00 (1H, t, *J* 12.2 Hz, H2), 2.83 (1H, d, *J* 4.2 Hz, H6), 3.84 (1H, m, H3). ^{13}C NMR (100MHz, $CDCl_3$): ppm 11.9, 15.9, 18.7, 20.7, 22.5, 22.8, 23.8, 24.1, 27.9, 28.1, 28.8, 29.9, 31.1, 32.4, 34.9, 35.8, 36.2, 39.4, 39.5, 39.9, 42.4, 42.6, 55.9, 56.9, 59.3, 65.7, 68.7. Elemental Analysis (%): Calc.: For $C_{27}H_{46}O_2$: C, 80.5 %; H, 11.5 %. Anal. Found: C, 78.3 %; H, 11.2 %.

8.13. 6β-Fluorocholestan-3β,5a-diol (12)[8]

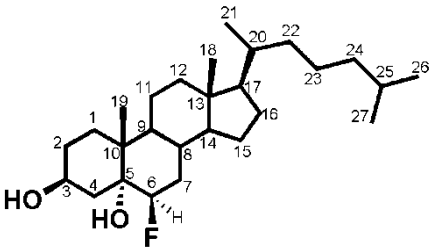

$BF_3{\cdot}OEt_2$ (0.4 mL, 3.00 mmol) was added to a solution of 5α,6α-epoxycholest-3β-ol (**11**) (0.33 g, 0.82 mmol) in dry diethyl ether (20 mL) under anhydrous conditions. The solution was allowed to stir at room temperature for 3 hours after which it was diluted with diethyl ether (10 mL), washed with aqueous $NaHCO_3$ (2 x 20 mL) and H_2O (2 x 20 mL). The organic layer was dried over $MgSO_4$, the solvent was evaporated and the residue subjected to column chromatography. The crude product was subsequently recrystallized from acetone and hexane to produce a white solid (0.14 g, 39 %).

M.p.: 216 – 218 ºC. Lit.[8] m.p.: 219 – 221 ºC. R_f (Hex:EtOAc, 2:8) 0.39. ^{1}H NMR (400 MHz, $CDCl_3$): ppm 0.68 (3H, s, H18), 0.86 (3H, d, *J* 1.6 Hz, H26), 0.87 (3H, d, *J* 1.6 Hz, H27), 0.90 (d, *J* 6.6 Hz, H21), 0.92 (3H, s, H19), 1.04 – 1.60 (14H, m, H8 – H17, H20, H25), 1.67 (2H, m, H1), 1.84 (4H, m, H2, H7), 2.06 (2H, m, H4), 3.72 (1H, m, H3) 4.05 (2H, m, OH x 2), 4.32 and 4.44 (1H, m, H6). ^{13}C NMR (100MHz, $CDCl_3$): ppm 11.9, 18.7, 19.3, 21.1, 22.8, 22.6, 23.8, 24.3, 28.5, 28.8, 29.7, 31.9, 35.8, 36.2, 36.3, 36.4, 36.6, 39.3, 39.5, 39.8, 42.4, 50.1, 56.2, 56.8, 92.0 and 93.7 (C6), 123.0, 139.4. Elemental Analysis (%): Calc. For $C_{27}H_{47}O_2F$: C, 76.7 %; H, 11.2 %. Anal. Found: C, 82.5 %; H, 11.9 %. M/Z 422.3 (8.8 % [M^+])

8.14. 9-Bromononanoic acid (13)[9,10]

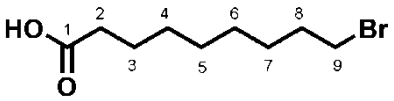

Method 1:

A solution of concentrated H_2SO_4 (0.6 mL) and H_2O (2 mL) was added to a solution of CrO_3 (0.68 g, 6.84 mmol) in H_2O (1 mL) at 0 ºC. The resulting solution was added to a solution 9-bromononanol (1.10 g, 4.48 mmol) in acetone (20 mL) at - 5 ºC. The solution was stirred at 0 ºC for 2 hours followed by stirring at room temperature for 16 hours. An extraction with diethyl ether (4 x 25 mL) was carried out and the organic layers combined. This was then washed with H_2O (2 x 60 mL) and brine (60 mL) and the organic layer dried over anhydrous $MgSO_4$. The solvent was evaporated and purified by column chromatography to yield (**13**) as a colourless oil (0.82 g, 77 %).

Method 2:

9-Bromononanol (1.07 g, 4.48 mmol) was added to concentrated HNO_3 (10 mL, 0.24 mol) over 30 minutes while maintaining the temperature between 25 – 30 °C. The solution was stirred at room temperature for 4 hours followed by stirring at 80 °C for an additional hour. After cooling to room temperature, H_2O (100 mL) was added and the solution extracted with diethyl ether (4 x 25 mL). The organic layers were combined and dried over anhydrous $MgSO_4$ and the solvent evaporated. The resulting residue was purified by column chromatography to yield (**13**) as a yellow solid (0.64 g, 60 %).

M.p.: 28 – 30 ºC. Lit.[10] m.p.: 31 – 33 ºC. R_f (Hex:EtOAc, 5:5) 0.58. ^{1}H NMR (400 MHz, $CDCl_3$): ppm 1.34 (8H, m, H4 – H7), 1.57 (2H, m, H3), 1.79 (2H, m, H8), 2.28 (2H, t, *J* 7.4 Hz, H2), 3.34 (2H, t, *J* 6.9 Hz, H9). ^{13}C NMR (100 MHz, $CDCl_3$): ppm 24.5, 28.1, 28.6, 29.0, 29.1, 32.8, 33.9, 34.0, 180.1.

General procedure for the synthesis of thiastearic acids.

Solid KOH (2.00 mmol) was added to a solution of the appropriate bromo-carboxylic acid (1.00 mmol) and the corresponding alkylthiol (1.00 mmol) in absolute EtOH (20 mL). After refluxing the solution under nitrogen for 3 hours it was allowed to cool to room temperature, acidified with glacial acetic acid and the solvent removed *in vacuo*. DCM (20 mL) was added to the resulting residue and washed with H_2O (2 x 20 mL). The organic layer was dried over anhydrous $MgSO_4$ and the solvent evaporated. Recrystallization from acetone afforded the thiastearic acid.

8.15. 9-Thiastearic acid (14)[11]

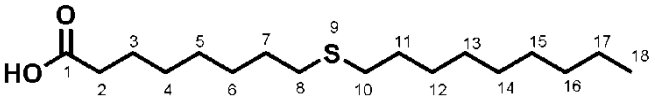

Compound (**14**) was produced from 8-bromooctanoic acid (0.58 g, 2.77 mmol) and 1-nonanethiol (0.4 mL, 2.39 mmol) as a white crystalline solid (0.47 g, 35 %).

M.p.: 43 - 45 °C. Lit.[12] m.p.: 51 – 52 °C. R_f (Hex:EtOAc, 8:2) 0.52. ^{1}H NMR (400 MHz, $CDCl_3$): ppm 0.88 (3H, t, *J* 6.6 Hz, H18), 1.27 – 1.41 (18H, m, H4 – H6, H12 – H17), 1.61 (6H, m, H3, H7, H11), 2.35 (2H, t, *J* 7.4 Hz, H2), 2.49 (4H, t, *J* 7.4 Hz, H8, H10). ^{13}C NMR (100 MHz, $CDCl_3$): ppm 14.1, 22.7, 24.6, 28.7, 28.8, 28.9 (2C), 29.3 (2C), 29.5, 29.6, 29.8, 31.9, 32.2, 32.3, 33.9, 179.2.

8.16. 10-Thiastearic acid (15)[11]

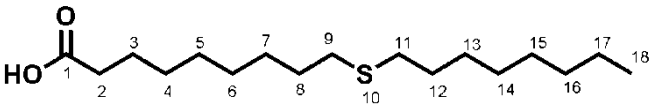

Compound (**15**) was synthesized from (**13**) (0.59 g, 2.48 mmol) and 1-octanethiol (0.4 mL, 2.48 mmol) to produce a pale pink solid (0.78 g, 78 %).

M.p.: 40 - 42 °C. Lit.[12] m.p.: 46 – 47 ºC. R_f (Hex:EtOAc, 8:2) 0.58. ^{1}H NMR (400 MHz, $CDCl_3$): ppm 0.88 (3H, t, *J* 7.9 Hz, H18), 1.31 (18H, m, H4 – H7, H13 – H17), 1.58 (6H, m, H3, H8, H12), 2.34 (2H, t, *J* 7.5 Hz, H2), 2.49 (4H, t, *J* 7.3 Hz, H9, H11). ^{13}C NMR (100 MHz, $CDCl_3$): ppm 14.1, 22.7, 24.7, 28.8, 28.9 (2C), 29.0, 29.1, 29.2, 29.3, 29.7, 29.8, 31.8, 32.2, 32.3, 33.9, 179.3.

8.17. 11-Thiastearic acid (16)[11]

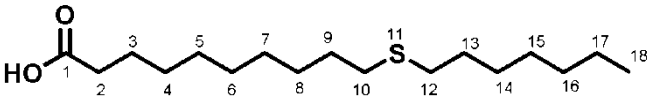

Compound (**16**) was obtained from 10-bromodecanoic acid (1.01 g, 3.98 mmol) and 1-heptanethiol (0.70 mL, 4.00 mmol) to produce a white solid (0.38 g, 32 %).

M.p.: 47 – 49 ºC. Lit.[11] m.p.: 45 – 46 ºC. R_f (Hex:EtOAc, 5:5) 0.84. ^{1}H NMR (400 MHz, $CDCl_3$): ppm 0.87 (3H, m, H18), 1.37 – 1.29 (18H, m, H4 – H8, H14 – H17), 1.59 (6H, m, H3, H9, H13), 2.34 (2H, t, *J* 7.6 Hz, H2), 2.49 (4H, t, *J* 7.6 Hz, H10, H12) ^{13}C NMR (100 MHz, $CDCl_3$): ppm 14.1, 22.8, 24.9, 29.1 (2C), 29.2, 29.4 (2C), 29.5, 29.9, 30.0, 32.0, 32.4 (2C), 32.5, 34.1, 179.6.

General procedure for the oxidation of thiastearic acids.[13]

30 % H_2O_2 (6.67 mmol) was added to a solution of thiastearic acid (0.10 mmol) in acetone (4 mL) and the solution stirred at room temperature for 24 hours. On completion, the solvent was evaporated and the resulting residue recrystallized from acetone to yield the sulfinyl product.

8.18. 8-(Nonylsulfinyl)octanoic acid (17)[12]

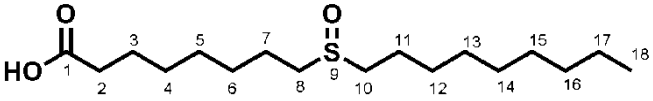

Obtained from 9-thiastearic acid (31.0 mg, 0.10 mmol) to yield a white solid (13.3 mg, 42 %).

M.p.: 81 – 82 ºC. Lit.[12] m.p.: 78 – 80 ºC. R_f (Hex:EtOAc, 8:2) 0.24. ^{1}H NMR (400 MHz, $CDCl_3$): ppm 0.88 (3H, , m, H18), 1.28 – 1.46 (18H, m, H4 – H6, H12 – H17), 1.63 (2H, m, H3), 1.77 (4H, m, H7, H11), 2.33 (2H, m, H2), 2.64 (2H, m, H8), 2.75 (2H, m, H10) ^{13}C NMR (100 MHz, $CDCl_3$): ppm 14.4, 22.9, 23.0 (2C), 25.0, 28.9, 29.0, 29.1 (2C), 29.2, 29.6, 29.7, 32.2, 34.3, 52.4, 52.6, 178.1.

8.19. 9-(Octylsulfinyl)nonanoic acid (18)[12]

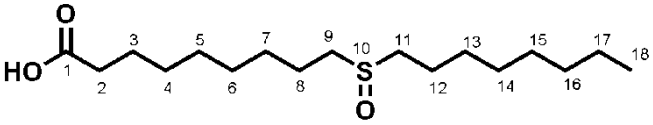

Obtained from 10-thiastearic acid (30.60 mg, 0.10 mmol) to yield a white solid (13.5 mg, 42 %).

M.p.: 76 – 77 ºC. Lit.[12] m.p.: 77 – 79 ºC. R_f (Hex:EtOAc, 8:2) 0.30. ^{1}H NMR (400 MHz, $CDCl_3$): ppm 0.88 (3H, , m, H18), 1.29 – 1.48 (18H, m, H4 – H7, H13 – H17), 1.63 (2H, m, H3), 1.77 (4H, m, H8, H12), 2.33 (2H, m, H2), 2.64 (2H, m, H9), 2.75 (2H, m, H10) ^{13}C NMR (100 MHz, $CDCl_3$): ppm 14.0, 22.5, 22.6, 24.7, 28.7 (4C), 28.9, 29.0, 29.1, 29.3, 31.7, 33.9, 52.1, 52.2, 177.7.

8.20. 10-(Heptylsulfinyl)decanoic acid (19)

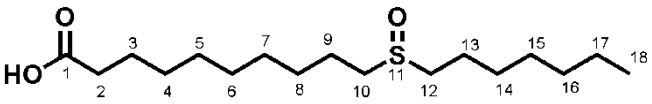

Obtained from 11-thiastearic acid (50.30 mg, 0.17 mmol) to yield a white crystalline solid (27.20 mg, 50 %).

M.p.: 68 – 70 ºC. R_f (Hex:EtOAc, 5:5) 0.26. ^{1}H NMR (400 MHz, $CDCl_3$): ppm 0.81 (3H, t, *J* 4.4 Hz, H18), 1.23 – 1.40 (18H, m, H4 – H8, H14 – H17), 1.55 (2H, t, *J* 6.8 Hz, H3), 1.67 (4H, t, *J* 6.8 Hz, H9, H13), 2.24 (2H, t, *J* 7.3 Hz, H2), 2.56 (2H, m, H10), 2.67 (2H, m, H12) ^{13}C NMR (100 MHz, $CDCl_3$): ppm 14.0, 22.5, 22.6, 22.7, 24.7, 28.7, 28.8, 28.9, 29.0 (4C), 33.6, 34.1, 52.1, 52.2, 177.8.

8.21. Enzymatic oxidation of sterols

The method reported by *invitrogen* was followed to enzymatically oxidize cholesterol and 23-thiacholest-4-en-3β-ol (**5**) and 3α-fluorocholest-5-ene (**10**)[14]

Reaction buffer

A reaction buffer was prepared by adding 2.5 mL of stock solution to 10 mL of H_2O. The stock solution consisted of 0.5 M sodium dihydroorthophosphate, pH 7.4, 0.25 M NaCl, 25 mM cholic acid and 0.5% Triton® X-100.

Cholesterol oxidase stock solution

A 200 U/mL cholesterol oxidase stock solution was prepared by dissolving 1 mg cholesterol oxidase in 0.12 mL of Reaction Buffer.

Oxidation procedure

Cholesterol (1 mg) was dissolved in Reaction Buffer (1 mL) and incubated at 37 °C. Cholesterol oxidase (20 µL) was added and the solution allowed to incubate for 45 minutes. Chloroform (0.5 mL) was added to terminate the reaction and samples were analysed by GC-MS.

8.22. Microorganism culture and growth conditions

M.smeg was grown on agar plates at 37 °C for four days. The culture was thereafter grown in three separate parts, following the procedure described by Wang and company.[15] A colony from the agar plate was inoculated into a glycerol stock solution and incubated at 37 °C for 24 hours. This was inoculated into an activation medium which was incubated for three days. This was followed by incubation into the transformation medium for seven days. Medium containing 0.1 % derivatized cholesterol was inoculated with culture from the transformation medium to evaluate the growth of M.smeg in the presence of the synthesized compounds.

Agar plates

The agar plates consisted of Middlebrook 7H9 broth base (0.52 g), NaCl (0.085 g), tween 80 (0.5 mL) and glycerol (450 µL) in H_2O (100 mL).

Glycerol stock solution

The stock solution was made up as described above for the agar plates with the exception of agar.

Activation medium

The activation medium contained Middlebrook 7H9 broth base (5.2 g), NaCl (0.85 g), tween 80 (5 mL), glycerol (4.5 mL) and cholesterol (2.5 g) in H_2O (1 L).

Transformation culture

The transformation medium consisted of Middlebrook 7H9 broth base (5.2 g), NaCl (0.85 g), tween 80 (5 mL) and cholesterol (2.5 g) in H_2O (1 L).

8.23. Growth curves of M.smeg with synthesized compounds as carbon source

The transformation culture was diluted by 1:500 in Middlebrook 7H9 broth of which 50 µL was added to medium (50 µL) containing the synthesized compounds (0.1 %) in a 96-well plate. Incubation was carried out for 4 days at 37 °C. OD readings were recorded at 595 nm every 4 hours.

8.24. Growth curves of M.tb with synthesized compounds as carbon source

All studies performed with M.tb were carried out by Krishnamoorthy Gopinath at the institute of infectious disease and molecular medicine, UCT. M.tb was grown in minimal media containing asparagine (0.5 g/l), KH_2PO_4 (1.0 g/L), Na_2HPO_4 (2.5 g/L), ferric ammonium citrate (50 mg/L), $MgSO_4 \cdot 7H_20$ (0.5 g/L), $CaCl_2$ (0.5 g/L), $ZnSO_4$ (0.1 mg/L), 0.2 % tyloxapol, 0.2 %

EtOH, and either 0.1 % glycerol or 0.01 % cholesterol or synthesized derivatives. Growth was monitored by OD at 600 nm for a period of 14 days.

8.25. Isolation of total protein associated with the cytoplasm[16]

M.smeg from the transformation culture (prior to dilution for growth curves) was harvested by centrifugation and the pellets washed with Tris-HCl buffer. The cell pellet was re-suspended in potassium phosphate buffer (20 mL) supplemented with protease inhibitor cocktail. Cells were disrupted by sonification for 6 minutes at 0 °C. The mixture was centrifuged and the supernatant collected and stored at - 80 °C until it was required for cell-free incubations.

8.26. Quantification of total protein[17]

Bradford method was used to determine the total protein concentration as detailed in Table 7.1 using bovine serum albumin (BSA) as the reference protein. A calibration curve was determined from a 2 mg/mL BSA stock solution. The protein extract (10.0 µL) was added to the Bradford"s reagent to determine its concentration and the absorbance read at 595 nm.

Table 7.1: *Protein quantitation by Bradford's assay.*

Concentration (mg/mL)	Blank	2.5	5.0	7.5	10	Sample
BSA (µL)	0	1.25	2.5	3.75	5.0	0
Tris-HCl Buffer (µL)	10	10	10	10	10	0
H_2O (µL)	790	788.8	787.5	786.2	785.0	790
Bradford Reagent (µL)	200	200	200	200	200	200

8.27. Cell-free incubations

Cell-free incubations were carried out by the addition of protein extract (1 mg/mL) to a solution containing synthesized compound (1 mg/mL), NaCl (0.2 mM), dithiothreitol (1 mM) and 10 mM Tris-HCl buffer (pH7.5) with a final volume of 500.0 µL. All compounds were suspended in EtOH (20.0 µL) prior to the addition of buffer. Incubations were carried for 24 hours. Reactions were stopped by the addition of15 % ethanolic KOH (500.0 µL) and samples heated at 90 °C for 2 hours. After samples were cooled to room temperature, samples were washed with brine, followed H_2O and extracted with chloroform (500.0 µL) containing an internal standard (0.30 mg). The organic layer was dried over anhydrous $MgSO_4$.

8.28. Whole cell incubations

Whole cell incubations were carried out as described for the growth curves of M.smeg and terminated as stated for th cell-free incubations.

8.29. Percentage recovery determination

Reactions were carried out as for the whole cell incubations and the reactions immediately terminated after the addition of M.smeg culture.

8.30. References

1. A. Bajaj, P. Kondaiah and S. Bhattacharya, *Bioconjugate Chem.*, 2008, **19**, 1640–1651.

2. A. Ternay, *Preparation of Potential Radioprotective Agents Derived from Aminothiols*, University of Texas, Arlington, 1986.

3. L. Nahar and A. B. Turner, *Tetrahedron*, 2003, **59**, 8623–8628.

4. P. Ferraboschi, A. Fiecchi, P. Grisenti, E. Santaniello and S. Trave, *Synth. Commun.*, 1987, **17**, 1569 – 1575.

5. S. H. Burstein and H. J. Ringold, *J. Biol. Chem.*, 1957, **224**, 4952–4958.

6. J. Liu, PhD Thesis, Texas Tech University, 2008.

7. E. Ma, H. Kim and E. Kim, *Steroids*, 2005, **70**, 245–250.

8. A. Bowers and H. J. Ringold, *Tetrahedron*, 1958, **3**, 14–27.

9. M. M. Meijler, N. Amara and J. Rayo, Patent, 2011001419 A1, 2011.

10. G. W. Buchanan, R. Smits and E. Munteanu, *J. Fluor. Chem*, 2003, **123**, 255–259.

11. M. D. Rahman, D. L. Ziering, S. J. Mannarelli, K. L. Swartz, D. S. Huang and R. A. Pascal, *J. Med. Chem.*, 1988, **31**, 1656–1659.

12. R. A. Pascal and D. L. Ziering, *J. Lipid Res.*, 1986, **27**, 221–224.

13. D. J. Hodgson, K. Y. Y. Lao, B. Dawson and P. H. Buist, *Helv. Chim. Acta*, 2003, **86**, 3688–3697.

14. Life Technologies, Amplex Red Cholesterol Assay Kit, http://www.lifetechnologies.com/order/catalog/product/A12216, 2010, (Accessed June 2011).

15. Z. Wang, F. Zhao, X. Hao, D. Chen and D. Li, *J. Mol. Catal. B Enzym.*, 2004, **27**, 147–153.

16. A. M. Upton and J. D. McKinney, *Microbiology*, 2007, **153**, 3973–3982.

17. M. M. Bradford, *Anal. Biochem.*, 1976, **72**, 248–54.

Appendix

Mass spectrum of cholesterol:

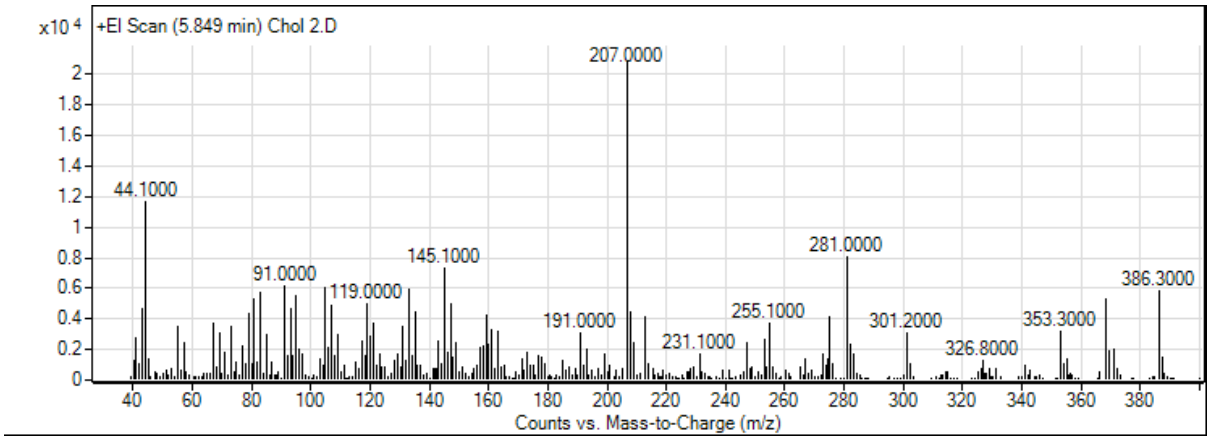

Mass spectrum of cholestenone

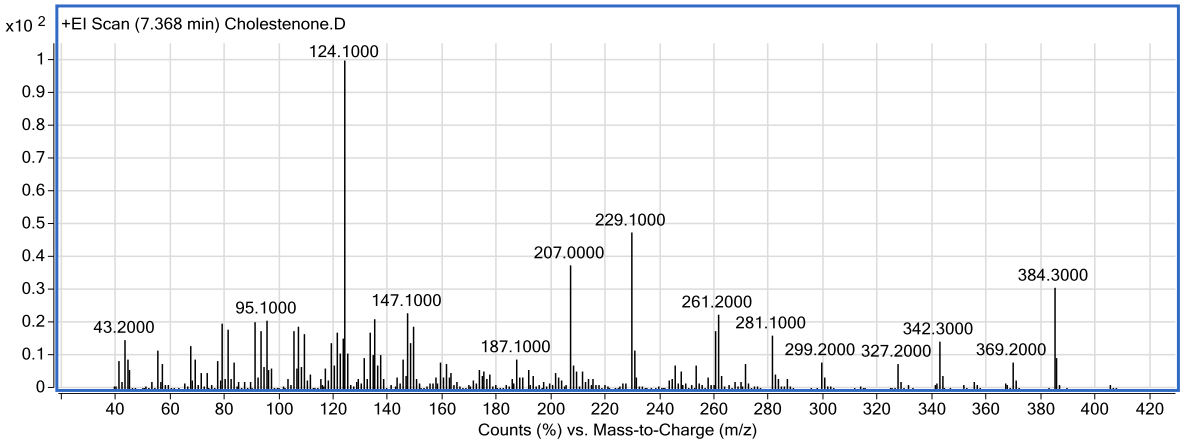

Mass spectrum of 3β-mercaptocholest-5-ene (**3**)

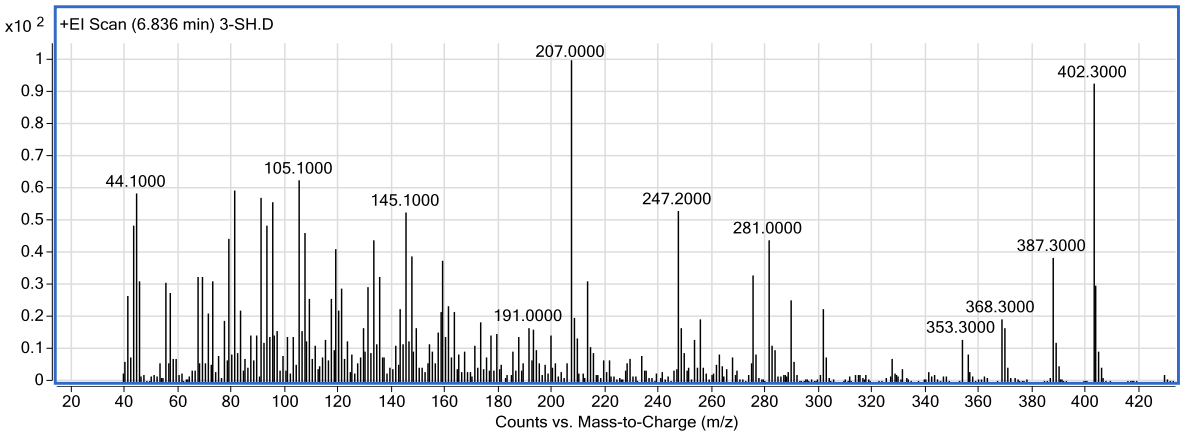

Mass spectrum of 23-thiacholest-4-en-3-one (**4**):

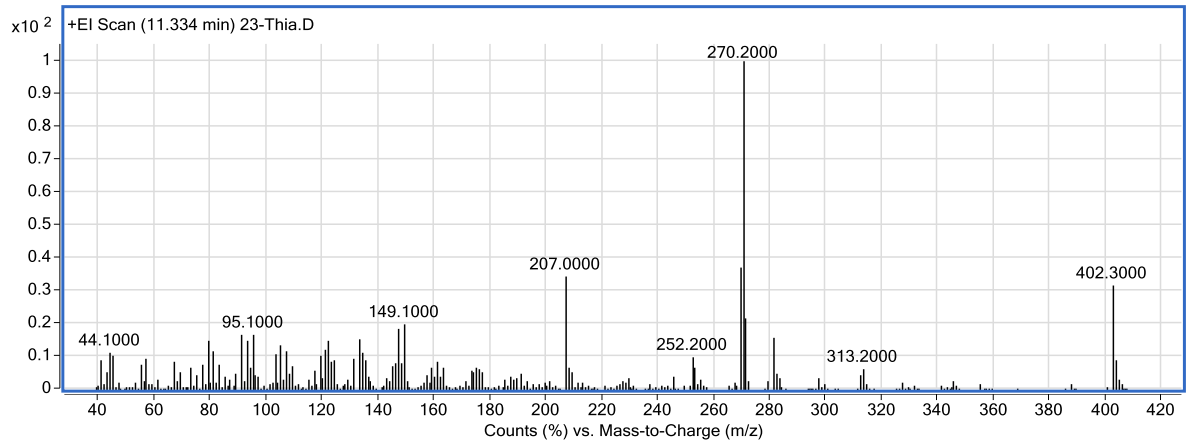

Mass spectrum of 23-thiacholest-4-en-3β-ol (**5**):

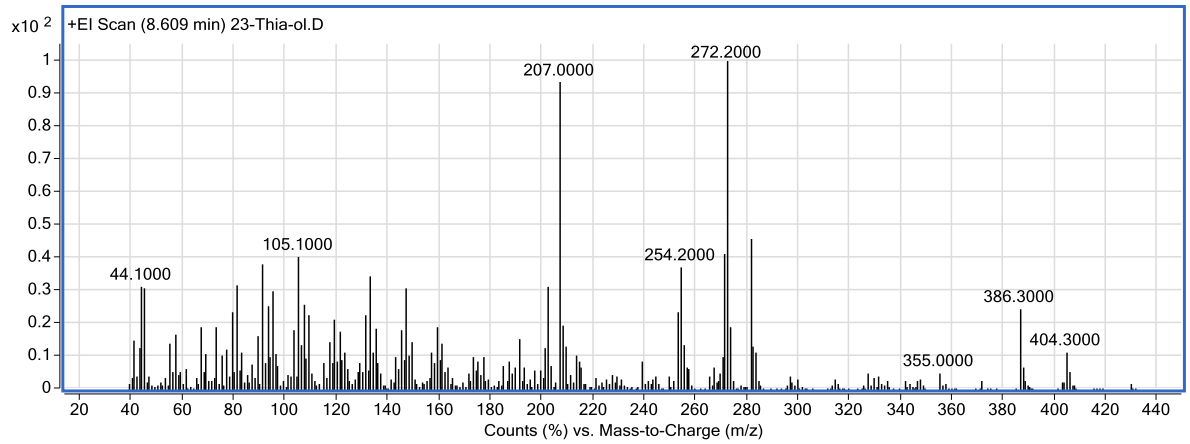

Mass spectrum of 3α-fluorocholest-5-ene (**10**):

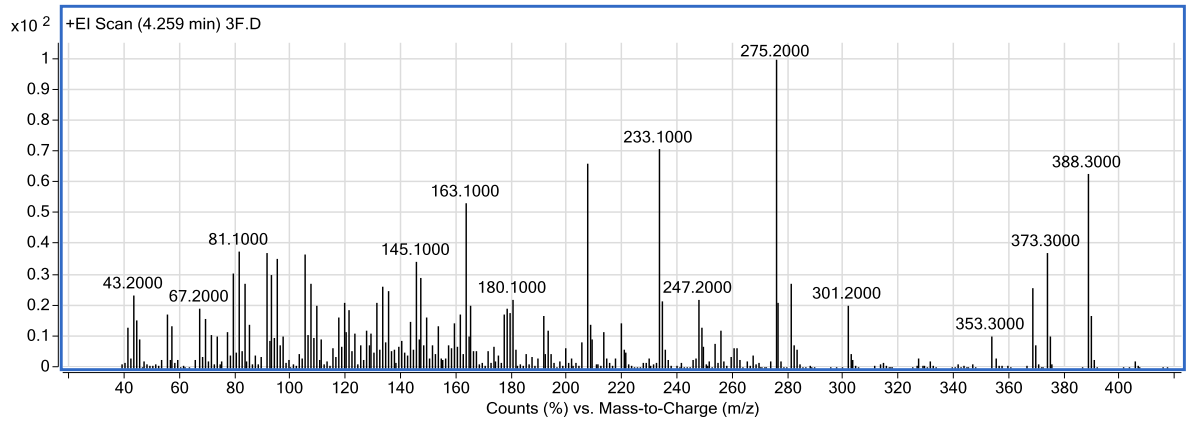

Mass spectrum of 6β-fluorocholestan-3β,5α-diol (**12**):